Fatigue Response of Notched Graphite-Epoxy Laminates

by

Gerald R. Kress

Thesis submitted to the Faculty of the
Virginia Polytechnic Institute and State University
in partial fulfillment of the requirements for the degree of
MASTER OF SCIENCE
in
Engineering Mechanics

APPROVED:

W.W. Stinchcomb, Chairman

M.W. Hyer

J.N. Reddy

D. Frederick, Dept. Head

May, 1983
Blacksburg, Virginia

FATIGUE RESPONSE OF NOTCHED GRAPHITE-EPOXY LAMINATES

by

Gerald Rolf Kress

(ABSTRACT)

Changes in the stiffness and strength of notched quasi-isotropic graphite-epoxy laminates were recorded and related to the fatigue damage. Two different laminates [0,90,+45,-45]s (type A) and [+45,90,-45,0]s (type B) were considered and the effects of stacking sequence were compared. Nondestructive testing techniques such as X-radiography, moire technique, acoustic emission, deply technique, and stiffness change were performed to observe damage development. Static properties and damage initiation were related to an approximate stress analysis.

Results show that the mechanical response and the fatigue damage depend strongly on the stacking sequence of laminates. In general, residual strength increased remarkably for both laminates due to stress redistributions while the continuous stiffness change curve is typical for each laminate and reflects damage characteristics. Buckling effects as well as matrix cracking and delaminations contribute to stiffness changes.

ACKNOWLEDGEMENTS

The author wishes to thank Dr. Wayne Stinchcomb who not only offered every help and answered every question but also left enough freedom for the author to follow his own ideas and gain his own experiences in research. He is also indebted to Mr. George Lough for maintaining and explaining the use of laboratory equipment and for performing delicate work on a load measuring device.

His fellow students spent time and patience to offer suggestions, discussions, and know how in experimental questions and helped setting up tests. Particularly mentioned here are Dr. Russell Jamison, Mr. Alton Highsmith, Mr. Anil Govada and Mr. Richard Stiffler.

Mr. Bob Davis, Mr. Archie Montgomery and Mr. Brent Farmer contributed with their excellent craftmanship performed on the loading fixture to successful results of the moire tests.

Mr. 'Mac' McCauley made photographic work and many times helped to obtain laboratory equipment.

The author remembers thankfully the cooperation with Dr. Dan Post, Dr. Anand Asundi and Mr. Robert Czarnek during the moire tests. Dr. Post helped designing the loading-fixture and made his laboratorium available for several days in

spite of his own tight schedule. Dr. Anand Asundi and Mr. Robert Czarnek spent much time attaching gratings to specimens. Dr. Anand Asundi made the setup for the moire tests and repeatedly spent many hours to supervise and perform the tests and to answer the technical questions of the author.

TABLE OF CONTENTS

LIST OF FIGURES

Chapter I

INTRODUCTION

The study of hole related fatigue damage in materials is motivated by the need to include holes into structures. For example, in an airplane, even a critical plate or shell may have to provide access from one side to another for electric lines, fuel pipes, or other supplementary equipment. Another, earlier, example concerning the response of the isotropic material steel is the effect of hatches on the strength of ship hulls. As of to-date, the knowledge of the fatigue response of notched composite laminates is much less complete than that of unnotched laminates. The main reason is that fatigue damage, residual strength, and stiffness degradation predicting models [1,2] for the unnotched situation are based on uniformities of damage that are reflected by terms such as 'characteristic state of damage (CDS)', for instance. These uniformities of damage do not apply, however, for notched specimens. An idea of the complexity of the fatigue behaviour of notched specimens may be given by studying an X-ray photo of damage around the hole of a notched specimen after high fatigue loading.

The objectives of the present work are to determine the nature of damage induced in graphite epoxy composite lami-

nates with center holes by cyclic tensile loading and to establish the influence of such damage on the strength, stiffness and life of the laminates.

The complexity of damage mechanisms in composite materials requires different techniques for complementary insight. Sendeckyj [3] found that the X-ray technique makes damage, namely matrix cracks and delaminations, visible but is restricted to observing spatial distribution of damage. The deply technique complements the X-ray photography because of its ability to identify specific planes of delamination. In the same sense the electron microscopy can detect fiber cracks as well as the results of debonding; that is, the pullout of fibers at fracture surfaces. X-ray photography and the deply technique are also opposite in the sense that the former is a nondestructive test (NDT) method while the latter inevitably destroys the test specimen.

The advantage of the ultrasonic C-scan technique, compared with X-ray photography, is that its sensitivity is not dependent on a contrast medium, thus enabling it to detect delamination-like flaws surrounded by undamaged material.

Damage events during the loading process can be detected by acoustic emission recording . It yields, in combination with the simultaneously recorded load-strain curve, information about the sequence and the interactive effects of subsequent damage events.

Since the strain field in notched specimens is nonuniform, it is difficult to decide what strain measurement technique gives the most valuable information. However, the moire technique [4] provides insight into the complete nonhomogeneous in-plane strain field. But the words 'complementary insight' used to describe different NDT methods have also a more general meaning than that one technique completes the picture of damage which is partially shown by another technique. A recently established investigative method is the use of stiffness change recording as an indicator for damage state or strength values [5].

E.T. Camponeschi and W.W. Stinchcomb [6] pointed out that a quasi-isotropic laminate exhibits a different response than its constituent sublaminates. For instance, the response of a [0,90,+45,-45]s laminate cannot be predicted by knowing the behaviour of the [0,90]s and of the [45,-45]s laminate. In contrast, if predictions for the response of yet untested laminates are desired, they should be based on considerations like stress analyses including edge effects or constraint effects. For designing as well as for research purposes many stress analyses for laminates with notches were developed [7,8,9,10,11,12,13,14]. Satisfactory solutions for hole induced edge effects require either FEM models [8,9,10,11,13,14] with many degrees of freedom, thus

demanding sophisticated economical storage and computation techniques [13], or the skillful use of simplifying assumptions [7,9,12] that lead to approximations of undetermined accuracy. Since most approximations for stress distributions around holes are principally straight edge solutions and not sensitive to the gradient of the circumferential stresses, we might suspect that their results do not closely agree with the true solutions. I.S. Raju and J.H. Crews, Jr. [9] compare a three dimensional FEM solution with a simplified FEM analysis [10] which divides the circular hole edge into straight edge segments. The data input of this approach includes the circumferential strains, calculated by Lekhnitskii's exact plane stress solution for anisotropic plates [15]. However, the results of the two models agree closely at least for the larger stress concentration values, thus indicating that the error encountered by the lack of sensitivity to circumferential gradients of approximate solutions is not too large.

On the other hand, knowing an even less accurate stress distribution may help to understand and predict the onset of damage and the probability of delamination development.

However, static strength predicting models for notched specimens were developed that do not require a laminate stress analysis. Instead, the notched and the unnotched situation are compared.

J.M.Whitney and R.J.Nuismer in 1974 [16] suggested a failure criterion for notched laminates that predicts the uniaxial tensile strength and is based on a simple consideration of the isotropic stress distribution rather than on the actual state of laminate stresses. Their failure criterion features two versions: the first one predicts failure, if the material is critically stressed over a certain distance from the hole, the second one says that a specimen will fail if the average stress over some other distance away from the hole exceeds a certain value.

However, their formulas determine the ratio of the notched strength versus the unnotched strength of a laminate so that the latter must be known; moreover, they are dealing with the different mechanisms of straight edge driven versus notch initiated failure simply by adjusting the material dependent constant 'a'. After collecting data for both unnotched and notched laminates, failure loads for various notch sizes can be predicted.

Three years later Whitney and R.Y. Kim [17] published the results of a test series which exhibit that notched failure mechanisms differ from the unnotched situation. They investigated the influence of two different stacking sequences, one of them producing tensile, the other producing compressive interlaminar normal stress througout the thickness of the straight edge on both notched and unnotched specimens.

The data indicate that unnotched tensile strength is reduced by the straight edge effects and is strongly dependent on the stacking sequence; while the strength of notched specimens is independent of the straight edge effects since tensile failure is initiated by the stress concentration at the notch before straight edge delamination comes into effect. Other investigations of the fatigue behaviour of notched specimens were conducted by Sendeckij [3], Stinchcomb and co-workers [2], and Whitcomb [14]. The work most comparable to the present one is that of Whitcomb, who described the damage state and the mechanical response of four different notched laminates after fatigue loading and related delamination onset to the results of an FEM stress analysis. The load levels of two-thirds of the initial strength of the laminates, respectively, were low enough to let the specimens survive a lifetime of ten million cycles. At this point, the damaged specimens were investigated using destructive and nondestructive methods. The residual strength of all laminates was equal to or higher than the initial strength of specimens, respectively. Stiffness degradations were found to be in the range from zero to minus 10 percent. Whitcomb also shows figures comparing initial stress distributions with delaminations at different locations through the thickness on the hole edge that suggest that interlami-

nar normal stress and shear stress distributions govern the locations of first fatigue delaminations. Later in the lifetime, the direction of delamination growth can be changed by an altered stress distribution.

Sendeckyj's work is mainly concerned with the introduction of stereo X-radiography and describes the damage that is made visible on X-ray stereo pairs.

The emphasis of the paper of Stinchcomb and co-workers is on the investigation of constraint effects on the development of initial damage. Notches were introduced in specimens by cutting notches out of single plies before lamination. The surface plies of the laminates to be produced, respectively, were left undamaged. The results of their work can be partially related to damage-pattern characteristics found in the present work which are dependent on the stacking sequence.

In the first phase of the present study, the fatigue damage pattern was observed in laminates with four different stacking sequences. For further investigations, two of the laminates, with relatively little straight edge initiated damage, were chosen in order to isolate notch effected damage from straight edge driven damage as much as possible.

The damage induced by static and by fatigue loading was observed by nondestructive inspection and other methods.

Quasi-static tests were performed to compare the development of damage under cyclic with that under static loading. Experimentally observed initiation of matrix cracks was compared with the results of an approximate stress analysis.

Chapter II

EXPERIMENTAL PROCEDURES

2.1 MATERIAL AND SPECIMENS

The material in this study is T300-5208 graphite epoxy. The Specimens for the preliminary study were ten inches long, 1.5 inches wide and had a 0.25 inch diameter hole in the center. The four stacking sequences were :

[0,+45,-45, 90]s

[0, 90,+45,-45]s

[45, 0,-45, 90]s

[+45,-45, 0, 90]s

From the results of tests on these laminates, two stacking sequences were chosen for further investigation. They were :

[0, 90,+45,-45]s type A

[+45, 90,-45, 0]s type B

The new specimens had a 0.375 inch diameter hole machined using an ultrasonic drilling machine. A third stacking sequence,

$$[+45,-45,\ 0,\ 90]s \qquad \text{type C}$$

was used to determine the critical strain energy release rate for delaminations in the batch of material used for this study. These specimens had no hole.

2.2 MECHANICAL TESTS

All mechanical tests were conducted in load control on a 20 kip servo hydraulic closed loop MTS testing machine.

Mechanical tests are performed to obtain strength and stiffness data for the undamaged and damaged specimens and to impose cyclic loading histories on the specimens.

The test machine was equipped with MTS hydraulic grips. The ends of the specimens seated in the grips were wrapped with a double layer of sandpaper folded around the upper and the lower edge such that the vertical edges of the specimens remained uncovered. This is merely a precaution to avoid slipping in the grips under high tensile loading. The sandpaper was replaced regularly. Alignment plates filling in

the gaps between the specimen edges and the inner surface of the grip housing helped to align and position the specimen and, therefore, to reduce unintentional load components like bending moments. Correcting a relative twist between the upper and the lower grip avoided unintended twisting moments acting on the specimens. Any relative twist was minimized by placing alignment bars between the grips and rotating the lower grip until the pointer and the crossmark on the alignment bars matched. The specimen, equipped with sandpaper and the alignment plates, was placed in the lower grip, and the gripping pressure was adjusted so that the specimen was still moveable against friction. Then the lower grip and specimen were moved up by hydraulic pressure until the upper part of the specimen with the alignment bars was in the right position within the upper grip. While the control set point was adjusted such that the lower grip was moving down at a very low time rate, both grips were slowly tightened. This procedure guaranties an almost buckle free positioning of the specimen under a slight tensile load. However; it was necessary to clean the grip housing and the wedges periodically because dirt on their contacting surfaces can cause unintended relative twists of the wedges while tightening.

2.3 MONOTONIC LOADING TESTS

The specimens were loaded with time rates between 25 lbs/sec and 50 lbs/sec using the ramp function of the MTS function generator.

Each of the four laminates used in the preliminary study was loaded until failure occured in order to obtain the stiffnesses and strengths of these laminates.

Strain was measured by a 1"-extensometer attached by rubber bands to the specimen. Slipping of the extensometer was prevented by pressing the knife edges into stripes of double adhesive tape attached to the specimens. The extensometer was centered with respect to the notch and oriented for measuring the longitudinal strain only.

Stiffness curves were recorded by a X-Y plotter. Some tests were performed with fatigued specimens to obtain changes of stiffness and strength dependent on the loading history.

Five specimens of each of the new laminate types A, B and C were subjected to strength tests with stiffness and acoustic emission recording to obtain the tensile strength, initial stiffness and informations on damage events during the loading process. Static tests were also performed on damaged specimens to measure the effects of cycling loading on strength and stiffness. Stiffness was measured during sev-

eral tests with not only the 1"-extensometer but also a 4"-extensometer to obtain information on the strain values around the hole based on short and long gage length.

2.4 SEQUENTIAL LOADING TESTS

Valuable information about a typical fatigue effected damage state distinguished from a damage state caused by static load was obtained from sequential loading tests. Two specimens, A22 and B16, were loaded in tension to a low load, treated with zinc iodide (a medium nearly opaque to X-Rays) unloaded, X-rayed, loaded again to a greater load, until failure. For each loading procedure, a stress-strain curve was recorded. The specimens were instumented with the four-inch extensiometer. Beginning at a very low load level, the specimens were sequentially loaded in increments of 10 percent of the mean tensile strength until a stress equal to the tensile strength of the virgin specimens was reached. Then the load increment was reduced to 5 percent of the tensile strength and the sequential loading was continued until the specimen failed.

2.5 FATIGUE TESTS

All fatigue tests were run in the tension-tension mode with a load ratio of R=0.1 and a frequency of 10 Hertz.

Specimens were tested at several different load levels evaluated as percentages of the mean tensile strength of five samples. The load levels spanned the range from 70 to 95 percent; i.e., from long-life-load levels to short-life-load levels.

Several specimens were run to failure to obtain lifetime-over-load (s-n) curves, others were monotonically loaded to failure after a certain number of cycles to obtain the typical strength-versus-loading-history curves. Many of these specimens were subjected to nondestructive inspections such as X-radiography or moire tests, at selected numbers of cycles.

Continuous stiffness degradation curves were produced using a Z-80 microprocessor and a peak-detector program. The input for the microprocessor was the load signal, generated by the MTS-testing machine, and the signal of the strain response of the tested specimen. The microprocessor evaluated the average load range and strain range during a time period of one second (10 cycles). These data were used as the input for a peak detctor program. The first recieved load and strain range information was used to define an ini-

tial stiffness value based on the unnotched cross-sectional area. All following data were related to as percentages of the initial stiffness. Results were printed at each 0.5 percent stiffness loss. Additionally the continuously updated stiffness-cycles curve was displayed on the terminal screen and could be plotted on paper. The printed results were used to produce stiffness degradation plots in both real and logarithmic lifetime scales. However, it was not possible to record the very values of stiffness degradation during approximately the first 100 cycles since the peak detector program is not started until the desired loading conditions are imposed on the specimen.

2.6 X-RAY RADIOGRAPHY

The X-ray photographs were taken using a Hewlett Packard N Faxitron X-ray system,using the same voltage of 25 Kv for all exposures.

The specimens were held by a device which allowed angular positions from 0 deg to about 45 deg with respect to the horizontal plane. The distance of the film from the beam source was about 18 inches.

Stereoscopic investigation is possible by taking two negatives of the same specimen, but with different angular positions with respect to the direction of the X-ray beam. For

the stereo negatives Kodak-R-film was exposed for 0.6 minutes. If a 3-D investigation was not intended, Kodak M-film was exposed for 0.3 minutes.

To make damage, especially matrix cracks but also delaminations, visible on X-ray photographs, the specimen must be prepared by filling the openings of the damage zone with a contrast medium. In the present study the specimens were moisturized at the edges of the hole and at the straight edges with zinc iodide which is nearly opaque to X-rays. The zinc iodide was applied shortly before the end of a cyclic test so that the relative movement of material adjacent to cracks helped it penetrate into the damage zone; however, the time period of fatigue loading with contrast medium in the specimen was kept short to avoid effects of zinc iodide on the fatigue behavior. In case of static tests the zinc iodide was allowed to soak in under load for some minutes. Load levels for the purpose of letting the contrast medium penetrate were the maximum load applied during the test; respectively, or a somewhat lower load in cases where the testing load approached or exceeded the tensile strength of a specimen.

After penetrating, the excess of zinc iodide on the surface had to be washed out carefully using acetone in order to avoid concealing the damage pattern by the image of the

surface. Although this method of detecting damage within a specimen gives highly precise information about the location and the size of even single matrix cracks, it must be critically mentioned that only those cracks which are penetrated by the contrast medium are visible; on the other hand, the zinc iodide can only penetrate along present cracks. Therefore, those cracks which are not connected with the surface were the zinc iodide was applied can not be made visible on X-ray photographs. There is, however, an advantage in this weakness: applying the contrast medium only at the edge of the hole gives good information on what part of the damage initiates there. Similar observation can be made for the damage associated with the straight edges. Using the moire test device, specimens could be loaded during X-ray exposure; however, only a few photographs of loaded specimens could be taken. In agreement with Sendeckyj's [3] observations, delaminations appear as dark regions with diffuse edges and sometimes have lighter areas embedded which are sharply distinguished from the surrounding spot. As in the present study, the light areas usually appear on X-rays of highly damaged specimens. It is believed that the variations in darkness are formed by mechanisms illustrated in Figure 1.

Penetrant Distribution

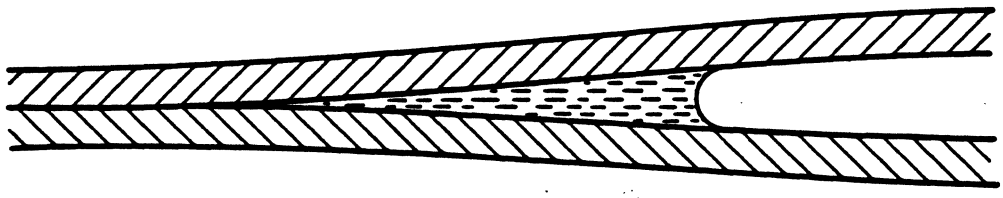

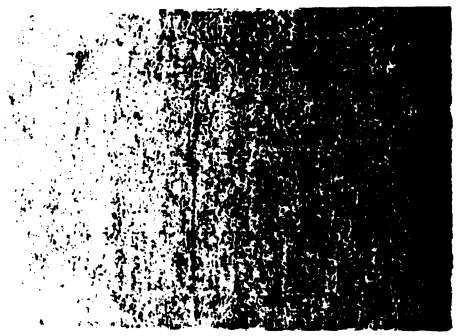

Effect on X-Ray Photograph

Figure 1: Penetrant Distribution in a Delaminated Area

At the periphere of a delaminated area, the gap between the delaminated plies is small, offering space for a only thin layer of penetrant that slightly reduces the intensity of passing X-ray beams and leads to the effect of diffuse edges. With increasing distance from the periphere, the thickness of the penetrant layer increases up to the point where the bond between the fluid and the solid material is no longer sufficient to form an uninterrupted layer. This transition phase is small and gives the distinct limits of the light spots. Thus, the light areas indicate a minimum gap width between delaminated plies.

2.7 DEPLY TECHNIQUE

The deply technique gives information on the location and extent of delaminations and fiber cracks in space. The specimens were kept at a temperature of 785 deg Fahrenheit for 30 to 50 min. in an electrically heated oven with controlled air exchange. This process effects the destruction of the resin-rich layer between the fiber carrying plies (the ply interface), which could then be separated and filed on paper cards for investigations like photography or microscopy. Applying gold chloride solution to specimens before the temperature treatment helps identify regions of delaminations and fiber cracking. Layers to be deplied were

first fixed by applying sticky tape and then disconnected from the remaining laminate by using a knife edge to systematically enlarge already present gaps.

As a general result of the experimental part of this study, the interlaminar surface patterns of deplied specimens consist of four elements. A surface showing exposed fibers looks typically silky or shiny and covers the largest part of the area. The ply surface contains evenly distributed spots of residual resin that are oriented in the fiber direction of the adjacent layer of the intact laminate. More significant for damage are the spots colored by gold chloride and characteristic dark blue areas. These are often accompanied by a concentration of resin-rich spots and match the locations of the before mentioned dark areas on X-ray photos. It is believed that the blue color arises from zinc iodide since the deplied specimen underwent X-radiography before deplying. However, the contrast on the deplied surfaces was so poor that instead of a photographic documentation sketches of the damage zones were drawn.

2.8 MOIRE TECHNIQUE

2.8.1 Purposes

The moire technique can be used as an accurate tool to obtain the complete two - dimensional displacement field at the plane surface of loaded elastic bodies. Because of its accuracy it is widely used to obtain experimentally elasticity solutions that cannot be determined analytically or to judge the aptitude of approximate solutions. Another importance of the technique lies in its ability to show the effects of structural damage within a body on its elastic behavior. In other terms, using the moire technique, it is possible to obtain the stiffness changes in damage zones.

2.8.2 Theoretical Background

Mechanical Interference or coarse moire produces the same fringe pattern as moire interferometry. Here the test setup consists simply of two coarse gratings with frequencies between 1 lines/mm and 40 lines/mm. One is fixed in space and is called the reference grating; the other undergoes in-plane deformations and is called an active grating. In practise, the active grating is attached to a body whose deformations under certain loading conditions are to be measured.

If for instance the active grating is uniformly stretched, a fringe pattern of equidistant light and dark

zones appears. Any of these fringes is the location of equal displacements of points on the active grating. The moire fringe orders N_x and N_y are the number of subsequent changes of intensity experienced at a certain point during the loading process from zero to the final value. The corresponding displacements u and v can be calculated by :

$$u = gN_x$$
$$v = gN_y \qquad (2.1)$$

where g is the pitch of the reference grating.

The same principle of using a fringe pattern to measure in plane displacements is used for moire Interferometry, which uses much finer gratings with pitches of the order of magnitude of the wavelength of light and therefore involves the effects of diffraction and interference of light.

Figure 2 illustrates the principle of a transmissive moire test setup as it can be used in practise for a investigation of the elastic behavior of a transparent body. In Figure 2a, the beam of coherent parallel directed light is diffracted at the reference grating into only two symmetrically oriented beams of diffraction order 0 and 1.
The conditions for this arrangement can be calculated using the grating equation :

$$\sin\theta_m = m\lambda f + \sin\alpha \qquad (2.2)$$

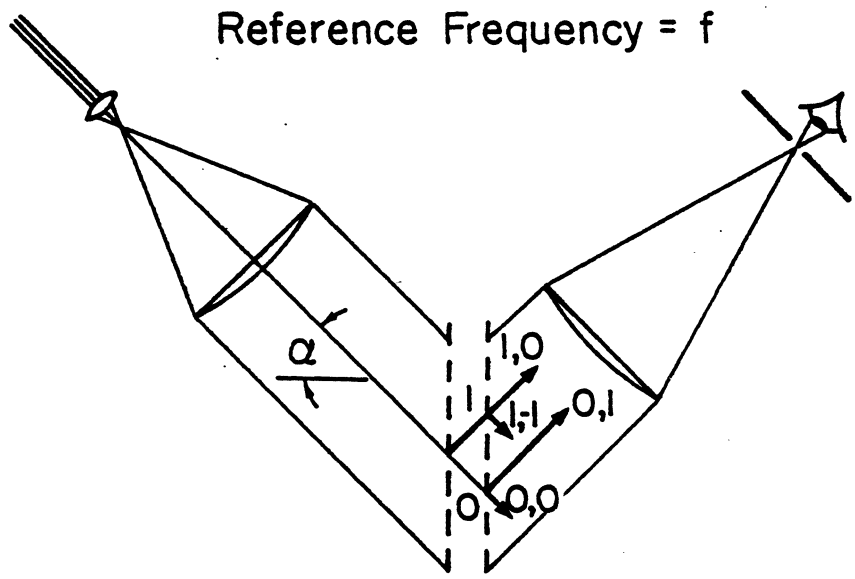

a) Active Frequency = $\frac{f}{1+\epsilon}$

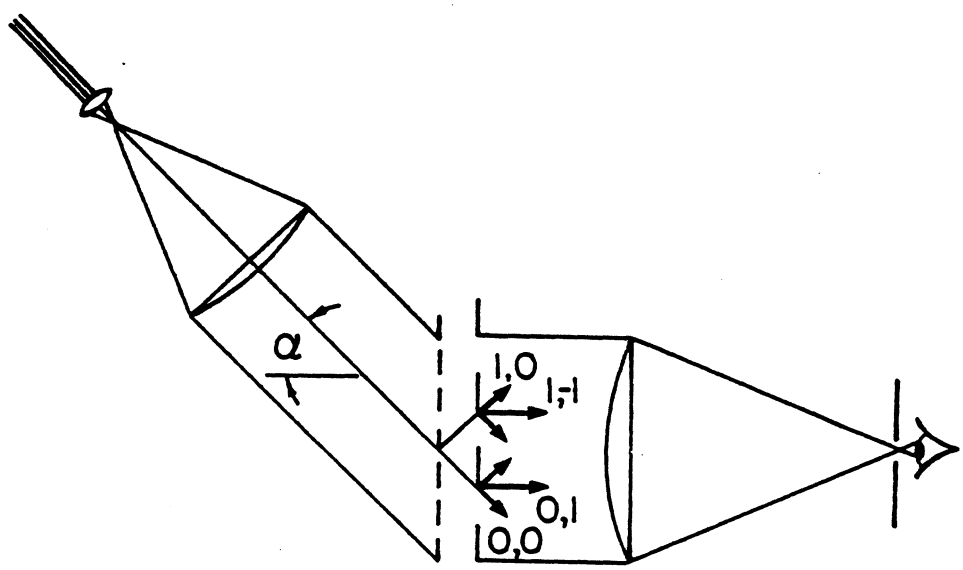

b) Active Frequency = $\frac{f}{2(1+\epsilon)}$

Figure 2: Transmissive Moire Test Set Up

and implementing the condition of symmetry of the diffraction orders 0 and 1.

$$\sin\alpha = \frac{\lambda}{2}f \tag{2.3}$$

with

α = angle of incidence

θ_m = direction of the diffracted light

m = diffraction order, counted anti-clock wise

λ = wave length of the coherent light

f = frequency of the optical grating

Two, and only two, diffraction orders are produced if

$$\frac{2}{\lambda} > f > \frac{2}{3\lambda} \tag{2.4}$$

The beams of the diffracted light are diffracted again at the active grating. Since the strain is zero, both grating frequencies are equal and the beams of the diffractions orders 1,0 and 0,1 are parallel, thus having parallel wavefronts.

If the active grating is deformed; however, the angles of the beams of diffraction order 1,0 and 0,1 are different according to the grating equation. The angle orientations of their wavefronts differ by the same value and produce a fringe pattern in space as is depicted in Figure 3.

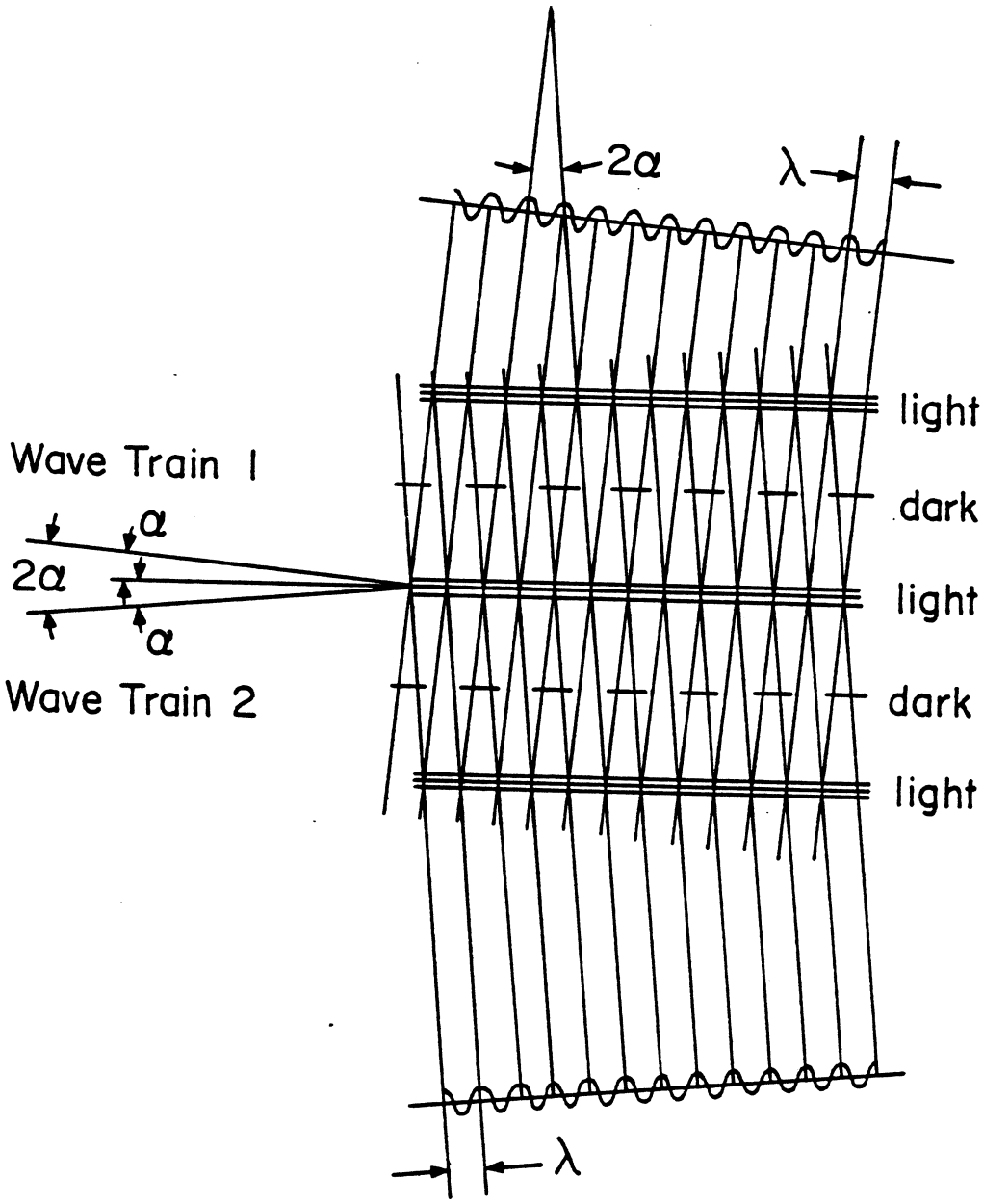

Figure 3: Interference of Two Wavefronts of Coherent Light

An important improvement of this setup is to choose an active grating with an undeformed frequency being one half of the value of the reference grating so the beams of the order 1,-1 and 0,1 emerge perpendicularly from the plane and allow an unforeshortened view of the fringe pattern, Figure 2b.

Another effect of decreasing the pitch of the reference grating by even multiples is called moire fringe multiplication. For a given active grating frequency there are β times as many fringes produced if the reference grating frequency is β times higher than the active grating frequency.

Another modification is inevitable if the body to be investigated is opaque. Without changing the theory or the resulting fringe pattern the transparent active grating is replaced by a reflecting grating, and the effect of the reference grating has to be achieved by a so called virtual grating. A virtual grating produces two beams of coherent light just as the reference grating did, as is illustrated in Figure 4.

2.8.3 Loading Fixture

The size of the investigated specimens required the construction of a new loading fixture for making moire measurements under load. The design, although kept as simple as possible, allows stresses as large as the tensile strength

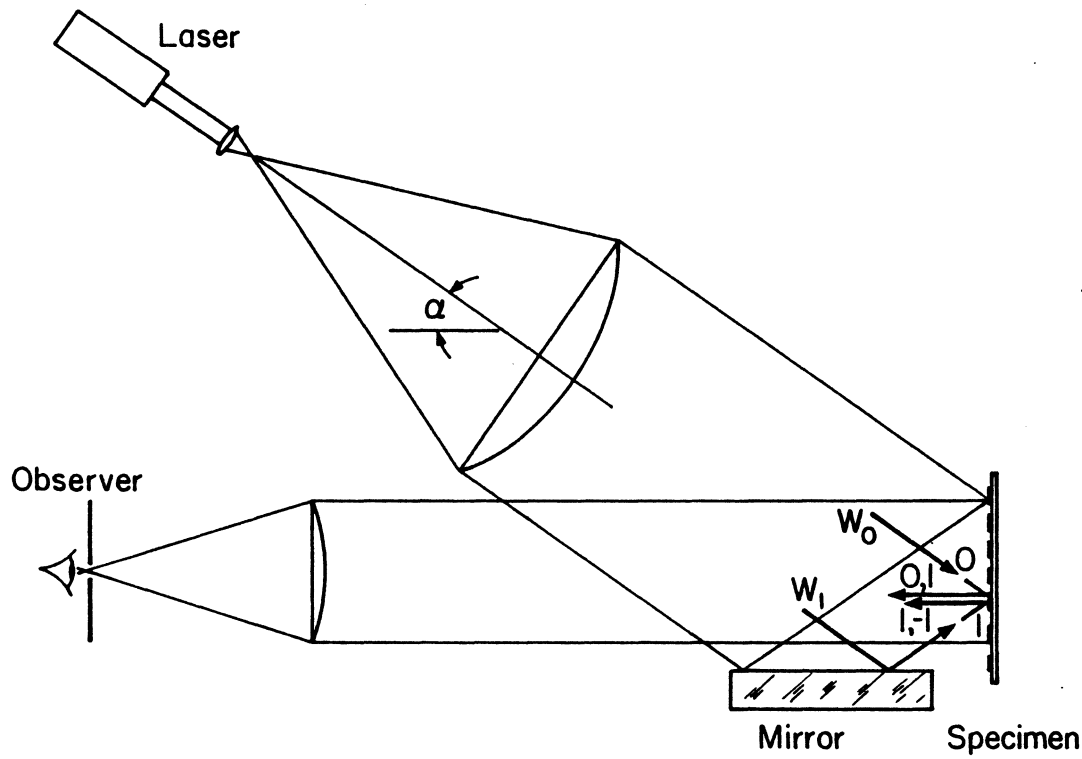

Figure 4: Reflective Moire Test Set Up With Virtual Grating

of the specimens to be applied. At the same time the creation of any out-of-plane effects is eliminated by making all forces colinear. The actual applied load can be measured through strain gages attached to a calibrated bolt, which is designed for undergoing suitable strains within the load levels in question.

For the moire test, the device is attached to a vertical surface and held by only one screw whose axis passes through the hole in the specimen. This allows the device to be turned around the axis to obtain displacement fields in both the X-direction and the Y-direction of the laminate.

The device consists of the frame, the carriage, the load cell, the torsion eliminator, the back plate, and two holders, Figure 5. The frame contains the lower grip for the specimen and guides the movable carriage and the torsion eliminator. The back plate is fixed to the end of the frame and holds the loading screw. The force, applied by turning the screw, is transmitted to the specimen through the torsion eliminator, the load cell, and the carriage. The torsion eliminator interrupts the transmission of the torsional moment from the screw on the load cell. For simplicity, the load is transmitted to the specimens not by friction but mainly through two pins in the center of each grip. The specimen ends are reinforced by glass-epoxy laminates. All

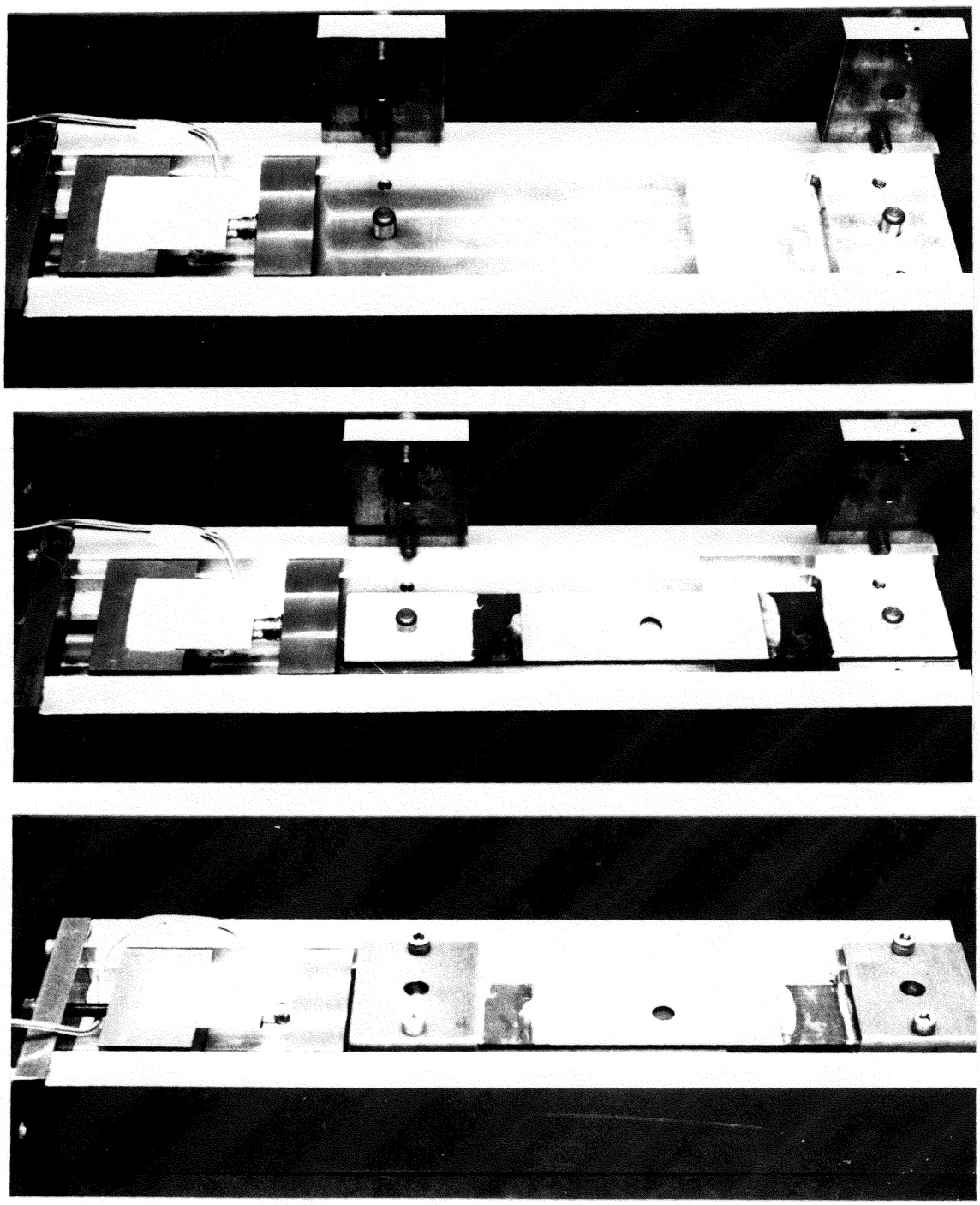

Figure 5: Loading Fixture

parts are dimensioned such that the forces in them have the same centerline, thus avoiding bending moments and other out-of-plane effects. As a result, the load cell, consisting of a steel rod with threads and attached strain gauges is free of torsional and bending moments. The four strain gauges are attached such that the first two measure the positive longitudinal strain on each side of the rod, giving a positive signal, while the second two measure the negative transverse strain (Poisson Effect) on each side, also giving a positive signal. So the sensitivity of the device is increased by the factor $2(1+\mu)$ (μ is Poisson's Ratio), while at the same time the effects of thermal expansions are eliminated. The load measuring device was calibrated using an Instron-test machine. The applied loads were measured and plotted against the corresponding strain recorded by the load cell.

2.8.4 Preparation of Specimens for Moire Tests

During a moire test the load is transmitted to the specimen through the pin and the edge of the holes drilled at the ends of each specimen. Since the magnitude of the load may come close to the static strength of the specimens, the ends were reinforced to prevent their breakage. The reinforcments consist of [0, 45,-45]s glass-epoxy plates which are glued

to both sides of each specimen, using a two-component epoxy adhesive.

To produce high quality moire fringe patterns, the specimen plane, with the grating, and the surface planes of the reinforced ends must be parallel. If those surfaces are not all parallel to each other,bending will be induced during a test and the result will be falsified. All surfaces to be glued together were sanded and cleaned with acetone. A thin layer of adhesive was spread onto the prepared surfaces, then the pieces were put together so that the reinforcement plates were attached to one side of the specimen at a time. The specimen was then placed on a thick glass plate, another plate was set on the middle of the specimen,and then a heavy weight with a plane surface was set on top of the specimen, thus improving the adhesive strength and ensuring the parallelism of reinforcement plates and specimen surfaces. The plate on the middle of the specimen helped avoiding bending during the curing time.

The drilling of the holes was performed as press fit so to achieve a distribution of pressure at the edge of the hole as equally as possible.

During the curing process while fabricating, the pattern of the curing cloth was formed in the matrix material of the specimen surface. To provide a surface that is plane and

smooth enough to support an optical grating two different things can be done. The first method is to polish the surface down until the curing cloth pattern is gone and a smooth surface is left. This method has two disadvantages. The first one is that there might still remain some of the pattern while at the same time the outside layer of fibers is exposed. Damaged fibers at the specimens surface reduce its adhesibility for the grating, may cause local distortion of the displacement fields, and may reduce strength. The other disadvantage is that removing of matrix material from the surface disturbs the balance of residual stresses within the laminate, thus leading to its bending in the unloaded state. This has probably only little effect on the specimen behavior during moire tests but makes proper attachment of the grating more difficult.

The second method tries filling the holes of the surface pattern with epoxy material rather then removing the embossed parts. For this purpose epoxy adhesive is spread out onto the surface and then covered by a teflon strip under firm pressure. Shrinkage of the hardening epoxy then leads to a less coarse reproduction of the original pattern rather than to its complete removal.

Therefore, a combination of the two methods seems to be recommendable. Instead of polishing down the whole pattern

we use fine sandpaper to remove the coarsest uneven patches only, then apply the epoxy adhesive method. This avoids disturbing the balance of residual stresses while at the same time the surface is fine enough to apply the epoxy technique successfully.

The optical grating was produced by exposing a photographic plate to two interferent beams of coherent light. After developing, the photo layer bears a pattern of equidistant bars and furrows, furrows at locations were the light sensitivity was lower and the remaining unreacted silver particles are washed out to a higher extent. The surface of the photolayer then was treated with photoflo, which lessens the adhesibility to the coating to be attached later. Using a vacuum chamber in order to minimize oxigeneous reactions, an aluminum layer was produced by evaporating this metal using electrically heated wire. The photographic plate was later glued to the prepared surface of specimens. After hardening of the glue, the glass plate bearing the photographic layer was removed and the very thin metal foil with the imprinted negative image of the grating was left; thus, the specimen was ready for the moire test.

2.8.5 Test Matrix

Moire tests were run for an A-specimen and a B-specimen at logarithmic distributed stages of lifetime from 10^0 to 10^5 cycles or 6 times 10^5 cycles, respectively. Fringe patterns of the displacement fields in both the x- and the y-direction were recorded. The specimens were tested under loads varying from a nominal load of 50 lbs to a load of 1550 lbs, which is about 60 percent of the static strength.

A mistake in the experimental procedure occurred in that the author unconsciously displaced the mirror creating the reference frequency, thus spoiling the fringe patterns of the later damage stages. After identifying this mistake the test of the highly damaged specimens was repeated. Fringe patterns obtained under correct test conditions are those of the undamaged and lightly damaged specimens and the new ones of the highly damaged situation.

For stiffness measurements; however, the effect of frequency mismatch is eliminated if there are two fringe patterns under different loads available. In this case, the difference in fringe order and the load increment can be used to obtain a correct stiffness value. It also must be determined if the actual reference frequency is lower or higher than the theoretically desired one. In the latter case, the null-field-fringe order must be counted negative in order to obtain a proper correction.

Chapter III

STRESS ANALYSIS

3.1 THEORY

The distribution of interlaminar stresses around the hole of the investigated laminates was estimated using a modification of the approximate straight-edge solution [7] by D. Engrand. The basic idea for this type of approximation was proposed by E.L. Reiss [18] and was developed for laminates by S. Tang [12].

Tang's basic idea is to develop an appropriate solution near the edge of an infinite symmetric laminate under unidirectional in-plane loading by superposing a plane-stress solution with an admissible three-dimensional state of stresses correcting the limitations of the plane-stress distribution near the edge such that the boundary conditions are satisfied.

However, the stress functions used by Tang neither satisfy the continuity of interlaminar stresses through the thickness nor the boundary condition of the normal stress acting on the surface of the laminate being zero. For these reasons this method is not conclusive enough to make close predictions for the onset of damage initiation or the static strength of laminates. Throughout this work, stresses act-

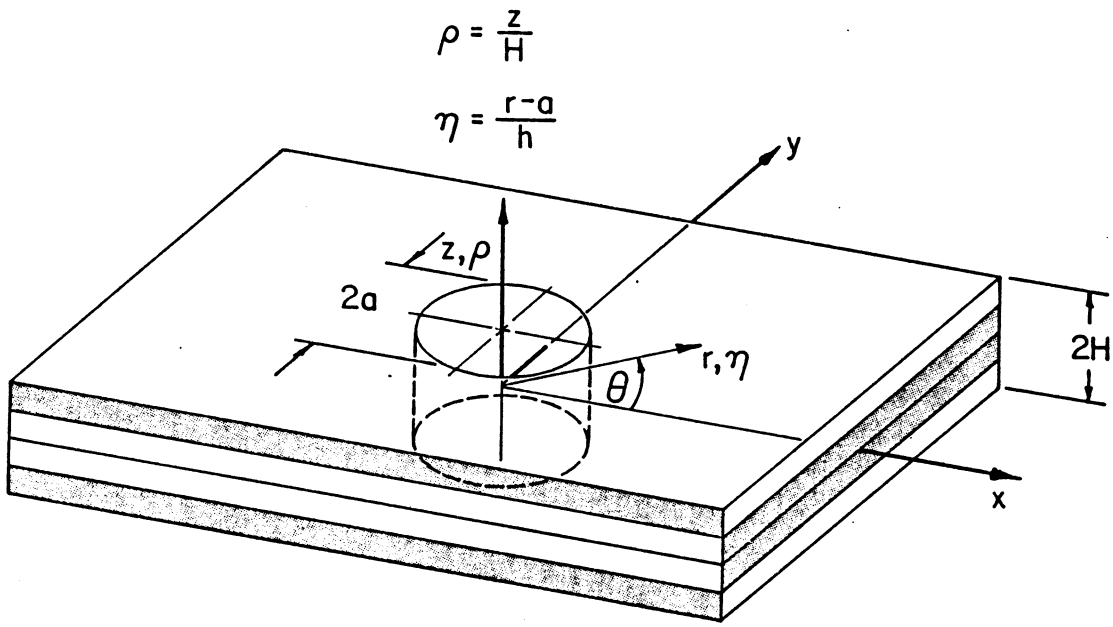

Absolute system coordinates	x, y, z
Absolute cylindrical coordinates	r, θ, z
Normalized cylindrical coordinates	η, θ, ρ

Figure 6: Coordinate Systems and Notations

ing on the planes perpendicular to the Z-axis will be referred to as interlaminar stresses, while stresses acting on planes parallel to the Z-axis will be called intralaminar. Figure 6 presents the coordinate systems and notations used in the following discussion.

The presently used form of Lekhnitskii's [15] plane-stress solution for anisotropic plates is taken from Tang's publication [12] :

$$\begin{aligned}
\sigma_{xx} &= p\cos^2\alpha + 2Re\{s_1^2\phi_0(Z_1) + s_2^2\psi_0(Z_2)\} \\
\sigma_{yy} &= p\sin^2\alpha - 2Re\{\phi_0(Z_1) + \psi_0(Z_2)\} \qquad (3.1) \\
\tau_{xy} &= p\sin\alpha\cos\alpha - 2Re\{s_1\phi_0(Z_1) + s_2\psi_0(Z_2)\}
\end{aligned}$$

where

$$\phi_0(Z_1) = -ip\,/\{4(s_1-s_2)(a+is_1b)\}\{1-Z_1(Z_1^2-a^2-b^2s_1^2)^{-0.5}\}$$

$$=b(s_2\sin2\alpha+2\cos^2\alpha)+ia(2s_2\sin^2\alpha+\sin2\alpha)$$

$$\psi_0(Z_1) = ip\,/\{4(s_1-s_2)(a+is_2b)\}\{1-Z_2(Z_2^2-a^2-b^2s_2^2)^{-0.5}\}$$

$$=b(s_1\sin2\alpha+2\cos^2\alpha)+ia(2s_1\sin^2\alpha+\sin2\alpha)$$

$$Z_1 = x + s_1y \qquad Z_2 = x + s_2y$$

Here, a and b are the major and the minor axes of ellipse. In the following calculations, b is set equal to a since we are dealing with a circular hole. Also, α, the angle between the x-axis and the direction of the principal uniaxial stress p uniformly distributed at a large distance from the hole, is zero. The complex numbers s_1 and s_2 are roots of the characteristic equation

$$b_{11}s^4-2b_{16}s^3+(2b_{12}+b_{66})s^2+b_{22} = 0$$

$$s_1=\alpha_1+i\beta_1 \quad s_2=\alpha_2+i\beta_2 \quad s_3=\alpha_1-i\beta_1 \quad s_4=\alpha_2-i\beta_2$$

The coefficients (compliances) of the characteristic equation are calculated by the subroutine 'FLEX' (Appendix B) and the complex roots are obtained by the IMSL (International Mathematics and Statistics Library) routine 'ZCPOLY'.
For the simpler case of quasi-isotropic laminates, the isotropic solution is given by Timoshenko [19], for example :

$$\begin{aligned}
\sigma_{RR} &= \frac{1}{2} S\{(1-a^2)+(1+3a^4-4a^2)\cos(\theta)\} \\
\sigma_{\theta\theta} &= \frac{1}{2} S\{(1+a^2)+(1+3a^4)\cos(\theta)\} \qquad (3.2) \\
\tau_{R\theta} &= -\frac{1}{2} S\{(1-3a^4+2a^2)\sin(\theta)\}
\end{aligned}$$

Timoshenko also states that the error that arises by estimating the stress distribution of a plate with finite width by taking a solution for an indefinite plate is less than 6 percent, if the width of the considered plate is at least four times larger than the diameter of the hole. The plane-stress solution is calculated by the subroutine 'PLANE' (Appendix B).

The next step of finding the lamina stresses is to calculate the laminate strains due to the average-stress distribution, where at first constant strains through the thickness are assumed.

$$\{\varepsilon\} = [b]\,\{\sigma\} \tag{3.3}$$

where [b] is the reduced compliance matrix of the laminate.

The stress distribution in the k^{th} is found by multiplying these strains by the lamina-stiffness matrices $[Q]^k$, respectively.

$$\{\sigma\}^k = [Q]^k\,\{\varepsilon\}^k \tag{3.4}$$

This is carried out by the subroutine 'LAMINA' (Appendix B).

However; although the overall laminate stresses σ_{RR} and $\sigma_{R\theta}$ satisfy the boundary conditions, the individual lamina stresses in general do not. This is called a state of self-equilibrated stresses. The deviation of the individual layer stresses from a state of stress that satisfies the boundary conditions is large only in the space (a thin layer) adjacent to the edge, called boundary layer.

The three dimensional stresses to be superposed with the imperfect plane-stress solution so that boundary conditions and continuity conditions are satisfied are referred to as boundary-layer stresses.

The boundary-layer stresses are functions of the dimensionless coordinates (see Figure 6)

$$\rho = \frac{z}{h} \quad , \quad -h < z < h$$

$$\eta = \frac{r-a}{h} \quad , \quad a: \text{hole radius} \qquad (3.5)$$

$$\theta = \theta$$

After substituting these boundary-layer coordinates, the equations of motion in cylindrical coordinates without body forces take the form :

$$\begin{aligned}
&\tau_{RZ',\rho} + \delta\{\sigma_{R',\eta} + \frac{1}{1+\eta}(\tau_{R\theta',\theta}+\sigma_R-\sigma_\theta)\} = 0 \\
&\tau_{Z\theta',\rho} + \delta\{\tau_{R\theta',\eta} + \frac{1}{1+\eta}(\sigma_{\theta\theta',\theta}+\tau_{R\theta}) \} = 0 \qquad (3.6) \\
&\sigma_{ZZ',\rho} + \delta\{\tau_{RZ',\eta} + \frac{1}{1+\eta}(\tau_{Z\theta',\theta}+\tau_{RZ}) \} = 0
\end{aligned}$$

where $$\delta = \frac{1}{(\eta+a/h)}$$

These equilibrium equations can be expanded into a power series of ε in terms of boundary-layer stress coefficients f^n.

$$\begin{aligned}
&\Sigma\{(f^n_{RZ',\rho}+f^n_{RR',\eta})(1+\varepsilon\eta)+\varepsilon(f^n_{R\theta',\theta}+f^n_{RR}-f^n_{\theta\theta}) \} = 0 \\
&\Sigma\{(f^n_{Z\theta',\rho}+f^n_{R\theta',\eta})(1+\varepsilon\eta)+\varepsilon(f^n_{\theta\theta',\theta}+f^n_{R\theta})\} = 0 \qquad (3.7) \\
&\Sigma\{(f^n_{ZZ',\rho}+f^n_{RZ',\eta})(1+\varepsilon\eta)+\varepsilon(f^n_{Z\theta',\theta}+f^n_{RZ})\} = 0
\end{aligned}$$

where $$f_{ij} = \Sigma f^n_{ij}\varepsilon^n \qquad (3.8)$$

The contributions of each power of ε must fulfill the equilibrium equations individually :

$$
\begin{aligned}
f^{n}_{ZR',\rho} + f^{n}_{RR',\eta} + \eta\left(f^{n-1}_{ZR,\rho} f^{n-1}_{RR,\eta}\right) + f^{n-1}_{R\theta,\theta} + f^{n-1}_{RR} - f^{n-1}_{\theta\theta} &= 0 \\
f^{n}_{ZZ',\rho} + f^{n}_{ZR',\eta} + \eta\left(f^{n-1}_{ZZ,\rho} f^{n-1}_{ZR,\eta}\right) + f^{n-1}_{Z\theta,\theta} + f^{n-1}_{ZR} &= 0 \qquad (3.9) \\
f^{n-1}_{Z\theta,\rho} + f^{n}_{R\theta',\eta} + \eta\left(f^{n-1}_{Z\theta,\eta}\right) + f^{n-1}_{\theta\theta,\theta} + 2 f^{n-1}_{R\theta} &= 0
\end{aligned}
$$

Finally, by dropping terms of less than zero order and setting n=0, the equilibrium equations reduce to :

$$
\begin{aligned}
f^{0}_{ZR',\rho} + f^{0}_{RR',\eta} &= 0 \\
f^{0}_{ZZ',\rho} + f^{0}_{ZR',\eta} &= 0 \qquad (3.10) \\
f^{0}_{Z\theta',\rho} + f^{0}_{R\theta',\eta} &= 0
\end{aligned}
$$

Advantageously we recognize that two of these equations represent a plane-strain problem, while the third one is of the form of the torsional problem.

The plain-strain problem associates the stresses f_{RR}, f_{RZ}, and f_{ZZ} with the stress function phi :

$$\begin{aligned} f^{O}_{RR} &= \phi_{,\rho\rho} \\ f^{O}_{RZ} &= -\phi_{,\rho\eta} \\ f^{O}_{ZZ} &= \phi_{,\eta\eta} \end{aligned} \tag{3.11}$$

The torsion problem involves the stresses $f_{R\theta}$ and $f_{\theta Z}$, compatible by the definition of the stress function psi :

$$\begin{aligned} f^{O}_{R\theta} &= \psi_{,\rho} \\ f^{O}_{\theta Z} &= -\psi_{,\eta} \end{aligned} \tag{3.12}$$

Since the now simplified problem depends on stress functions defined using the assumption of plane strain and; furthermore, the yet remaining stress components are acting only in planes defined by the radial and the vertical coordinate, the boundary-layer strain component $\varepsilon_{\theta\theta}$ is zero. Thus, after determining the other stresses, $\sigma_{\theta\theta}$ can be calculated (subroutine 'BOULAY', Appendix B).

by using the constitutive law :

$$f^{O}_{\theta\theta} = - \frac{1}{S_{22}} (S_{12} f^{O}_{R} + S_{23} f^{O}_{Z} + S_{26} f^{O}_{R\theta}) \qquad (3.13)$$

The elimination of $\varepsilon_{\theta\theta}$ and $\sigma_{\theta\theta}$ leads to a reduction of the compatibility matrix (subroutine 'FLEX', Appendix B) for the boundary-layer problem, using the algorithm :

$$A_{ij} = S_{ij} - \frac{S_{i2}\ S_{2j}}{S22} \qquad (3.14)$$

At the cylindrical surface of the hole the superimposed stress components must result in zero values :

$$\begin{aligned} f^{O}_{R\theta} + \sigma_{R\theta} &= 0 \\ f^{O}_{RR} + \sigma_{RR} &= 0 \\ f^{O}_{RZ} &= 0 \end{aligned} \qquad (3.15)$$

For the upper and lower free surface of the laminate all interlaminar stresses must be zero :

$$\begin{aligned} f^{0}_{\theta Z} &= 0 \\ f^{0}_{RZ} &= 0 \\ f^{0}_{ZZ} &= 0 \end{aligned} \qquad (3.16)$$

Far away from the edge the boundary effects must vanish, which is expressed by :

$$f^{0} \rightarrow 0 \quad \text{for} \quad \eta \rightarrow \infty \qquad (3.17)$$

The stress functions are defined as

$$\phi = a_{(\eta)} b_{(\rho)} \,, \qquad \psi = c_{(\eta)} d_{(\rho)} \qquad (3.18)$$

where the functions $b_{(\rho)}$ and $d_{(\rho)}$ are being determined by integration of the boundary conditions (subroutine 'FUNETA', Appendix B).

$$d_{(\rho)} = -\frac{1}{c(0)} \int_{-1}^{1} \sigma_{R\theta(0,\theta,\rho)} d\rho'$$

$$b_{(\rho)} = -\frac{1}{a(0)} \int_{-1}^{1} \left(\int \sigma_{RR(0,\theta,\rho)} d\rho'' \right) d\rho \qquad (3.19)$$

It follows that the two matching conditions in Eq. (3.15) can be satisfied by setting :

$$a_{(0)} = 1 \quad \text{and} \quad c_{(0)} = 1 \qquad (3.20)$$

while the simple boundary condition in Eq. (3.15) holds if

$$a_{,\eta} = 0 \qquad \text{for } \eta = 0 \qquad (3.21)$$

Clearly, for a symmetric laminate the values of $d_{(\rho)}$, $b_{(\rho)}$, and $b'_{(\rho)}$ are equal to zero at the flat surfaces of the laminate, so that the boundary conditions Eq. (3.16) are also satisfied.

The interlaminar stresses $f_{\theta Z}$, f_{ZZ} and f_{RZ} are functions of $d_{(\rho)}$, $b_{(\rho)}$, and $b'_{(\rho)}$ that are continuous through the thickness of the laminate, thus ensuring the continuity of all interlaminar stresses.

The functions $a_{(\eta)}$ and $c_{(\eta)}$ are to be determined by the compatibility equations in cylindrical coordinates. However; the chosen stress functions can not satisfy these equations exactly. So compatibility is achieved only in an approximate sense by minimizing the integral of the complementary energy through the thickness.

This calculus is carried out in Appendix A and the resulting eigenvalue problem is given by :

$$[M]\{\dddot{X}\} + [N]\{\ddot{X}\} + [P]\{X\} = 0 \qquad (3.22)$$

where the matrix elements M_{ij}, N_{ij}, and P_{ij} are defined as :

$$\begin{aligned}
M_{11} &= \int_{-1}^{1} A_{33} b^2 d\rho \\
N_{11} &= \int_{-1}^{1} (2A_{13} bb'' - A_{55} b'^2) d\rho \\
N_{12} &= \int_{-1}^{1} (A_{36} d'b - A_{45} b'd) d\rho \\
N_{22} &= -\int_{-1}^{1} A_{44} d^2 d\rho \qquad (3.23) \\
P_{11} &= \int_{-1}^{1} A_{11} b''^2 d\rho \\
P_{12} &= \int_{-1}^{1} A_{16} b'' d' d\rho \\
P_{22} &= \int_{-1}^{1} A_{66} d'^2 d\rho
\end{aligned}$$

All the integrands involved are only piecewise continuous functions or functions with piecewise continuous derivatives. The contributions of each layer have to be summed while the integration over an individual layer can be carried out using Gaussian Quadratures, where the exact integration of M_{11} requires the five-point formula, and that of the N-Matrix elements requires the three-point formula. The integrands of the P-matrix are piecewise constants.

Because the functions $b_{(\rho)}$, $b'_{(\rho)}$ and $d_{(\rho)}$ are defined as being integrals by themselves, they must be calculated and inserted into the integrands mentioned above simultaneously. These calculations are carried out by the subroutine 'NUMINT' (Appendix B).

The characteristic equation of the eigenvalue problem is written as

$$\det(\lambda^4 M + \lambda^2 N + P) = 0 \qquad (3.24)$$

and leads after substituting μ for λ^2 to the cubic equation in μ :

$$q_0\mu^3 + q_1\mu^2 + q_2\mu + q_3 = 0 \qquad (3.25)$$

The solution for the eigenvalue problem is of the type :

$$\{X\}_{(\eta)} = \Sigma\ \alpha_i \{X\}_i e^{-\lambda_i \eta} = \begin{Bmatrix} a \\ c \end{Bmatrix} \tag{3.26}$$

$\{X\}_1$, $\{X\}_2$, and $\{X\}_3$ are the eigenvectors associated with the eigenvalues λ_1, λ_2, and λ_3.
The constants α_1, α_2, and α_3 are determined by satisfying the before mentioned conditions (3.20) and (3.21), which lead to the system of equations :

$$\begin{aligned} a_{(0)} &= -\lambda_1\alpha_1 a_1 - \lambda_2\alpha_2 a_2 - \lambda_3\alpha_3 a_3 = 0 \\ a_{(0)} &= \alpha_1 a_1 + \alpha_2 a_2 + \alpha_3 a_3 = 1 \\ c_{(0)} &= \alpha_1 c_1 + \alpha_2 c_2 + \alpha_3 c_3 = 1 \end{aligned} \tag{3.27}$$

The complex eigenvalues λ_i are obtained by the routine 'KUPO' which is called within the subroutine 'FUNETA' (Appendix B). This subroutine finds also the complex eigenvectors $\{X\}_i$ and solves for the constants α_i. The boundary layer stresses are then calculated directly as functions of the actual coordinate η, as is carried out in the subroutine

'BOULAY' (Appendix B). Opposing Engrand's statement [7] the presently obtained eigenvalues are usually complex. It is not excluded that the mistake in Engrand's paper [7] concerning the matrix element M_{11} (defined as $M_{11} = \int A_{22} b_{(\rho)} d\rho$ in [7]) is also contained in his calculations. After implementing the wrong definition of this matrix element into the program of the present study, real eigenvectors were found and, under consideration of a stress concentration factor of three at the location θ = 90 deg, Engrand's results for the quasi-isotropic laminate were reproduced.

3.2 STRESS DISTRIBUTIONS

The stresses represented in the figures in this subsection are related to a uniform-stress field at a large distance from the hole with σ_x being a unit value, σ_y and σ_{xy} being zero. Therefore, the presented stresses can be referred to also as stress concentrations.

The stress curves are represented along the hole edge from zero deg to 180 deg. The magnitude of stresses is obtained by measuring the distance of a point on the stress curve from the circle in inches and multiplying this value by the given scale per inch. To better distinguish the circle from a stress curve close to it, the circle is plotted using a slightly thinner pen. Intralaminar stresses are

shown in the middle of layers, and interlaminar stresses are shown on the interfaces between layers, respectively. The 'Z' coordinate is expressed in the figures in units of the layer thickness H. The in-plane stresses are plotted in lamina (also natural or material) coordinates which provides a better understanding of stress situations likely to cause matrix cracks. Identification of stresses in these plots is possible by recalling the boundary conditions. For instance, a zero deg layer has a σ_{11} distribution with zero values at θ = 0 and θ = 180 deg and a σ_{22} distribution with a zero value at θ = 90 deg. The shear stress in this example has zero values at all three of these locations. The interlaminar stresses are plotted in cylindrical coordinates in order to simplify the figures, since the stress component σ_{RZ} is zero at the boundary. The identification of these stresses is aided by additional plots showing their through-the-thickness distributions. The normal stress component is a piecewise quadratic function and the shear stress component is a piecewise linear function through the thickness.

3.2.1 In-Plane Stresses in the A-Laminate

Figure 7 shows the in-plane stresses in the A-laminate. Note the high stress concentration in the fiber direction for the zero-deg layer at locations θ = 90 deg. The first visible damage observed in X-ray photos consists of matrix cracks. High stresses σ_{22} and σ_{12} indicate the likelyhood of matrix breakage. It may be confusing that the plots have different scale factors. For instance, the maximum value of the shear stress for Z = 3.5H is actually about 50 percent higher than for Z = 0.5H. It is also important to note that σ_{22} in the 90-deg layer and σ_{12} in the zero-deg layer have actually higher maximums there than in the other layers.

3.2.2 Interlaminar Stresses in the A-Laminate

Figure 8 shows the distribution of σ_{ZZ} and $\sigma_{\theta Z}$ within the A-laminate. The symmetry of the geometry and the loading situation leads to zero values of the interlaminar shear stresses in the midplane (Z=0) and the tensile concentrations of the normal stress are less than 0.5. Combinations of tensile normal stress and high shear stress occur between the +45-deg and the 90-deg layer, Z=2H. We may note that the values of $\sigma_{\theta Z}$ are higher between 90 deg and 180 deg than between zero deg and 90 deg angle orientation. The same holds for the 90-deg/zero-deg interface (Z=H), although the

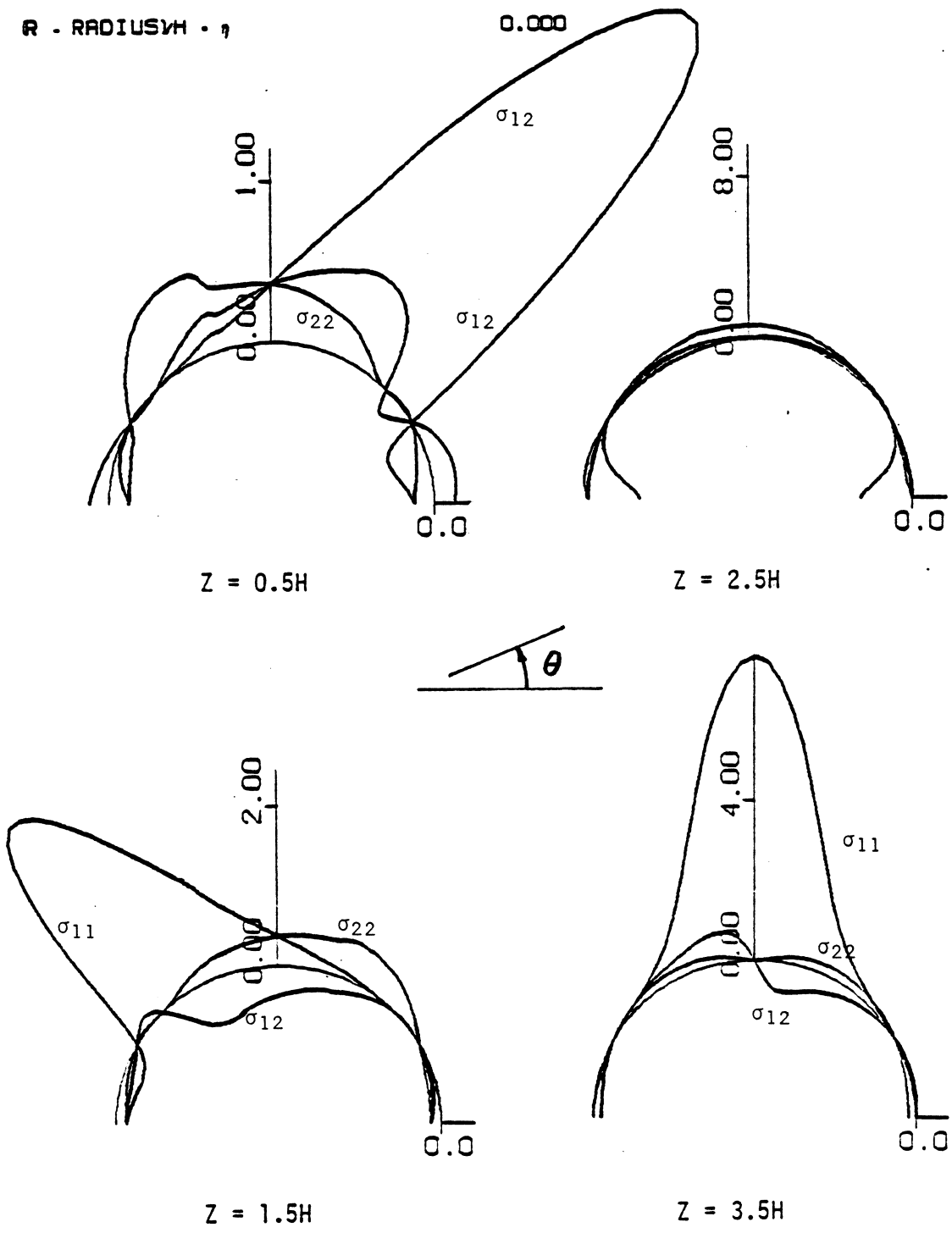

Figure 7: In-Plane Stresses in the A-Laminate

stresses are generally less at this interface than at the +45-deg/90-deg interface, Z=2H.

Figure 9 represents the variation of the interlaminar stresses through the thickness from the midplane to the surface at θ = 90 deg. Note the precise satisfaction of the boundary conditions at the surface.

3.2.3 In-Plane Stresses in the B-Laminate

We note in Figure 10 that the stresses in layers of same directions in the A- and in the B-laminate are quite similar but not exactly equal. Maximum stress concentrations are slightly higher for the B-Laminate than for the A-Laminate, but the differences are too small to explain the differences in the initial strengths of A- and B-specimens, respectively.

3.2.4 Interlaminar stresses in the B-Laminate

Figure 11 shows the distribution of σ_{ZZ} and $\sigma_{\theta Z}$ at the hole on the different interfaces. In contrast to the remark concerning the similarity of the in-plane stresses in the A- and the B-laminates, we observe a completely different distribution of the interlaminar stresses in the two laminates. A high shear concentration occurs between the zero-deg and the -45-deg layer (Z=H) at a angle of about θ = 70 deg and

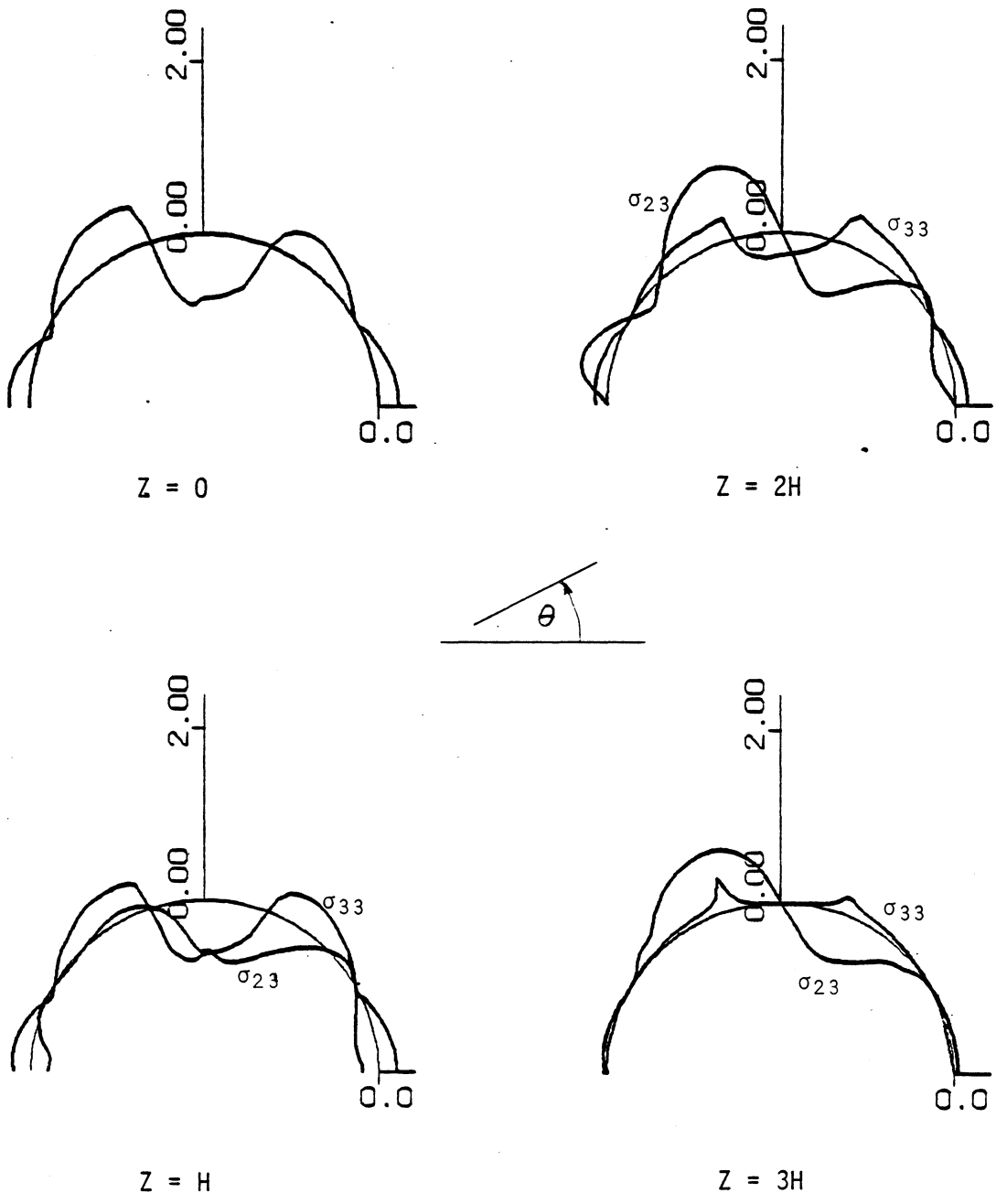

Figure 8: Interlaminar Stresses in the A-Laminate

MATERIAL GRAPHITE EPOXY	
STACKING SEQUENCE	[0 , 90, 45, -45]$_s$
HOLE DIAMETER	0.375 INCHES
LAMINATE THICKNESS	0.044 INCHES
ANGLE THETA	90.000
R - RADIUS/H - η	0.000

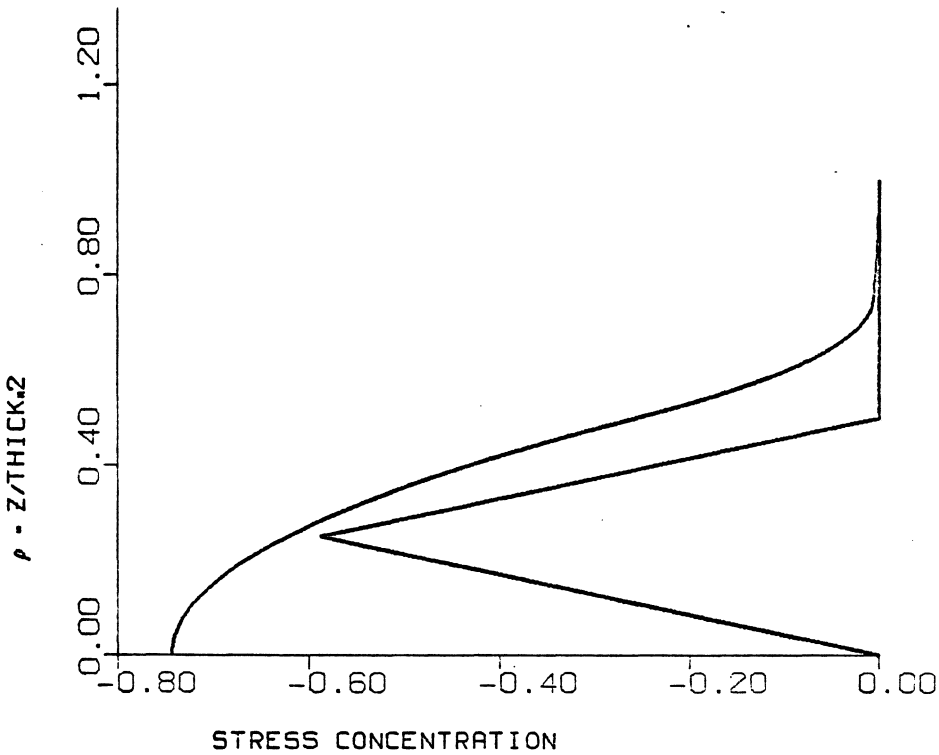

σ_{zs} σ_{zs}

IN CYLINDRICAL COORDINATES

Figure 9: Interlaminar Stresses Through the Thickness in the A-Laminate

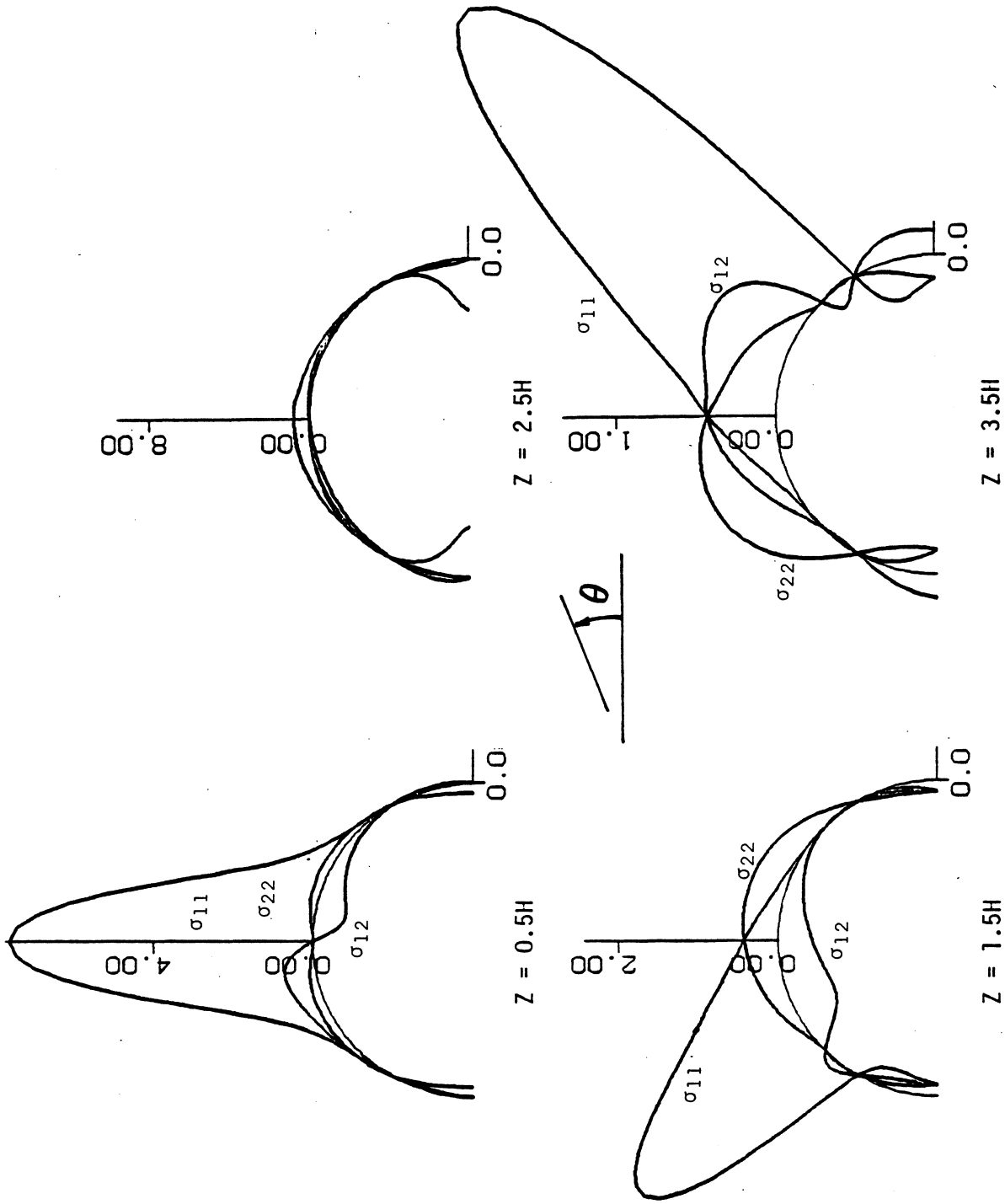

Figure 10: In-Plane Stresses in the B-Laminate

is accompagnied by compressive normal stress. Combinations of both tensile normal and and high shear stresses are found on the interfaces between the -45-deg and the 90-deg layers (Z=2) and between the 90-deg and the 45-deg layers (Z=3) at similar locations.

Figure 12 shows the distribution of the interlaminar stresses through the thickness in the same manner as in Figure 9.

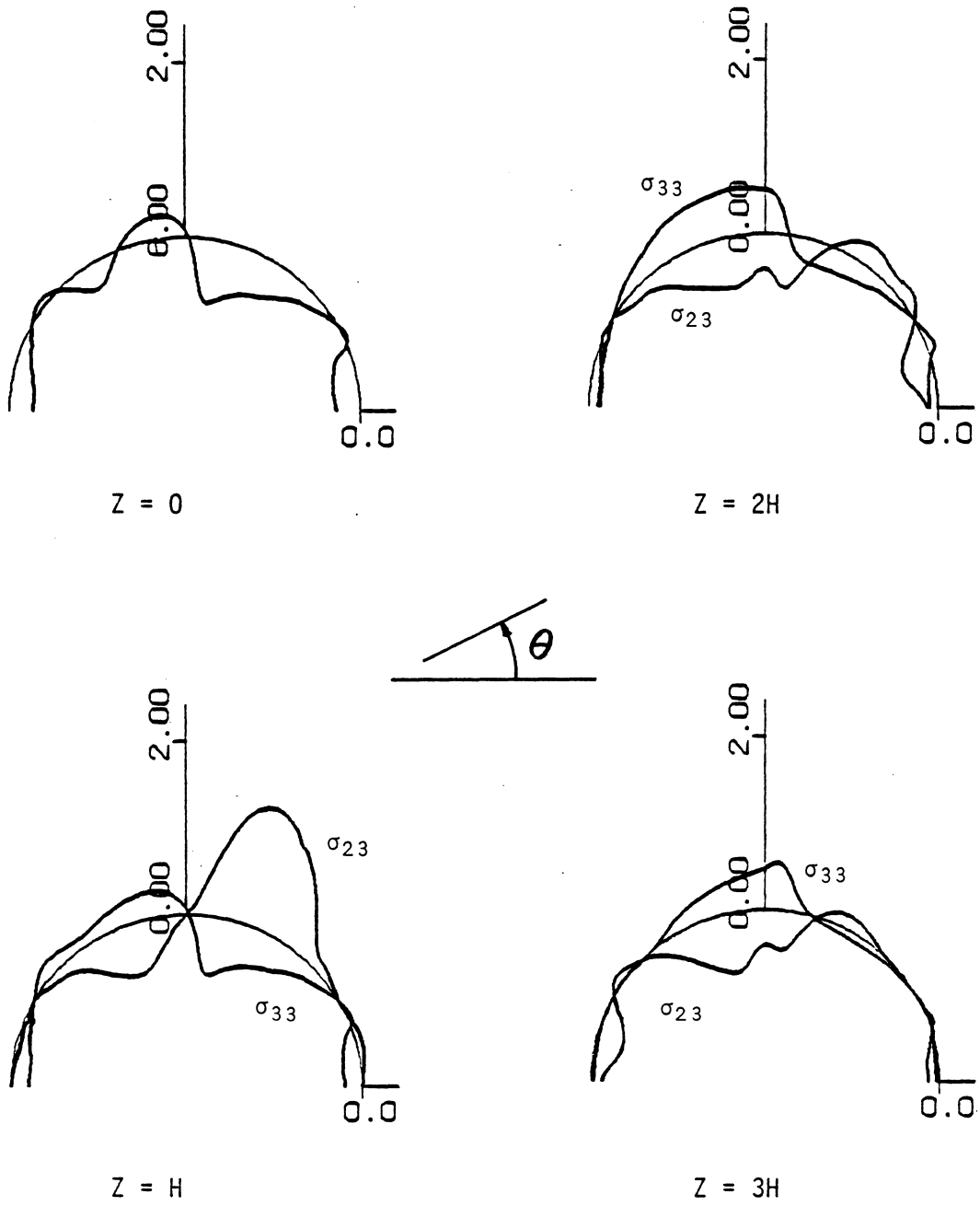

Figure 11: Interlaminar Stresses in the B-Laminate

MATERIAL GRAPHITE EPOXY	
STACKING SEQUENCE	[45, 90, -45, 0]$_s$
HOLE DIAMETER	0.375 INCHES
LAMINATE THICKNESS	0.044 INCHES
ANGLE THETA	90.000
R - RADIUS/H - η	0.000

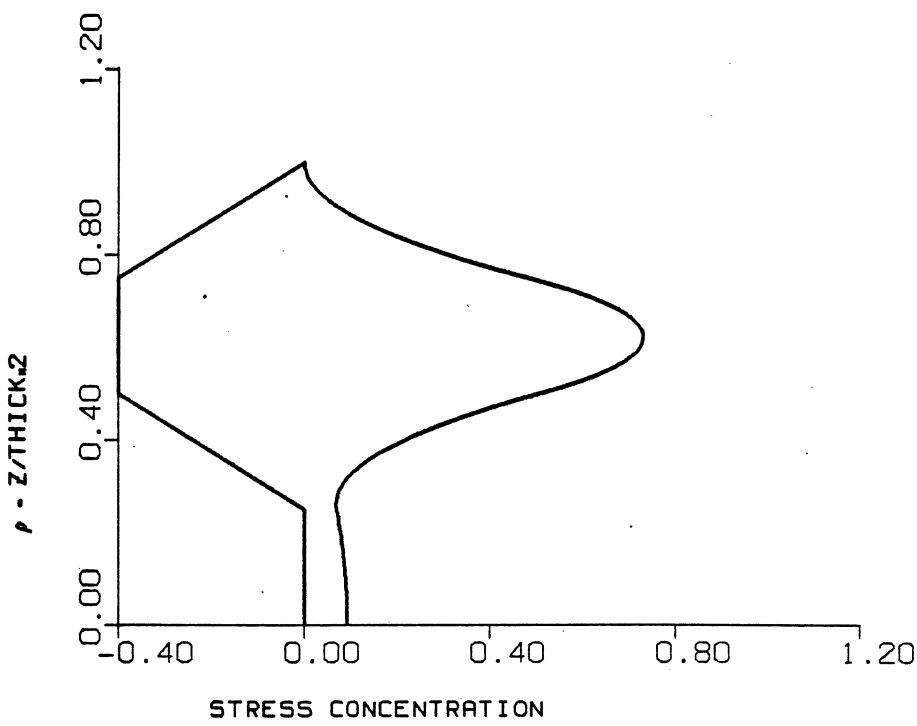

σ_{zz} σ_{rz}

IN CYLINDRICAL COORDINATES

Figure 12: Interlaminar Stresses Through the Thickness in the B-Laminate

Chapter IV

DISCUSSION OF TEST DATA

4.1 X-RAY PHOTOGRAPHY

During the following discussion cracks that are initiated at the hole boundary or the straight edge will be called primary cracks. Other, usually smaller cracks, which initiate along the primary cracks are located in adjacent plies and will be called secondary cracks.

4.1.1 A-Specimens

4.1.1.1 Quasi-Static Damage Patterns

The radiographs of sequential-loading tests with repeated and increasing load applications give some evidence about the onset of damage.

The first visible cracks for the specimen A-22 appear at 60 percent of the average initial strength for A-laminates, Figure 13a. They are zero-deg cracks on both sides of the hole, having equal extensions in both directions, and 90-deg cracks also on both sides of the hole but of smaller length than the zero-deg cracks and extending along the 90-deg direction less than one fifth of the hole hole diameter. This very early pattern of damage in zero-deg and 90-deg plies is completed by matrix cracks in the 45-deg plies.

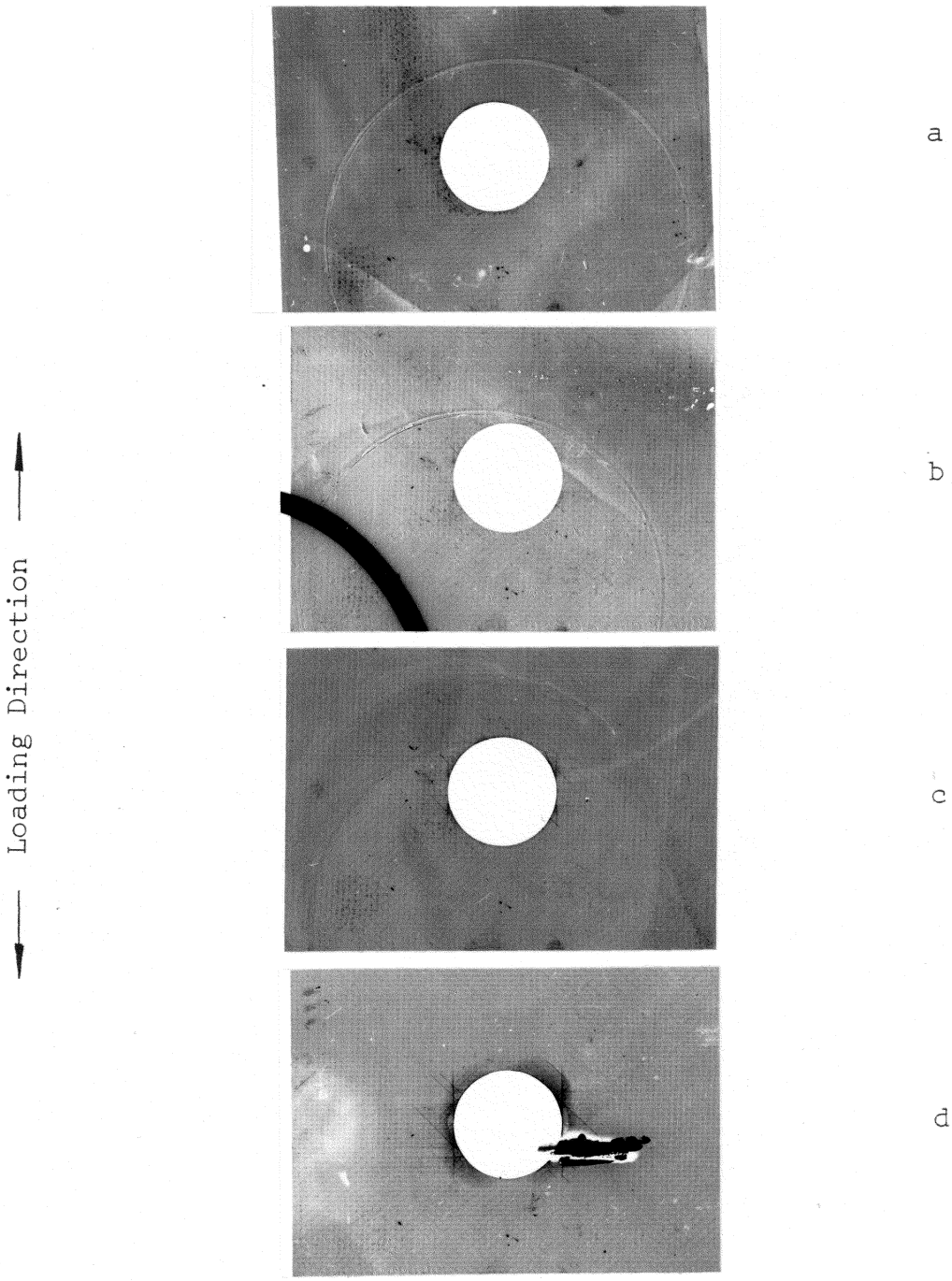

Figure 13: Quasi-Static Damage in an A-Specimen

The 70 percent radiograph of the same specimen shows very well defined +45-deg cracks along a line passing through the center of the hole. The cracks tangent to the hole are much smaller. Very small secondary -45-deg cracks develop along the other cracks, Figure 13b.

In the radiographs following the 80 percent and 90 percent steps the tangent zero-deg cracks appear darker but do not increase in length very much. The number and then the length of the 90-deg cracks, still confined to the area governed by the zero-deg cracks, increase considerably. The plus 45-deg cracks tangent to the hole grow rapidly into the area which is already occupied by the 90-deg cracks. Although the clarity of the radiographs does not allow a very distinct judgement, it seems that delaminations on the edges of the hole, start as early as on the 80 percent load level, initiating in the corners made up by the tangent 45-deg cracks and 90-deg cracks, Figure 13c.

On the 90 percent load level, delamination also starts on the corners between the zero-deg cracks and the other major plus 45-deg cracks.

The highest load levels are characterized by a greater number and increased length of minus 45-deg cracks and by a butterfly pattern of delamination around the hole. The observations let suggest that the onset of delamination is at

least assisted, if not caused by, the existing matrix crack pattern, Figure 13d.

4.1.1.2 Fatigue Damage Patterns

The damage patterns discussed in this section belong to different specimens which were subjected to different numbers of cycles on the 80-percent-load level for A-specimens to prepare them for strength tests. The X-radiograph of A-14, Figure 14a, shows damage after 10 cycles at the 80 percent load that is very similar to that shown in Figure 13c. A lower concentration with zinc iodide is the probable cause for the 90 deg cracks not showing up as clearly in this figure. The matrix crack pattern after 1K cycles shown in Figure 14b is shows an increase in length for all cracks. Additionally, the cycled specimen developed delaminations at the hole edge at θ=-45 deg and θ=315 deg, if the positive x-direction is defined as the zero-deg direction. After 10K cycles these delaminations are more developed and new delaminations at -135/45-deg locations are initiated. The zero-deg-tangent cracks now extend beyond the area of the hole while cracks in the other plies are also longer. The damage in specimen A-4 with 10K cycles fatigue loading, Figure 14c, contradicts a generalization of the delamination development as was shown in the previous photographs. Name-

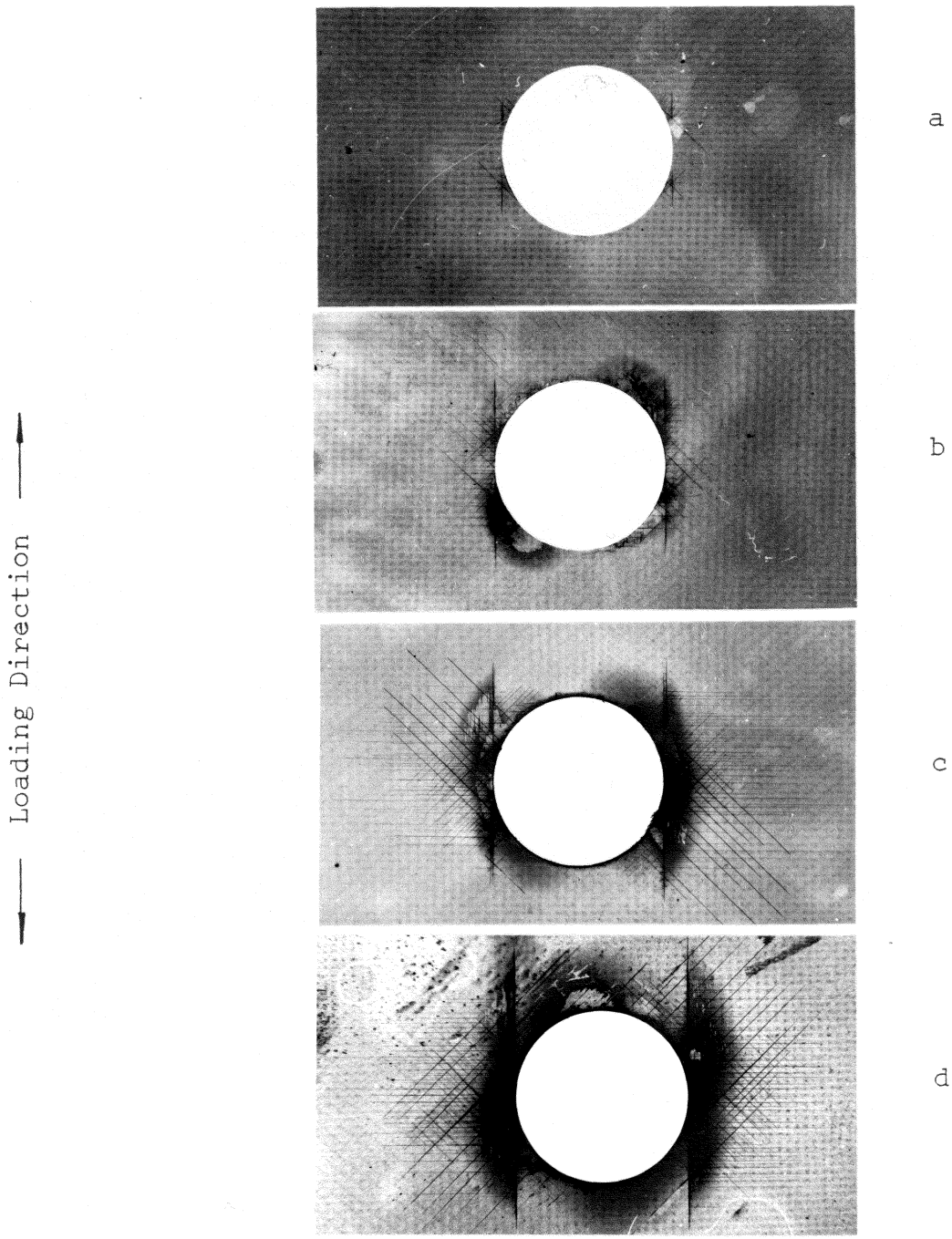

Figure 14: Fatigue Damage an in A-Specimen

ly, the delaminations on the -45/135-deg locations are less developed than in A-4. The delaminations are now following the path of the tangent cracks which are 40 percent longer than the hole diameter. Cracks in 45-deg direction are longer than those in -45-deg direction. A large number of 90-deg cracks have developed, many of them initiated at the tangent zero-deg cracks, and some approach the straight edge.

The damage state after 100K cycles in A-39 is shown in Figure 14d. The zero-deg cracks have an extension of 190 percent of the hole diameter and are still accompanied by delaminations, mostly on the side facing the straight edge. Delaminations developed also along the hole edge between the tangent cracks.

Figure 15a and b show the highly developed damage state after 600K cycles in specimen A-39. The two prints are made from the same negative but received different exposure times in order to enhance the delamination details (short exposure) or to enhance the matrix crack pattern (long exposure). Other specimens, cycled on the 80-percent-load level, survived 900K to 1300K cycles.

The damage zone includes large delaminations of an obviously complex distribution and the tangent zero-deg-matrix cracks still passing through it, matching its extension. New

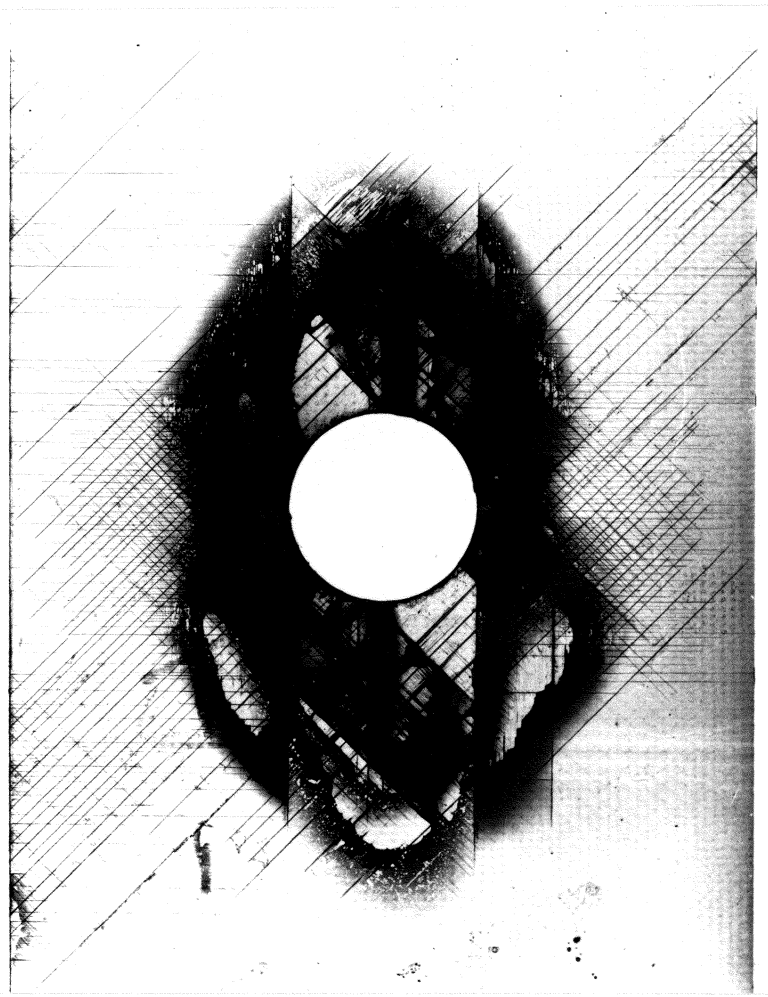

Figure 15: A-39 after 600K cycles at 80 percent load level

zero-deg cracks of a large size have formed in the middle between the tangent cracks, and one is seen between the hole and the straight edge. We also note that some areas that appeared dark in the X-ray of the same specimen, taken after 100K cycles are now light like the surrounding undamaged zones. The +45-deg and the 90-deg cracks extend from the edge of the hole to the straight edges. Some matrix cracks and a delamination are initiated on the straight edge.

It is mentioned here that this specimen at this stage of fatigue loading had a residual strength of 122 percent of the averaged values for new specimens, and the 1-inch extensometer measured a stiffness of approximately 65 percent of the averaged values for new specimens.

4.1.2 B-Specimens

4.1.2.1 Quasi-Static Damage Pattern

The radiographs taken during the quasi-static test on specimen B-16 show the first matrix cracks in the +45-deg plies on lines which pass through or near the center of the hole at the 50 percent load level, Figure 16a.

The next picture, Fig. 16b, taken after application of a 60 percent load, already shows cracks in all plies. While the previous cracks grew only a small amount, new cracks in plus 45-deg direction are added. These are following lines that

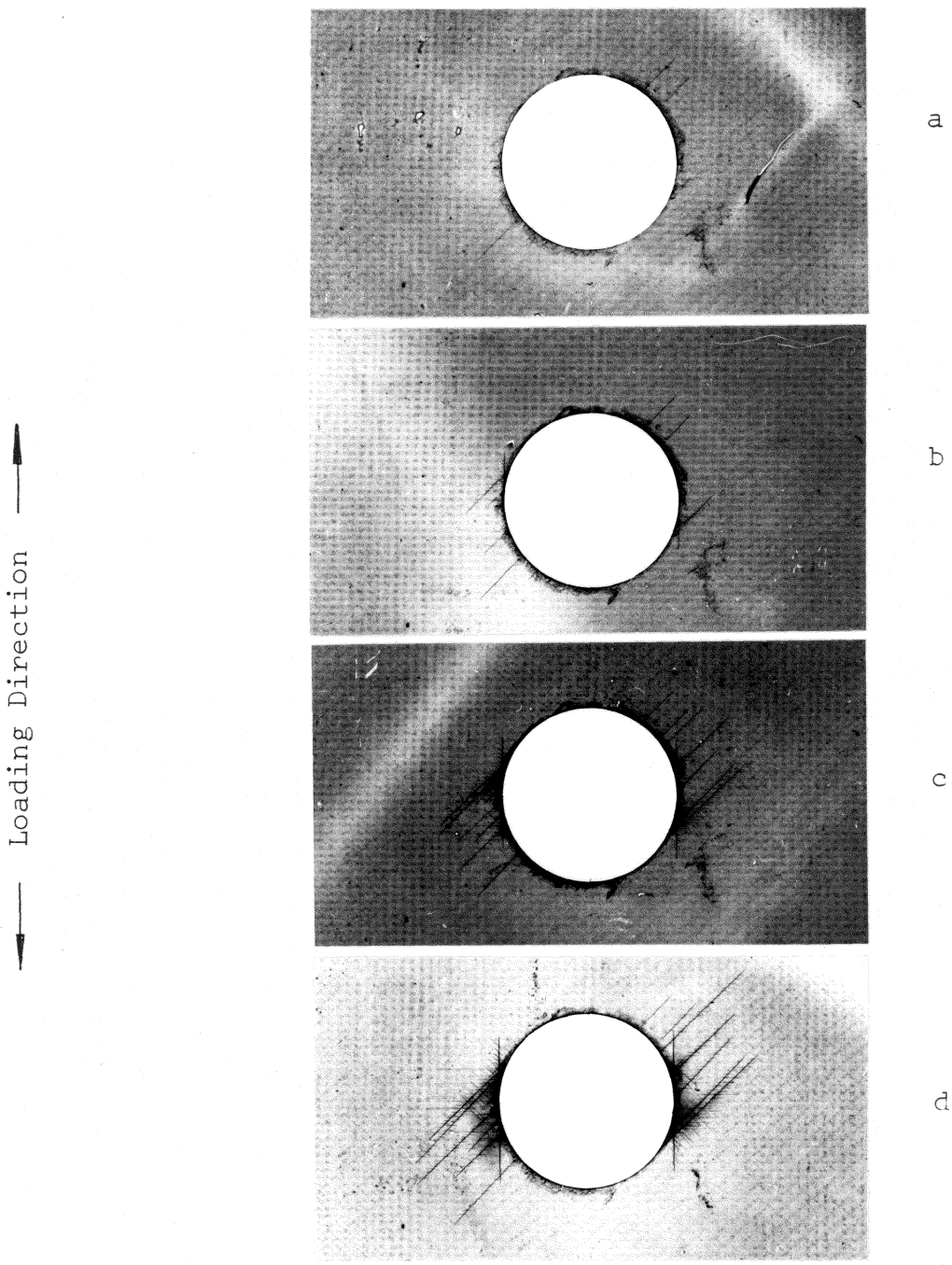

Figure 16: Quasi-Static Damage in B-Specimen

pass through the hole but closer to the periphere than to the center, and extend away from the boundary of the hole. The new cracks in the plus 45-deg direction have the same size as the initial ones. Cracks in the zero-deg plies initiate tangent to the hole and extend into the region containing cracks in the +45-deg plies. Along the new +45-deg cracks, equidistantly distributed, small 90-deg cracks appear, while the tangent zero-deg cracks are accompanied by similar cracks in the minus 45-deg direction. The spacing of the cracks in the -45-deg plies is less than that of cracks in the 90-deg plies.

The 80 percent load level radiograph, Fig. 16c, shows some additional +45-deg cracks located in the area between the very first cracks and those which followed. The zero-deg cracks also extend in the other direction; and shadowed areas, stronger in the corner between the zero-deg and the plus 45-deg cracks, indicate the onset of delamination.

Loading to 90 and 95 percent causes continued growth of the tangent zero-deg cracks away from the delaminated region and increases the intensity and size of the shadowed area. The number and extent of cracks in the 90- and -45-deg plies also increases. At the same time only one of the straight edges developed +45-deg cracks, Figure 16d.

Until the 110 percent load level is reached, especially all primary +45-deg cracks increase in number and length with the secondary 90-deg cracks associated with them. At a load level of 115 percent of the average tensile strength, the first pair of cracks, one developing from the hole, the other from the straight edge, grow together and form a single, continuous crack, Figure 17a.

Cracks in the 90-deg plies initiate along the edge of the specimen at locations such that,in a plan view, they shape triangles defined by themselves, the free edge and the already present +45-deg cracks in the adjacent ply.

In the radiographs for the 125 percent and the 130 percent loads, Figure 17b, edge initiated damage, consisting of 90- and +45-deg ply cracks can be seen.

The specimen broke while applying a 135 percent load level. Until then, the damage pattern consisted of matrix cracks with a major extent only in the zero-deg and the +45-deg plies and in the 90-deg plies only where +45-deg cracks did not develop. The delaminations extended as far as two tangent zero-deg matrix cracks.

We may suspect an interaction between these zero-deg cracks, the delaminations and the plus 45-deg matrix cracks which were seen on the 60 percent radiograph.

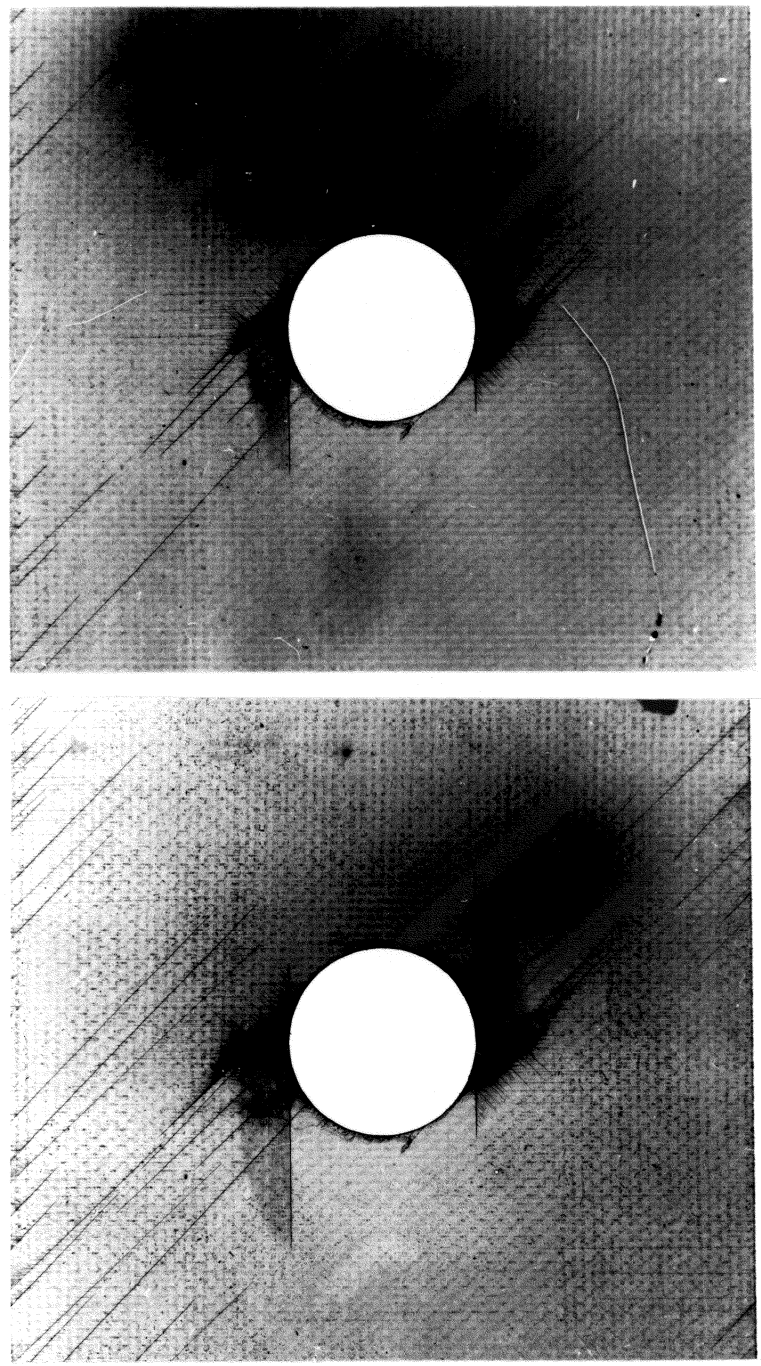

Figure 17: Quasi-Static Damage in a B-Specimen

4.1.2.2 Fatigue Damage Patterns

First, we consider fatigue damage due to a low load level of 70 percent, applied on specimen B-11. Comparing the radiographs of B-11 with that of B-16 after applying the 50 percent load level (Figure 17a), it is noted that the only visible damage in B-16 does not occur in B-11 during its whole life.

The damage states of B-16 after the 70 percent load step and B-11 after 100 cycles (Figure 18a) on that load level are similar. While the major or primary cracks in zero-deg and plus 45-deg directions are comparable in number and size, the fatigued specimen developed more and longer secondary cracks than the quasi-statically loaded specimen, and the the delaminations are more distinct. Apparently delamination develops at locations where the major plus 45-deg cracks meet the projection of the tangent zero-deg cracks.

After one thousand cycles, all previous damage modes are increased, but there is no new type of damage (Figure 18b).

The radiograph taken after ten thousand cycles shows the two zero-deg cracks now having the length of the hole diamater and are arranged symmetrically. The tips of the primary plus 45-deg cracks extend as far into the longitudinal direction of the specimen as the zero-deg cracks. The secondary cracks in the minus 45-deg and 90-deg direction now

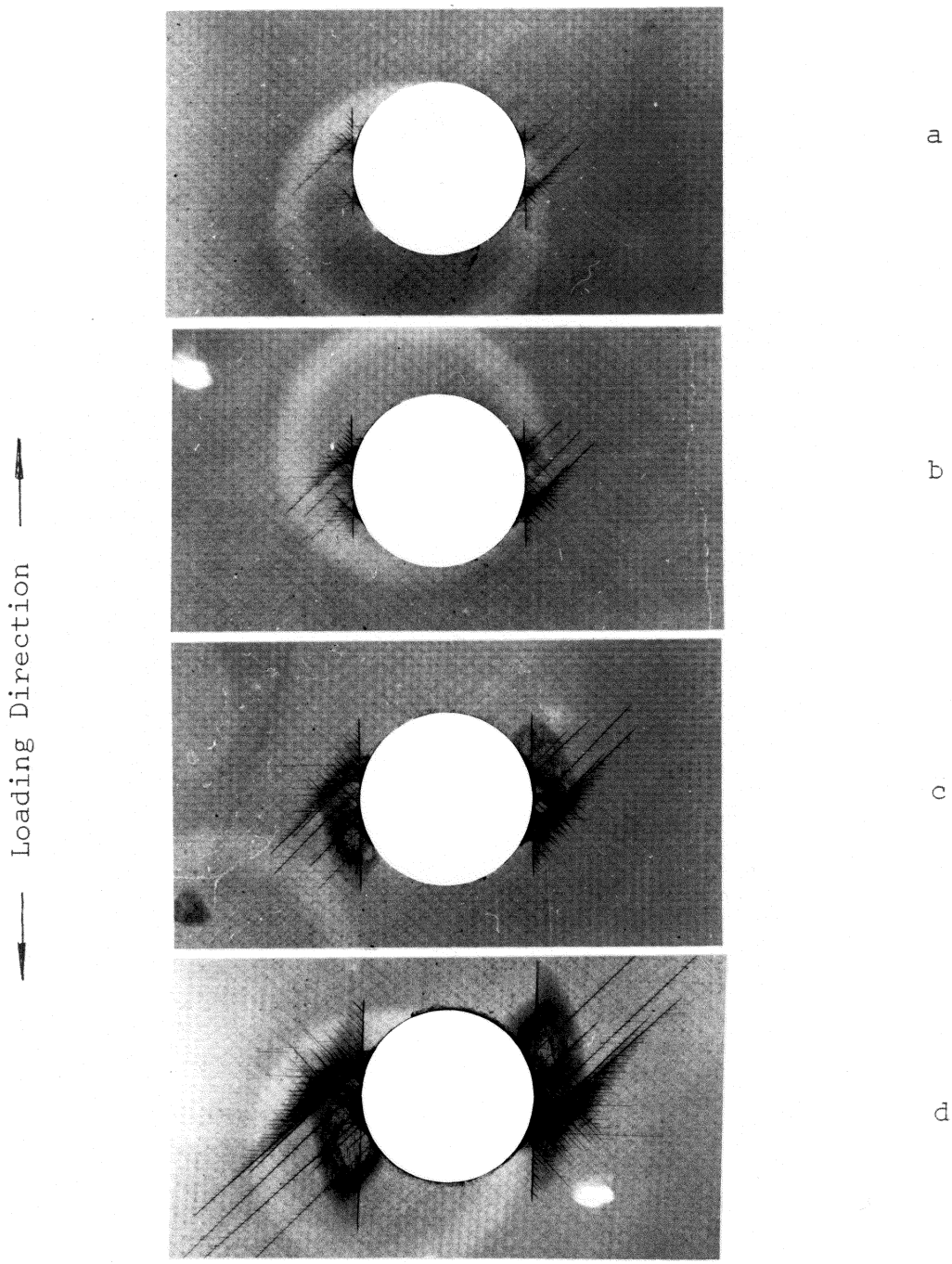

Figure 18: Fatigue Damage at Low Load Level in a B-Specimen

form a dense mesh. The four original delamination areas grew together, extending from the hole edge along the zero-deg cracks and the darkest and longest plus 45-deg cracks. One of the two edges has a damage pattern consisting of plus 45-deg / 90-deg crack combinations, each shaping a little triangle, Figure 18c.

After one hundred thousand cycles the primary plus 45-deg cracks doubled in length while the tangent zero-deg cracks extend into the direction of advancement of the cracks in the 45-deg plies. Delamination now fills the region between the hole edge and the zero-deg cracks and, between these cracks and the straight edges, follows them very precisely. Delamination also extends in the direction of the plus 45-deg cracks which are nearly tangents to the hole edge. At the previously damaged straight edge, the plus 45-deg cracks became longer, as shown in Figure 18d.

The last recorded state of damage at one million cycles shows the primary plus 45-deg cracks connecting the hole and the straight edges, the zero-deg cracks having a length of twice the hole diameter, and associated by delaminations. The delamination also follows the path of the plus 45-deg cracks as described previously, now covering about two thirds of the distance to the straight edge, Figure 19.

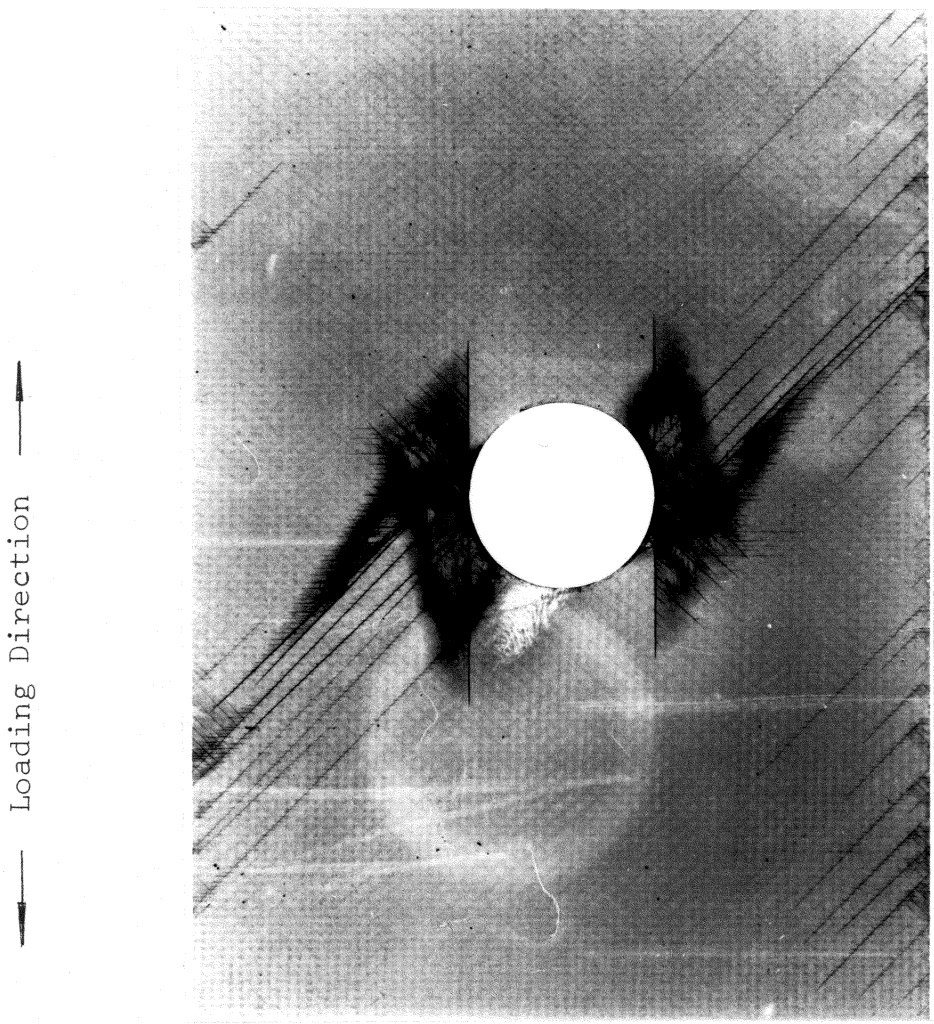

Figure 19: Fatigue Damage after 1 Million Cycles in B-11

The strength test performed on the damaged specimen gave a very high residual strength of 137 percent of the average initial strength of B-specimen, thus indicating that this radiograph shows a very advanced state of matrix damage and delamination while most of the load carrying fibers are still intact.

4.1.3 Fatigue Damage at High Load Level

The state of damage in B-6 cycled ten times at 95 percent of the initial strength value is shown in Figure 20a. The damage state is very similar to that of B-16 after reaching the 95 percent load step. The only remarkable difference is the greater extent of the secondary 90-deg matrix cracks into areas of the cyclically loaded specimen which appear free from other cracks. Some of those cracks nearly reach the straight edge.

After one hundred cycles all cracks grew only a little while the delamination spread out following the pattern indicated previously, as shown in Figure 20b.

The following nine hundred cycles produced an increase in the length of plus 45-deg cracks and an increase of number and length of the secondary 90-deg cracks, which reach the straight edges. Only little damage initiates on these edges, as can be seen in Figure 20c.

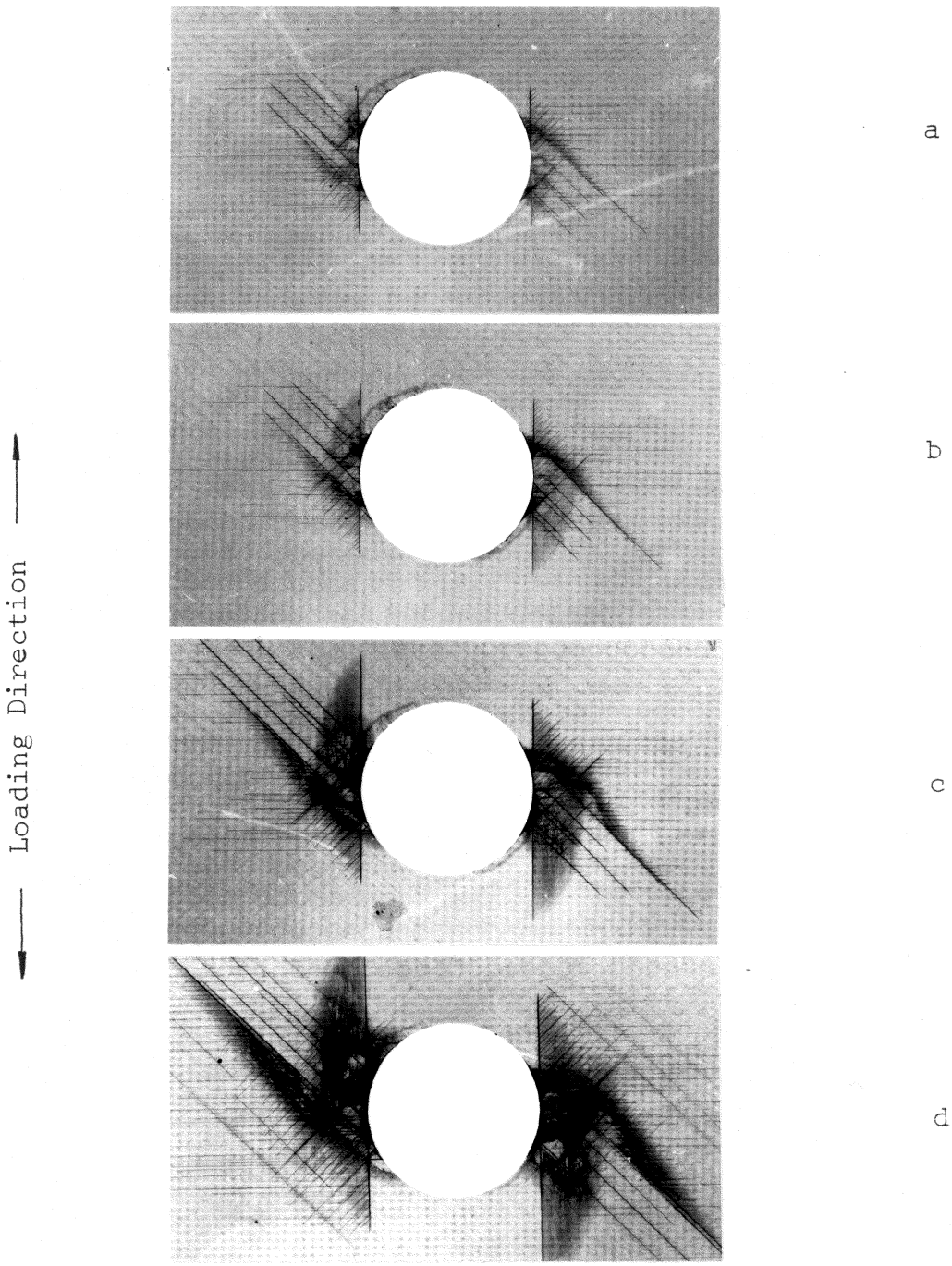

Figure 20: Fatigue Damage at High Load Level in a B-Specimen

Comparing the damage in the late stage of life of B-6 and B-11 (see Figure 20 and Figure 19d), the similarities consist of a nearly identical delamination pattern and the arrangement of the primary plus 45-deg and zero-deg matrix cracks. While B-11 shows many straight edge induced matrix cracks in plus 45-deg, 90-deg, and minus 45-deg plies, B-6 has only a few of these cracks - an effect that is hard to explain due to the load levels. A possible cause for the difference might be a less careful finish (polish) of the B-11 edges, thus inducing additional local stress concentrations.

An additional effect in B-6 is the much more developed pattern of secondary 90-deg cracks, most of which come are near the straight edges. Another effect is the presence of large plus 45-deg cracks that neither belong to the primary cracks nor are initiated by these. This damage is probably a 'third order effect' in the sense that the new plus 45-deg cracks are initiated by the secondary 90-deg or minus 45-deg cracks or by the combined effect of these. Recalling that the 45-deg layer and the minus 45-deg layer are not adjacent but separated by the 90-deg layer, it is noted that interactive effects between cracks in separated layers may exist.

4.2 DEPLY TECHNIQUE

The deplied specimens A35 and B35 contain a maximum of damage. Both underwent continuous stiffness measurement tests that were halted late in the fatigue life just prior to failure, see Figure 34. Figure 21 depicts the essential pattern of the blue coloured areas on the interfaces of adjacent plies whose fiber orientation is indicated by the crossing lines. Since the color results from zinc iodide concentrations, the outer limits of these blue areas mark the extent of delaminations as well as the positions of matrix cracks containing a relatively large amount of zinc iodide. Experience shows that it is difficult to deply two adjacent layers of the same fiber direction. It seems likely to the author that there is no significant delamination between the layers of identical orientation adjacent to the laminate midplane since, because of the symmetry of both the loading and the geometry, interlaminar shear stresses are zero in this plane.

4.2.1 A-Specimen

The characteristic 'spider'-shape defined by the blue areas on the zero-deg/90-deg interface of the A-specimen marks the extent of delaminations. The central stripes between the tangent cracks are not locations of delamination expansion

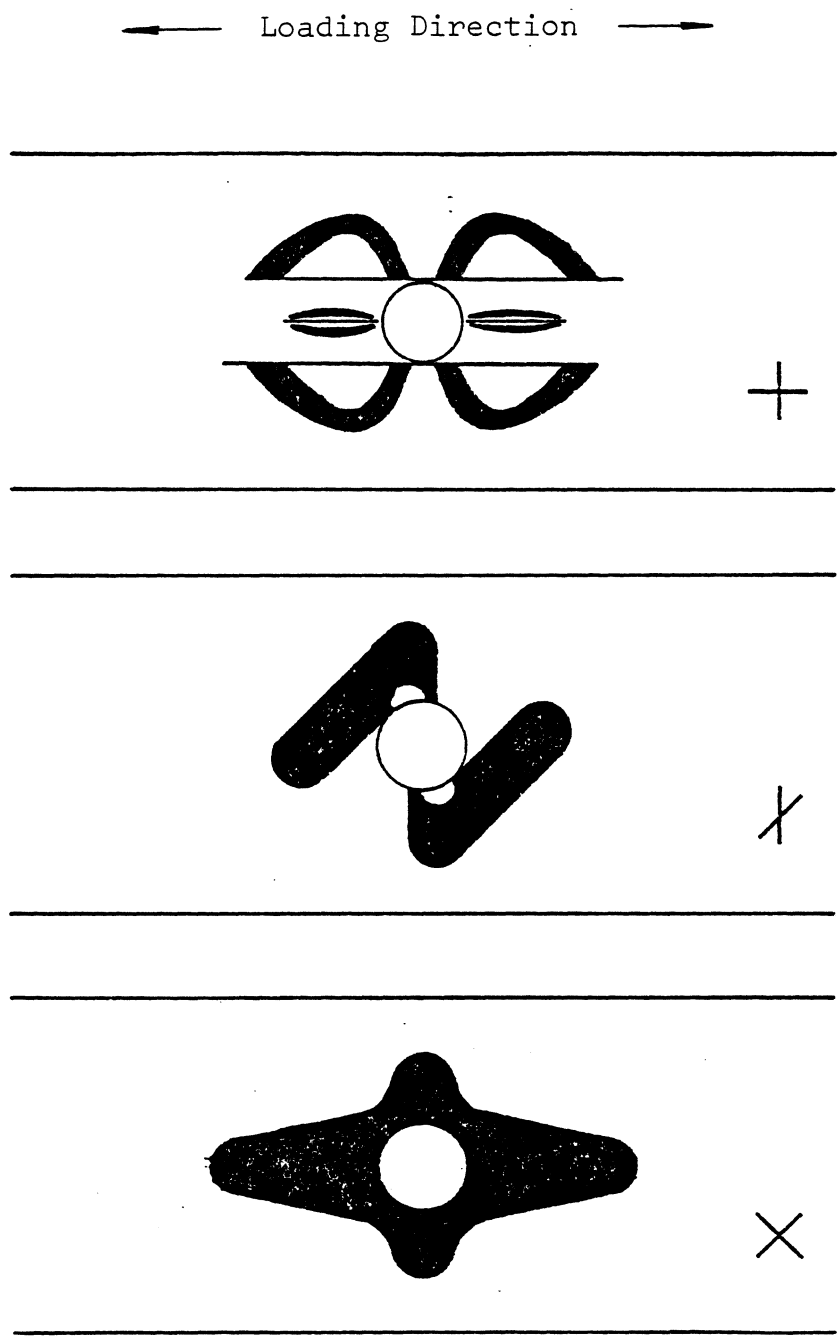

Figure 21: Delaminations on A-Specimen Interfaces

since delamination has fully taken place already (see X-rays, Figure 14 and Figure 15). They are probably caused by the zinc-iodide in the middle zero-deg cracks. The tangent zero-deg cracks did not leave such a trace. This seemingly inconsistent observation may be rationalized using the previously mentioned model based on the adhesive relations between the fluid and the solid material. The width of the tangent zero-deg cracks is larger than that of the middle cracks so that the fluid is not kept in the wider cracks. The interface between the 90-deg and the 45-deg layer shows a blue shadowed area resembling a 'Z'. This pattern can also be found on the X-ray in Figure 15. The typical pattern between the 45-deg and -45-deg plies is sketched in Figure 21 and may be called the 'Flying Saucer' pattern.

4.2.2 B-Specimen

In contrast to the A-specimen, B35 was not treated with zinc iodide but more thoroughly penetrated with gold chloride. However, delaminations can be identyfied and are sketched in Figure 22. Straight edge delaminations developed on the 90-deg/-45-deg interface. The larger extent of delaminations on the 45-deg/90-deg interface, compared with that on the 90-deg/-45-deg interface, indicates interactive effects between delaminations and matrix cracks. The shapes of de-

laminations on 45-deg/90-deg interfaces in the A- and the B-specimen, respectively, are quite different. While the larger extent of the cracks towards the straight edges in the B-specimen can be explained by the influence of matrix cracks in the outer layer, the larger extent of the delaminations in the A-specimen towards the x-axis of the laminate could be related to buckling effects in this specimen. These buckling effects were observed by eye-inspection during fatigue loading and are discussed in the section on continuous stiffness tests. At the stage of lifetime of the deplied specimens, the delaminations can not be related to the initial distribution of interlaminar stresses in the laminates.

4.3 MOIRE INTERFEROMETRY

All Moire-fringe patterns show the surface layer damage in detail and show the effect of damage on the surface displacement field. Although damage in the inner layers can not be measured directly, its collective effect on the overall laminate response is included in the surface displacement. In other words, the Moire technique is much more sensitive to damage in the surface layer than to damage anywhere else. For this reason, the fringe patterns of the damaged A-specimen and the damaged B-specimen, respectively,

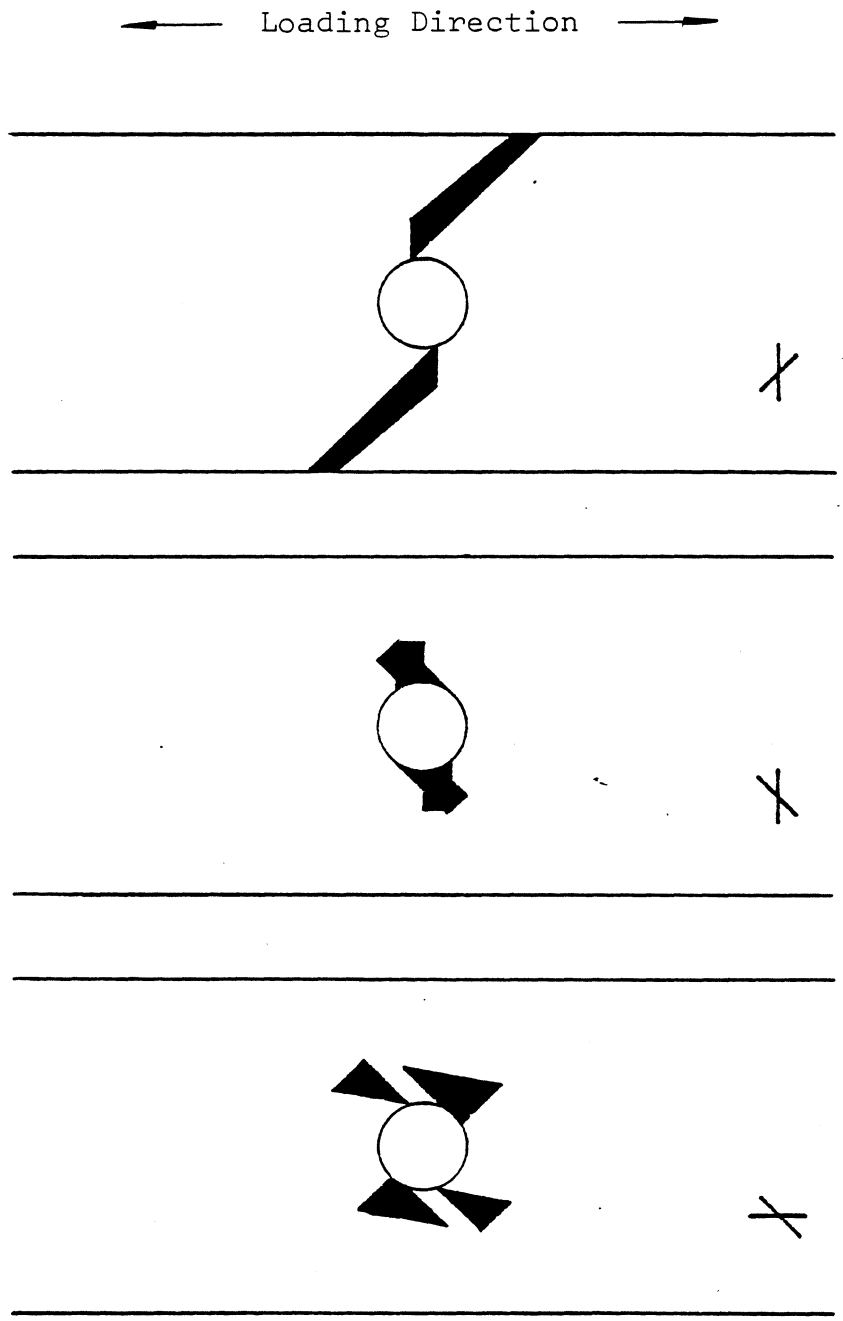

Figure 22: Delaminations on B-Specimen Interfaces

look quite different. None of the photographs shows a perfectly undamaged laminate - not even those taken under a 550 lbs load. This may be related to a mistake in the experimental procedure since after machining of the loading fixture and calibrating of the load cell the author tested the operability of the device by loading specimens up to more than 1000 lbs. To compare with the value given by a series of static stiffness tests performed using a 1"-extensometer, an equivalent stiffness was calculated from the fringe pattern. Two symmetrically located points on the x-axis at a distance of one inch from each other were taken and the number of fringes between them was counted. This number was corrected by a low-load fringe order and gave a stiffness of 53.3 msi and 51.75 msi for the A- and the B-specimen, respectively. Both values lie within the range of stiffness values determined using the 1"-extensometer but are about 6 percent and 4 percent above the average of the extensometer values, respectively. There is an agreement between the results of the two methods in that the initial stiffness of an A-specimen is slightly higher than that of an B-specimen. Since the part of the specimen reproduced on the moire negative is too small, it was not possible to compare the 2"- and the 3.625"-extensometer measurements with values obtained from the fringe patterns. At a distance from the

hole edge of less than two diameters the u-displacement field appears to be almost uniform. Another demonstration shows that the 1"-extensometer stiffness measurement is almost insensitive to excentricities of the extensometer with respect to the hole. For the A-specimen, for instance, a shift of 0.1 inches lead to a fringe order deviation of 2 from the correct value of 97.

4.3.1 A-Specimen

4.3.1.1 Fringe Pattern of the Undamaged Specimen

The fringes for the u- and for the v-displacements are shown in Figure 23a and b, respectively. One of the four peaks of the tangent matrix cracks is not yet fully developed and in this area the highly increased density of the u-displacement fringes can be studied. On the opposite side of the hole, along he zero-deg-matrix crack, the fringes are less dense than in the area spoken of above. At a distance from the hole edge of less than two diameters the u-displacement field appears to be almost uniform.

4.3.1.2 Onset of Fatigue Damage

Figures 24a and b show the damage state of the specimen under 1050 lbs load before the load is cycled and that of the specimen after 10 cycles under 1550 lbs load, respectively.

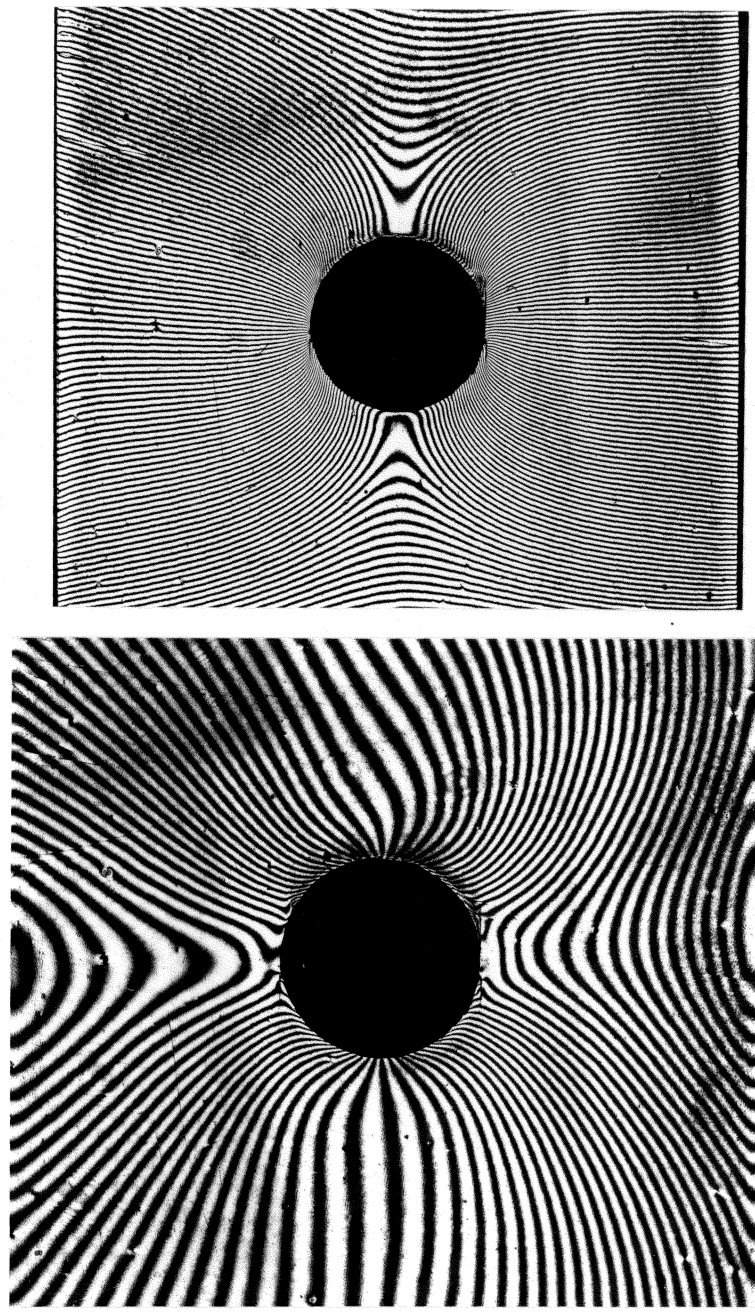

a

b

Figure 23: Fringe Patterns of the Undamaged Specimen

a

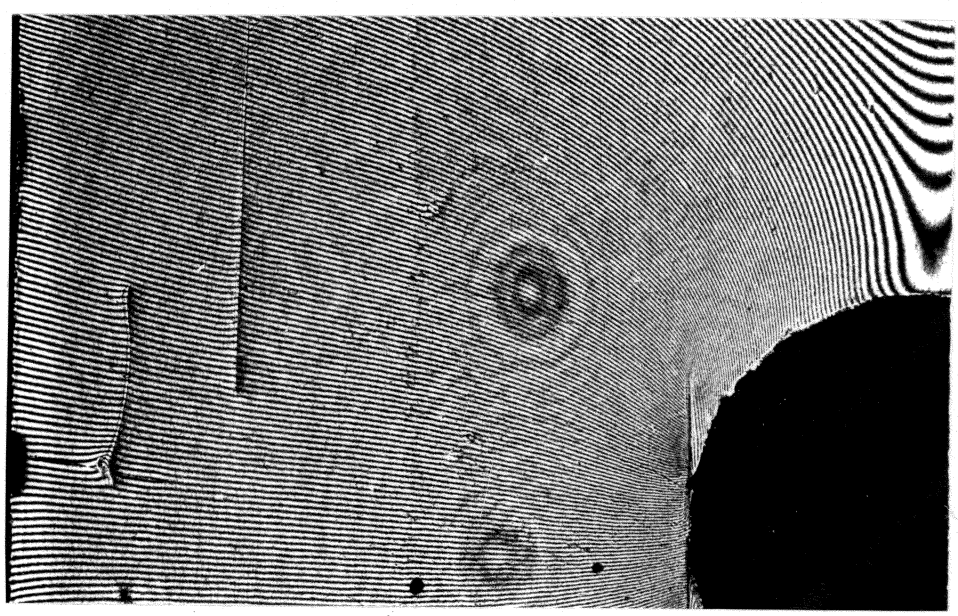

b

Figure 24: Undamaged Versus Low Damage Situation

We note that after 10 cycles of fatigue loading the crack that is not fully formed in the specimen before cyclic loading has grown and we can study its immediate effect on the stress field close to the hole edge. Apparently the crack redistributes and relaxes the strain field and lowers the strain concentration . According to the results for isotropic plates with a circular hole under unidirectional tension [19], we may assume a strain concentration of three for ε_x for an idealized undamaged situation and compare this value with the new strain concentraton along he crack. It is difficult to determine the maximum fringe density at the crack. Therefore, fringes emerging from the crack tips are followed to straight edge where the distance between them is measured. This value, in comparison to the crack length, may serve as an averaged strain concentration, still having in mind that there might be a higher value at the crack tips, which is difficult to estimate. We can also determine how the relaxation of strain at the tangent cracks influences the strain distribution on the straight edge by relating the length of a chosen segment to the number of fringes within this segment. This procedure should lead to correct numbers even under the condition of frequency mismatch by subtracting the null-field fringes.

4.3.1.3 Fringe Pattern of the Highly Damaged Specimen

Figure 25a and b shows clearly the areas of delaminations between the zero-deg matrix cracks and the influence of the damage on the lamina behaviour. The former complete symmetry of the fringe pattern is now reduced to a mere point symmetry with respect to the specimen center. Looking at the photograph, the crack above the hole is shifted toward the negative x-direction while the areas of low strain are shifted clockwise, possibly an effect of damage in the 45-deg plies.

The tongue-like shaped areas confined by the hole edges and the tangent cracks undergo a relative displacement to the delaminated areas outside the cracks. Although the edge of the hole appears somewhat diffuse, it can be seen that the strain concentration factor for ε_x is approximately constantly distributed over the whole length of the cracks with only slight additional concentrations at the tips of the cracks. As an estimate, the average strain concentration along the cracks is 1.46 and that at the tips is not determinable. Considering a fringe-order difference of 149 between the idealized 1"-extensometer-measurement points minus 24 fringes of residual deformation found on the null-field pattern and an applied load of 550 lbs, we find a stiffness value of 79.5 percent of the value calculated for the undamaged specimen.

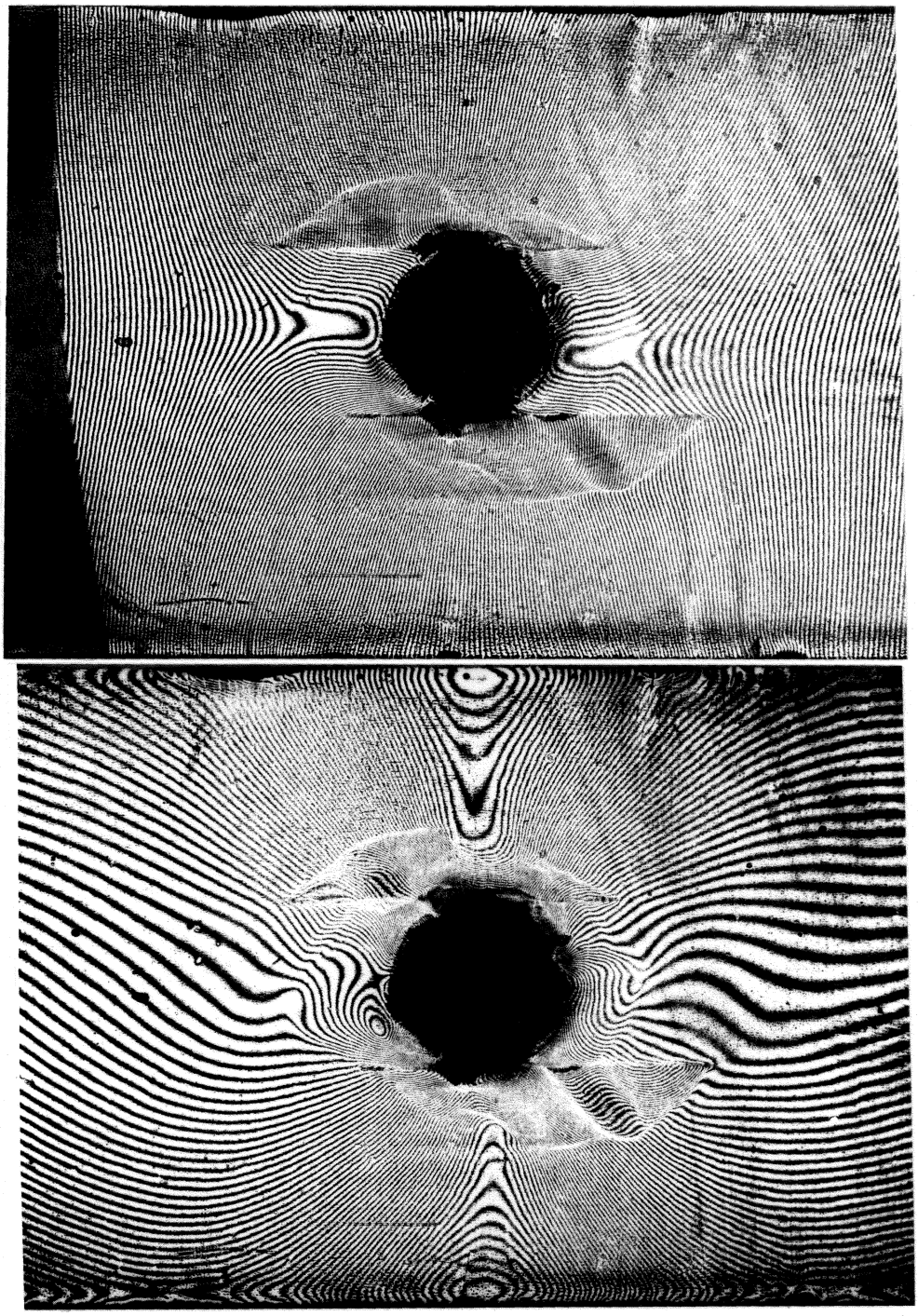

a

b

Figure 25: Fringe Pattern of the Highly Damaged Specimen

4.3.2 B-Specimen

4.3.2.1 Fringe Pattern of the Undamaged Specimen

The initial fringe pattern of the B-specimen is almost undisturbed by cracks as Figure 26a and b shows.

It seems that at this stage only the tangential +45-deg (here depicted in -45-deg direction) cracks lead to a significant reduction of the strain component ε_x at the hole edge.

4.3.2.2 Onset of Damage

Figure 27a and b indicates that the displacement field is heavily changed on locations where cracks cut fringes almost perpendicular and only slightly where cracks are almost parallel to the fringes.

The displacement field is most changed by the cracks tangent to the hole. We may reflect here that a more heavily change in the displacement field correlates to a higher stress relaxation and, going one step further, to a larger reduction of the elastic energy due to the regional stiffness of the laminate. In this context, let us remember that the X-ray photos document a quicker growth of the tangent +45-deg cracks than of the other +45-deg cracks after the onset of damage.

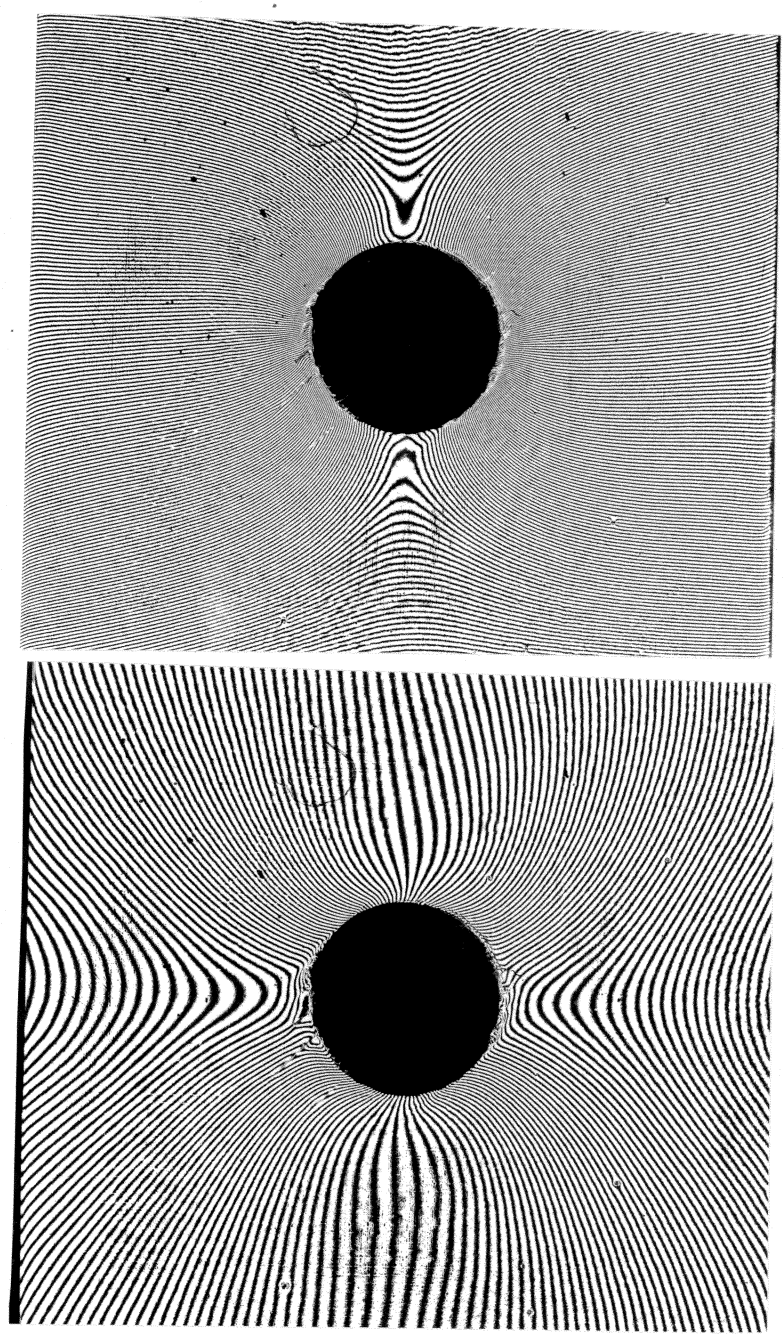

Figure 26: Fringe Pattern of an Undamaged B-Specimen

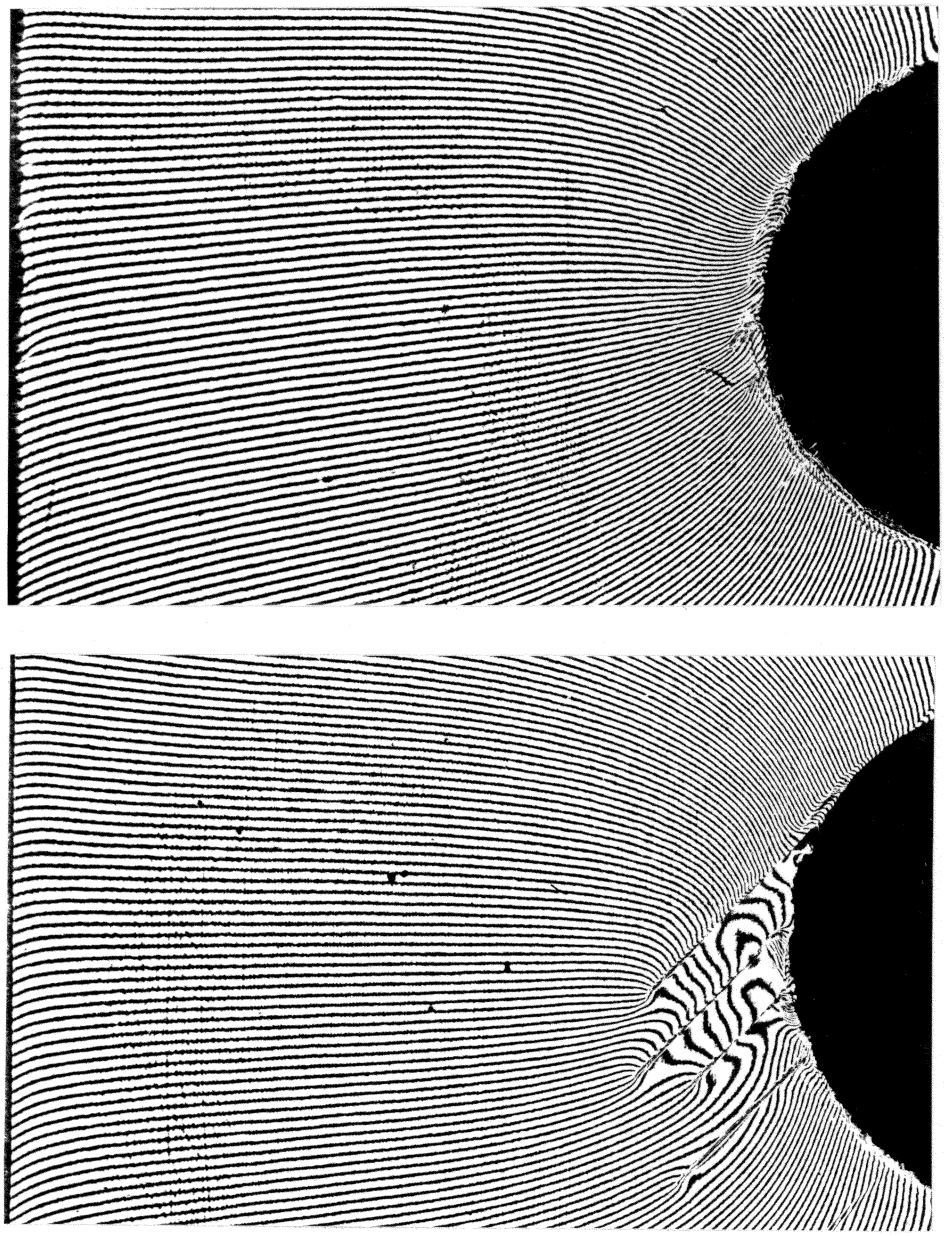

a

b

Figure 27: Undamaged Versus Low Damage B-Specimen

4.3.2.3 Fringe Pattern of the Highly Damaged Specimen

Figure 28a and b both show the delaminated areas along he tangent +45-deg cracks.

It is difficult to obtain a 1"-extensometer-stiffness equivalent since the large +45-deg cracks make it impossible to count fringes through this area. Particularly in Figure 28b the fringes have curvatures regularly placed along the +45-deg direction. A possible interpretation is that along these lines, cracks are anticipated but not yet fully formed. Such regularly distributed fringe shifts appear also between the hole and the straight edge in the 90-deg direction. It is possible that this fringe pattern shows a local displacement which precedes crack initiation or, in case of the fringe shifts along a 90-deg direction, is due to a crack in the adjacent layer. Unlike the fringe pattern of the A-specimen, fringe patterns of the B-specimens do not provide data to make quantified estimates on the residual strain concentration, since the strength governing zero-deg layers are located at the midplane of this laminate.

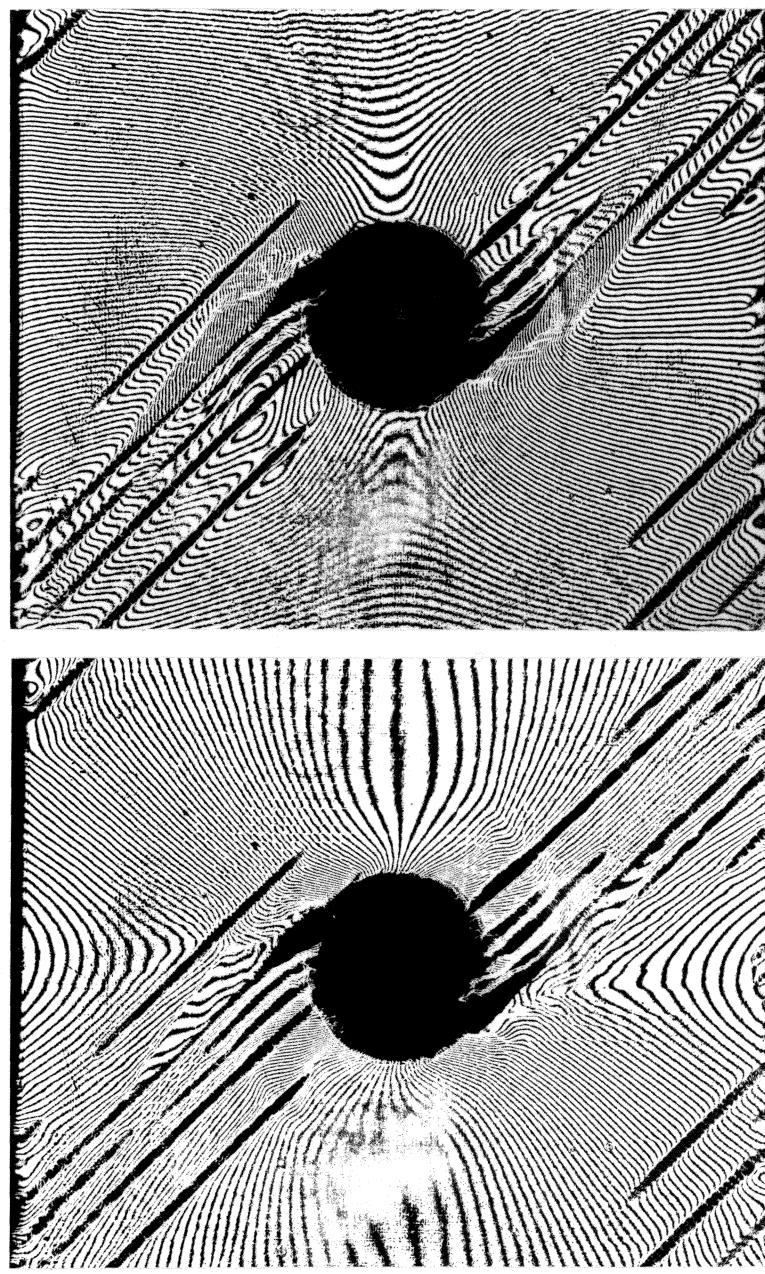

a

b

Figure 28: Fringe Pattern of the Highly Damaged B-Specimen

Chapter V

RESULTS

5.1 INITIAL TENSILE STRENGTH

Tensile strength tests were performed on five specimens of each type of laminate, including the unnotched laminate.

In Figure 29, the failure load of each specimen is represented by the length of a vertical line. The average failure loads of A,B and C specimens were 2620, 2240, and 4680 lbs., respectively, as indicated by the solid horizontal lines.

The lower, dashed horizontal lines indicate the averaged load levels for which major discontinuities in the strain-load curves, as well as the first strong acoustic emissions during the loading process, occurred.

The percentages refer to the average failure load of each type of laminate. The C-specimens typically had edge induced delminations accompanied by strong acoustic emissions at a strain of approximately 0.66 percent. The correlation between the onset of acoustic emission activity and this strain value was much better than the correlation with load values. The root of the sum of the squared deviations is 2.54 for the strains and 5.59 for the corresponding loads.

After the delamination point, indicated by an increase of strain for nearly constant load on the load- -strain curve,

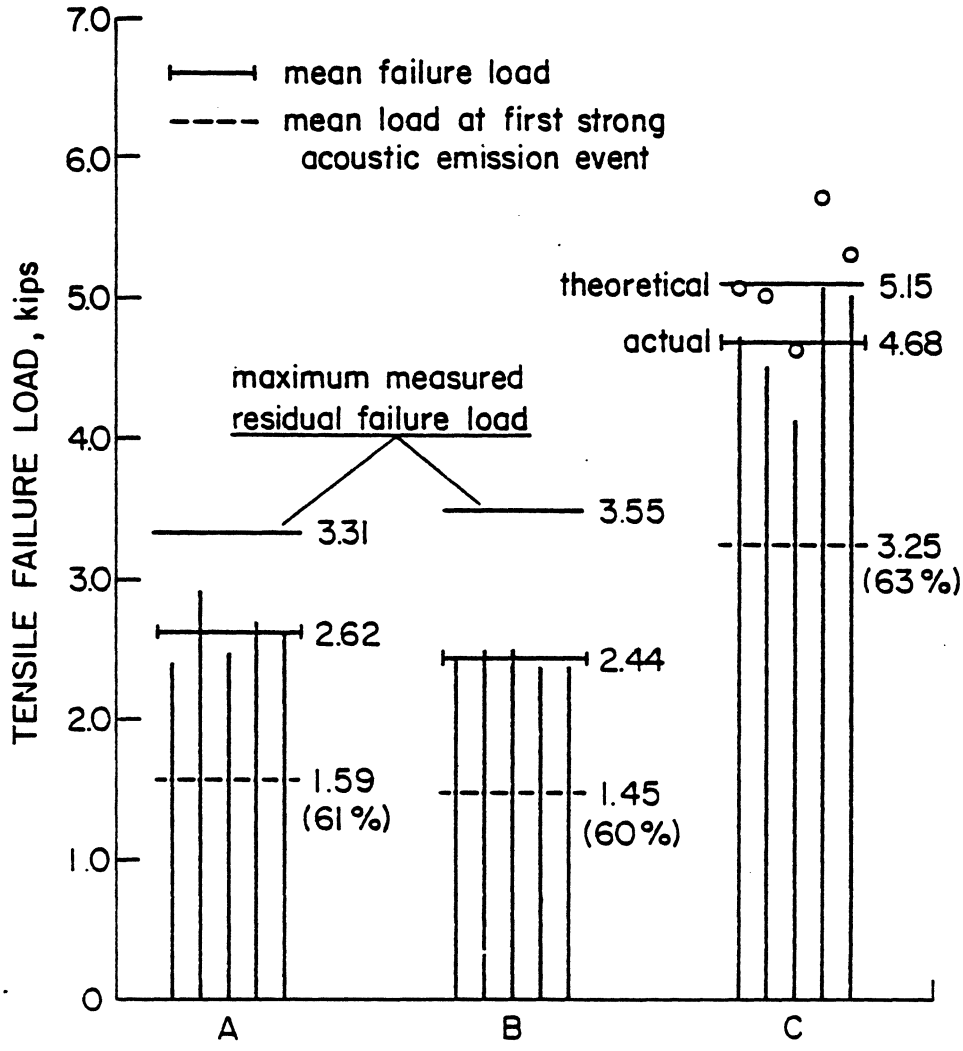

Figure 29: Static Strength

the averaged stiffness was reduced. Both the step in the curve and the reduced slope after the step suggested the idea of predicting strength values for the 'no delamination' situation by simply multiplying the averaged stiffness value taken from the initial part of the load-strain curve by the failure strain of each specimen. These values, indicated by the open circles, average to 5150 lbs. or 110 percent of the actual strength as indicated in the figure. Considering the critical, net cross sections, which are the notched sections for the A and B specimens, the average failure stresses are 52.8, 48.6 and 71.5 ksi for A-, B-, and C-specimens, respectively. The large difference between the strength values of notched and unnotched specimens is due to the stress concentrating effect of the hole. Yet, it must be noted, that the strength of the C-specimens is also reduced by straight, free edge effects. But the strength values indicate that a strength reduction factor for the hole must be much larger than one for the straight edge.

Furthermore, since edge effects in general (whether for curved or straight edges) decrease rapidly with increasing distance from the edge, the effects of the straight and the curved edges of the notched laminates are independent. In other words, we may assume that for the notched specimens used in this study, the effects of the straight edge do not

yield an additional contribution to the reduction of static strength caused by the hole.

It is important to note that the highest measured residual strengths, related to the notched crosssection, of A- (66.5 ksi) and B- (71.4 ksi) specimens approach the tensile strengths of C-specimens, thus indicating that fatigue damage redistributes local stresses to the extent of reducing the stress concentration due to the hole.

5.2 INITIAL STIFFNESS

Stiffness data were taken from the linear part of the load-strain curves recorded during the tensile strength tests by means of a 1.0 in. extensometer centered with respect to the hole. Each vertical line in Figure 30 represents the stiffness of a specimen. Average stiffness values, based on the area of the unnotched section, are indicated by the horizontal lines. The stiffness values of A- and B-specimens, based on the cross-sectional area, are lower than the stiffness values determined for unnotched C type specimens. This demonstrates the large, local deformation field associated with the local stresses due to the hole.

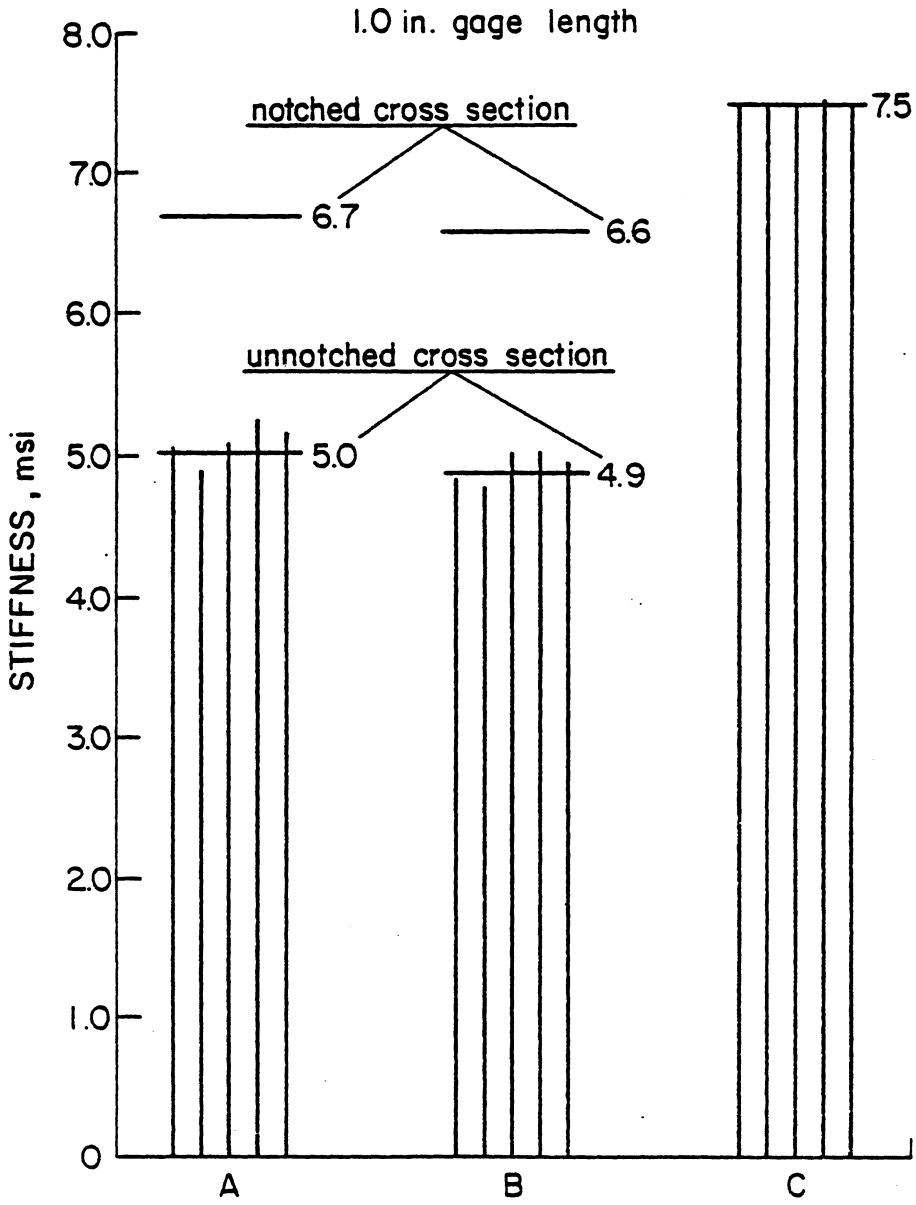

Figure 30: Static Stiffness

5.3 S-N DATA

A lifetime of more than 10^6 cycles under the condition of a sinusoidal load with a ratio $\sigma_{min}/\sigma_{max} = 0.1$ and a frequency of 10 Hz can be expcted at an 80 percent load level (2093 kips) for A-specimens and a 70 percent load level (1707 kips) for B-specimens. Load-log life curves for the two laminates are shown in Figure 31. A-specimens, cycled at a 95 percent load level (2485 kips), and B-specimens, cycled on an 85 percent load level (2073 kips) will survive 10^5 cycles.

Two A-specimens had an average lifetime of $1.1*10^6$ at the 80 percent load level while the B-specimen, cycled at the 70 percent level, had a residual strength of 137 percent of the virgin strength after 10^6 cycles. The residual strength data for type B laminates suggest that residual strength values of this magnitude occur during the final decade of logarithmic life.

5.4 STIFFNESS DEGRADATION

5.4.1 Interrupted Stiffness Recording

Figure 32 shows stiffness data for type B laminates cycled at the 85 percent level.

The two stiffness curves show the effect of gage length on the stiffness values. A clip type strain gage extensometer

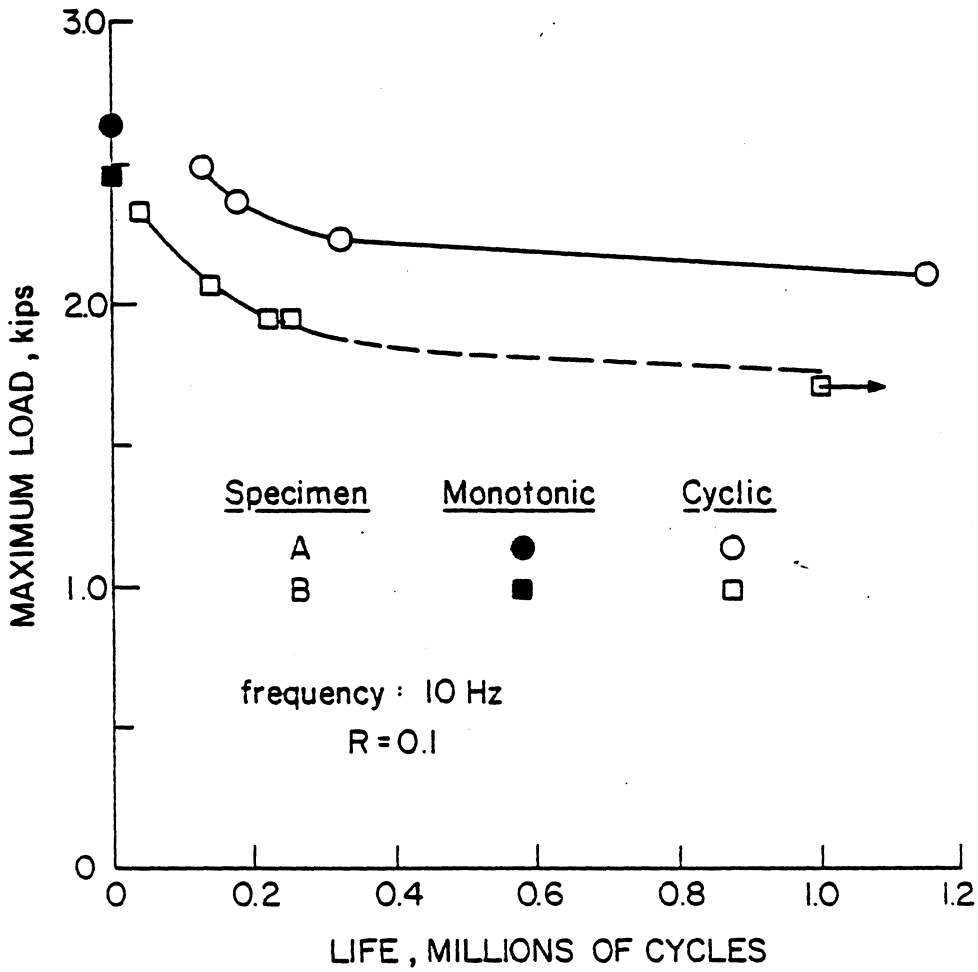

Figure 31: S-N Curves

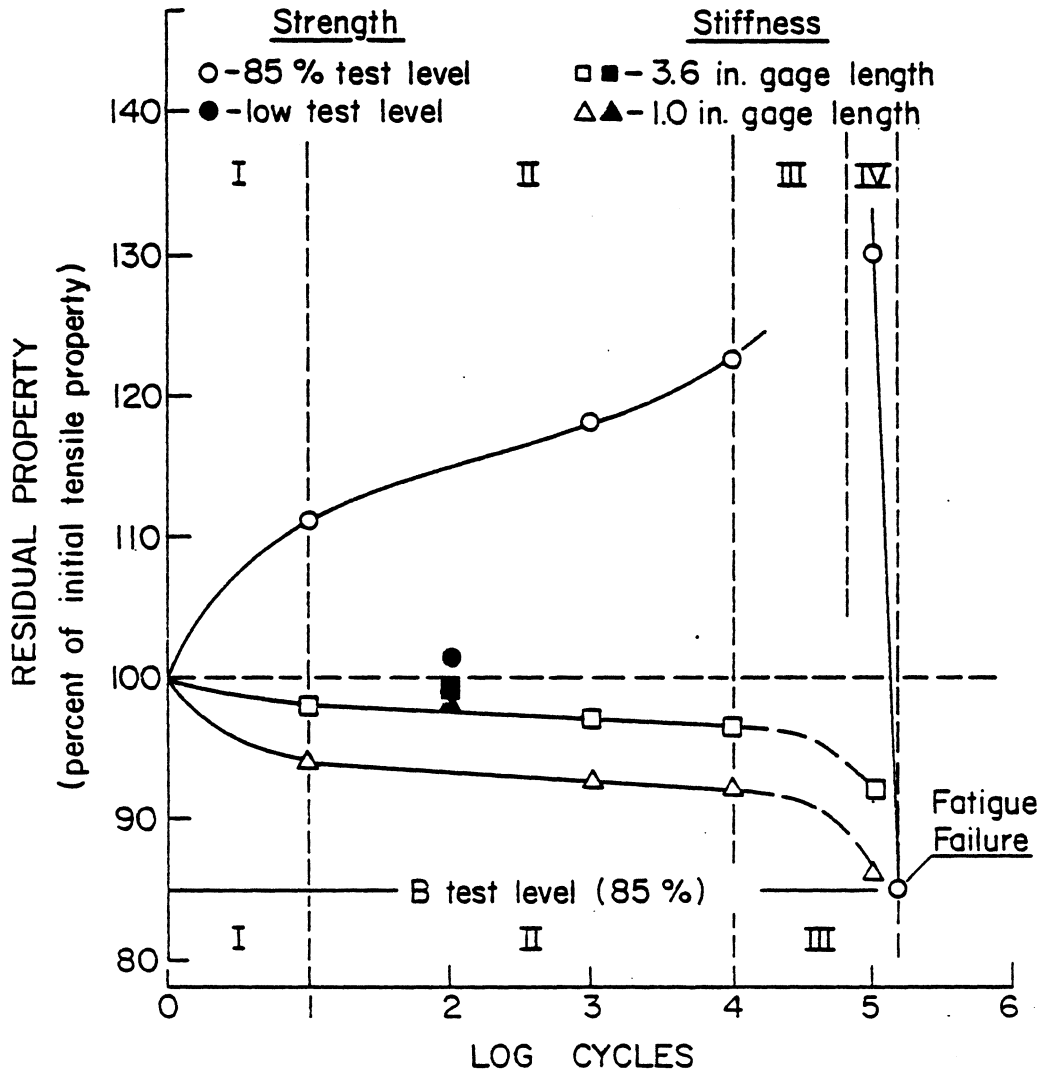

Figure 32: Stiffness and Residual Strength Versus Life

centered over the hole was used to measure displacement over a 1.0 in. gage length. A DCDT extensometer centered over the hole measured displacement over a 3.625 in. gage length. The stiffness change values based on the short extensometer data are larger. However, if the damage zone spreads outside the 1.0 gage length, the stiffness change values determined from the short extensometer are inaccurate.

The process of damage development around the hole of a type B laminate is indicated by the stiffness curves shown in Figure 32. The limits of the regions I, II, and III are somewhat arbitrary, but are chosen to reflect transitions in the damage growth process as represented by stiffness change. In region I, the stiffness decreases at a decreasing rate as small matrix cracks develop near the hole. In region II, the stiffness degrades linearly with log cycles and the matrix cracks in the zero and 45 deg. plies extend away from the hole and delaminations form in the region damaged by matrix cracks. Region III begins as the stiffness degradation rate increases. In this region, the sharp decrease in stiffness is associated with further extension of the cracks in the zero and 45 deg. plies, an increase in the density of the cracks in the 45 deg. plies, and growth of delamination along the 45 deg. matrix cracks. Early in the life of the laminate (region I) the damage is confined to

the approximate zone of stress concentration around the hole. In later stages of life, the stresses around the hole are redistributed and the stress concentration around the hole is changed due to the growth of the damage zone away from the hole. Radiographs of damaged type B specimens at several intervals in the loading history are shown in Figure 18 and Figure 20. The data in Figure 32 are presented in terms of percent change in stiffness because the exact values of stiffness are not repeatable in situations where the cyclic test is stopped, the extensiometer is removed from the specimen, and the specimen is removed from the grips for nondestructive evaluation at various cyclic intervals. However, if the stiffness values are determined at the beginning and end if each cyclic interval, or are recorded throughout a cyclic interval by the data aquisition system, the change in stiffnes during the cyclic interval can be determined. The total change is then computed as the sum of the stiffness changes for all intervals.

5.4.2 Continuous Stiffness Recording

The plots of the results of the peak detector program on a logarithmic lifetime scale confirm the estimated stiffness curves based on quasi-static tests. The suggestion of a five percent stiffness loss after 100 cycles at a 90 percent

cycling load for both laminates was taken into account by multiplying the first stiffness value, recieved by the peak detector after 200 cycles, by the factor 0.95.

Figure 33 shows the regions II and III of the stiffness degradation due to fatigue loading at the 90 percent level of the failure load of each specimen, respectively. The time axis is logarithmically scaled. In this representation, region II appears as an almost linear line leading into a sharp knee which connects region II with region III. Immediately beyond the knee, the degradation rate appears to be highly increased. At the end of region III, the stiffness decay accelerates again until failure.

Comparing the two curves shown in Figure 33, we find the B-laminate showing a lower stiffness degradation before the knee, a later and more distinct forming of the knee, and a higher degradation rate after the knee than the A-laminate. The stiffness loss at the end of fatigue life is 18 percent for the B-specimen and 40 percent for the A-specimen.
The data have been replotted using a linear scale for the life axis, Figure 34. Throughout the lifetime, the A-specimen has a lower stiffness than the B-specimen. Between 10 K and 50 K cycles, the degradation rates of both curves are similar; after that the A-specimen looses stiffness more rapidly than the B-specimen. Although the total stiffness loss

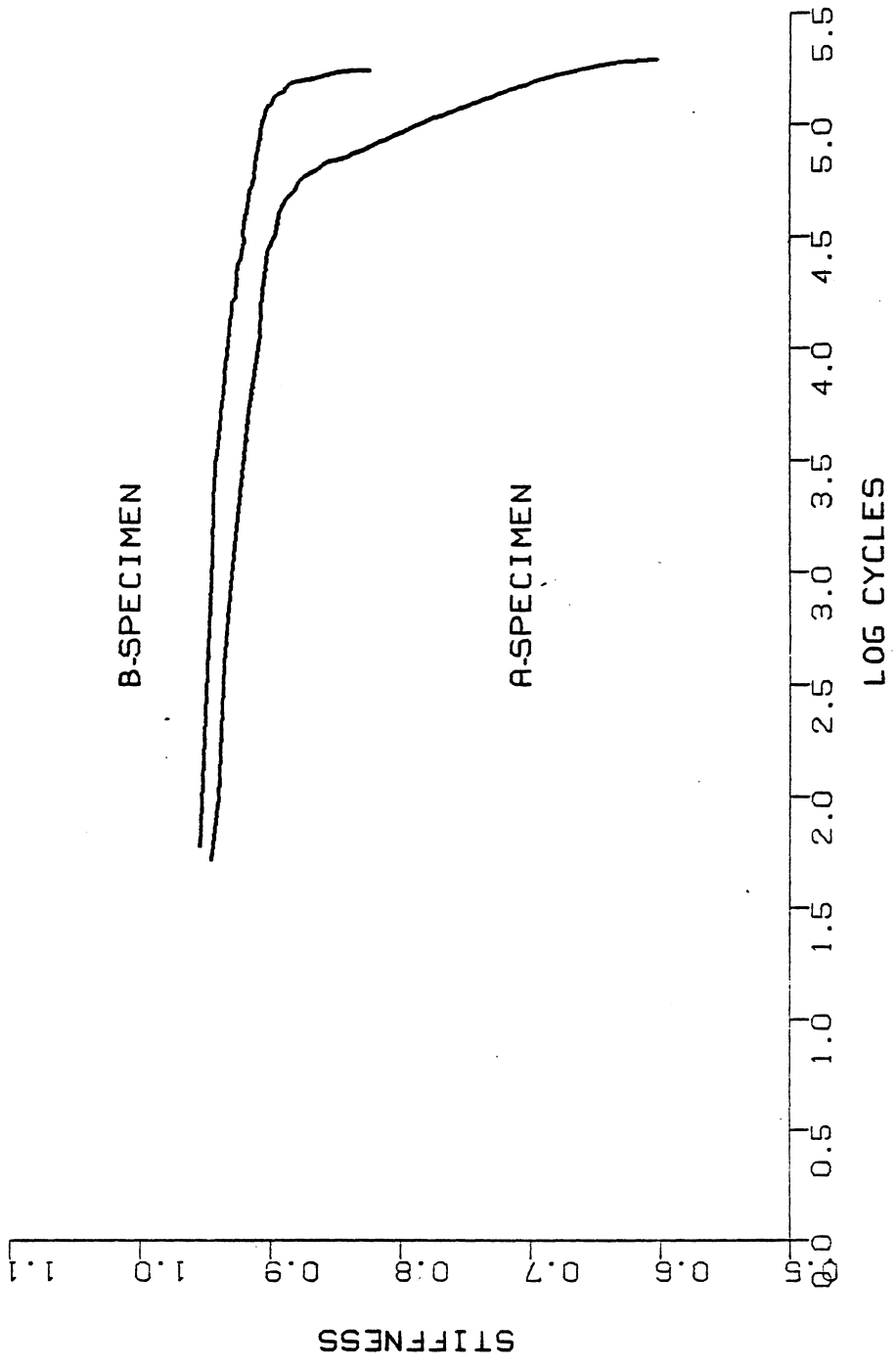

Figure 33: Stiffness Degradation Versus Logarithmic Cycles

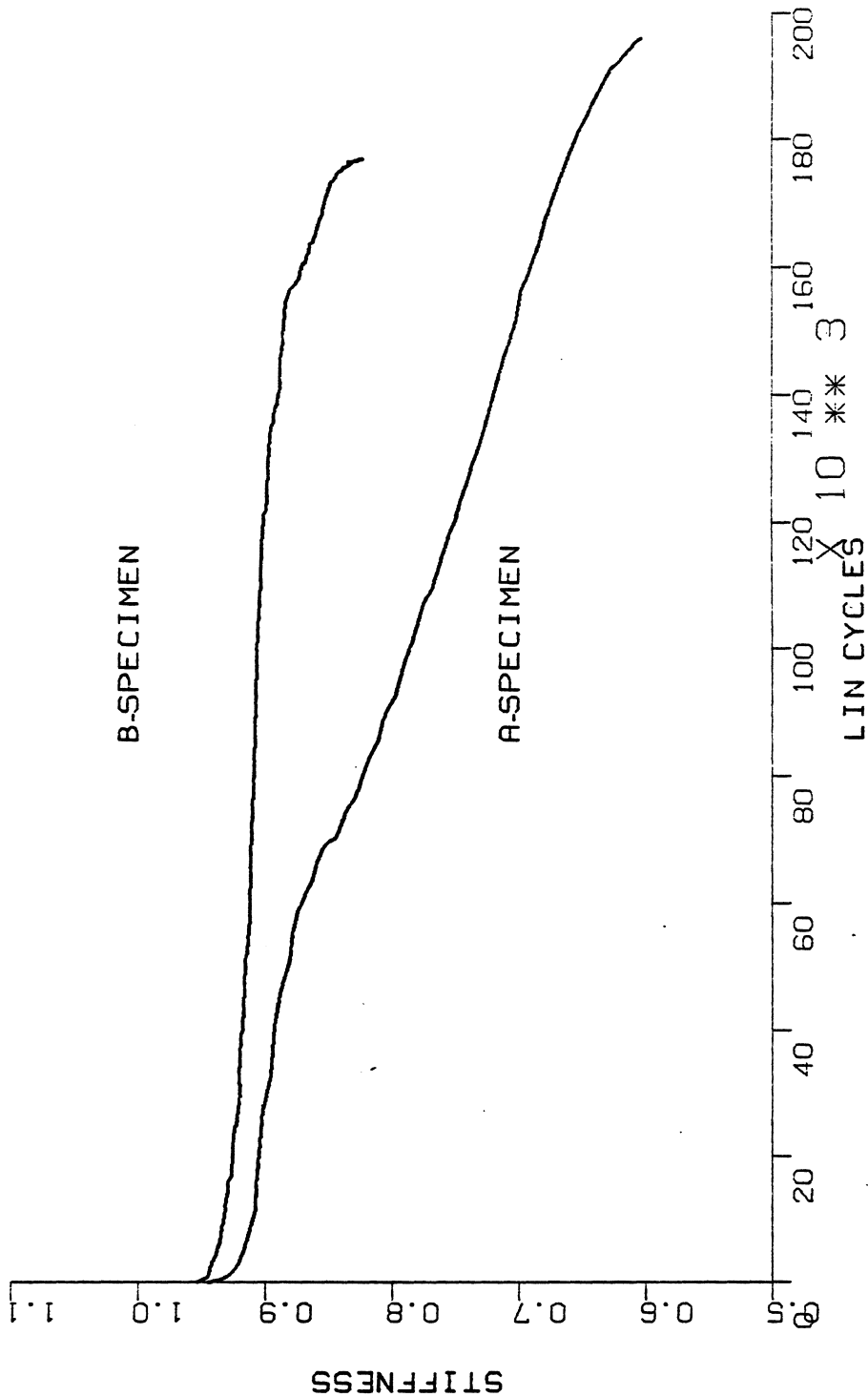

Figure 34: Stiffness Degradation Versus Linear Cycles

during its lifeyime is lower for the B-specimen, the stiffness degradation rate shortly before failure is very high. Both laminates exhibit three sudden stiffness changes during the fatigue life: the first one occurs during the very first cycles of loading, the second one occurs within the first half of the lifetime for the A-specimen and well before failure for the B-specimen, and the third, sudden stiffness loss leads into the failure of the specimens. The A-specimen has its second sudden stiffness loss at 70 k cycles and the B-specimen at 157 K cycles. Both events coincide with the onset of the knee in the logarithmic- -scale stiffness representation and are generally followed by an increased degradation rate. It should be mentioned here that locally confined buckling effects were seen during cyclic loading of the A-specimen. On both sides of the specimen, the zero-deg and the 90-deg plies, as a sublaminate, delaminated from the inner [45,-45]s block at locations governed by compressive circumferential stresses and buckled outwards. It could be hyphothetisized that the forming of these delaminations and in company the stiffness degradation is being rapidly accelerated after reaching a critical delamination size which faciliates buckling. The sudden stiffness change at 70 K for the A-specimen could then be related to the observed buckling effects. By eye-inspection, no buckling effects were

visible for the B-specimen. However, at the end of the fatigue life, it seemed to be obvious by eye-observation that the surface 45-deg ply contributed only little or nothing to the load transfer, since around the hole matrix cracks were formed and some of the surface material confined by those cracks was almost completely delaminated. The matrix cracks prevent the in-plane-load transfer and the delaminations make load transfer through interlaminar shear stresses impossible. These effects were visible at the end of the lifetime of the B-speceimen, thus suggesting the possibility of a relationship between them and the sudden stiffness change at 157 K cycles. Finally it should be recalled that the 90 percent load levels for the A- and the B-specimen are represented by the absolute values of 2354 lbs and 2195 lbs, respectively.

5.5 RESIDUAL STRENGTH

A number of the cyclic tests were halted at various stages of the loading history for nondestructive inspection of the damage zone and residual strength measurements. This series of tests provided a characteristic and repeatable curve of the change in residual strength throughout the loading history, Figure 32 and Figure 35.

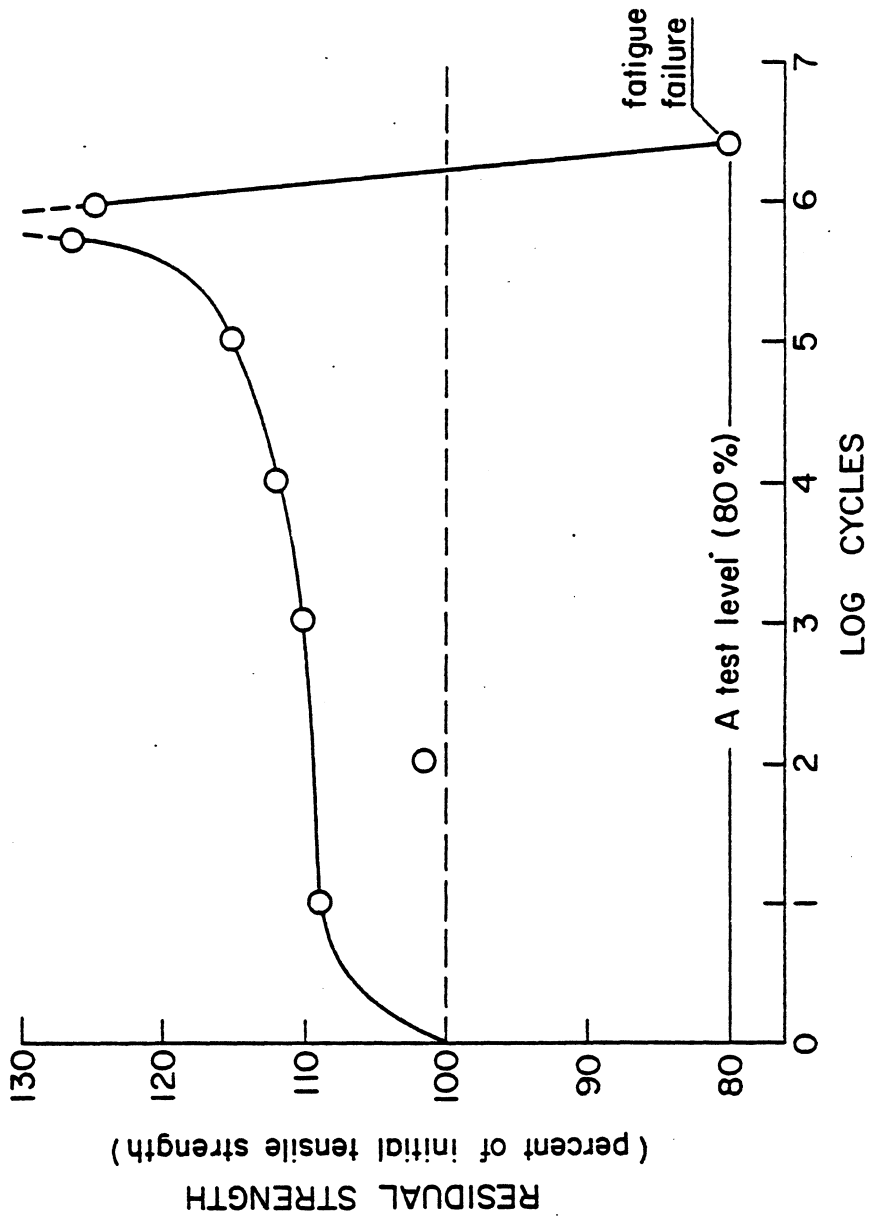

Figure 35: Residual strength of an A-Specimen

During the first few (ten) cycles, the damage, primarily matrix cracks, reduces the effect of the stress concentration at the hole and the residual strength increase is on the order of ten percent. The actual strength increase does depend on the cyclic stress level, with the higher stress levels corresponding to slightly higher strength increases than the lower stress levels.

Stiffness change and residual strength data for a type B laminate after 100 cycles at a low cyclic stress amplitude are also shown in Figure 32. Both the increase in residual strength and the decrease in stiffness are less than those for the same type specimen cycled at the 85 percent stress level. The second region of the residual strength curve, approximately ten percent of the fatigue life, is characterized by a slow, but constant increase in residual strength over a logarithmic cycles scale. At the end of the second region, the increase in residual strength is 115 to 120 percent. The limits of regions I and II for residual strength are approximately the same as observed for stiffness change.

The third region of the residual strength curve is marked by a further increase in residual strength. Although the data in this region is incomplete, it appears that the maximum residual strength is reached between 50 and 80 percent of the lifetime. The largest increases in residual strength

are 26 and 42 percent for the type A and B laminates, respectively. During the final region of the fatigue life, the residual strength decreases until the strength equals the level of maximum cyclic stress, as shown in Figure 32 and Figure 35. The last two regions of the residual strength-log cycles curve correspond to the third region of the stiffness reduction curve where the stiffness change shows a sharp decrease on the log cycles plot. The logarithmic scale used to represent the lifetime may cause some confusion in interpreting these results. The residual strength data have been replotted in Figure 36 using a linear scale to represent cycles.

The appearance of fracture surfaces depends on the loading history of the specimens, respectively. The typical static failure fracture surface is located along a straight line passing through the center of the hole, Figure 37.

Specimens with increased residual strength, loaded monotonically to failure, have a more distributed fracture surface as recorded in Figure 38.

Figure 39 shows the typical widely scattered fracture surface of a highly damaged specimen.

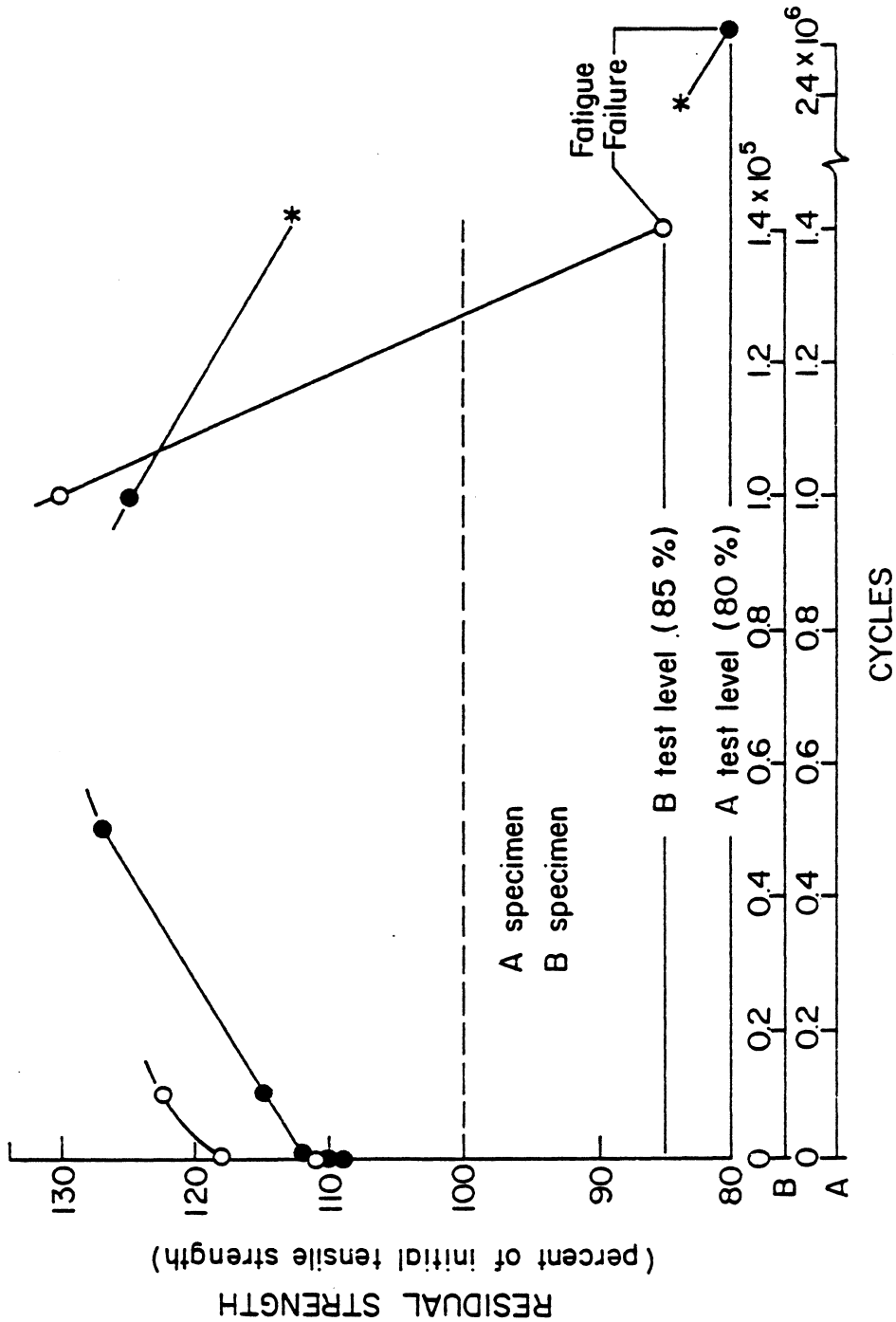

Figure 36: Residual Strength Versus Linear Cycles

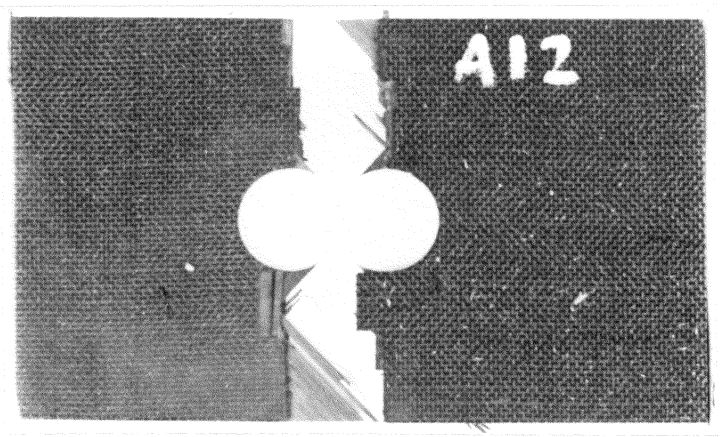

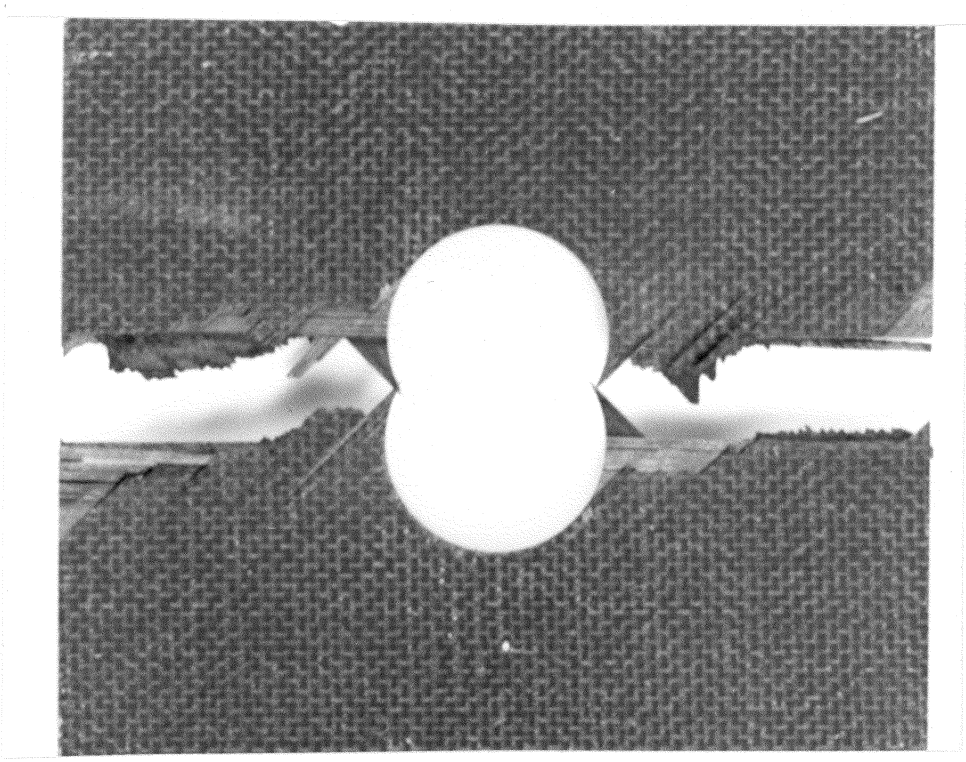

Figure 37: Static Fracture Surfaces

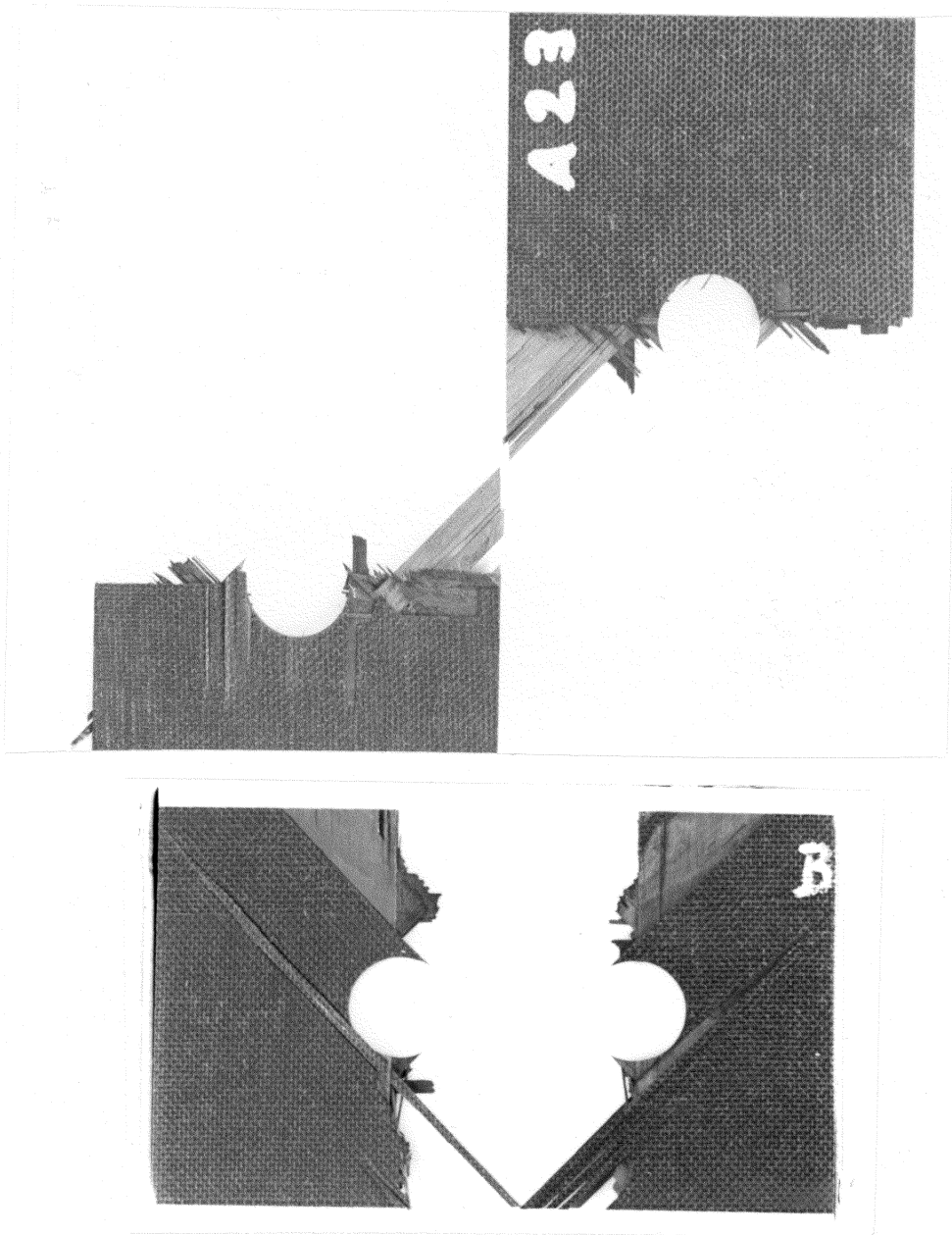

Figure 38: Fracture Surfaces of Low Stress Level Fatigue Specimen

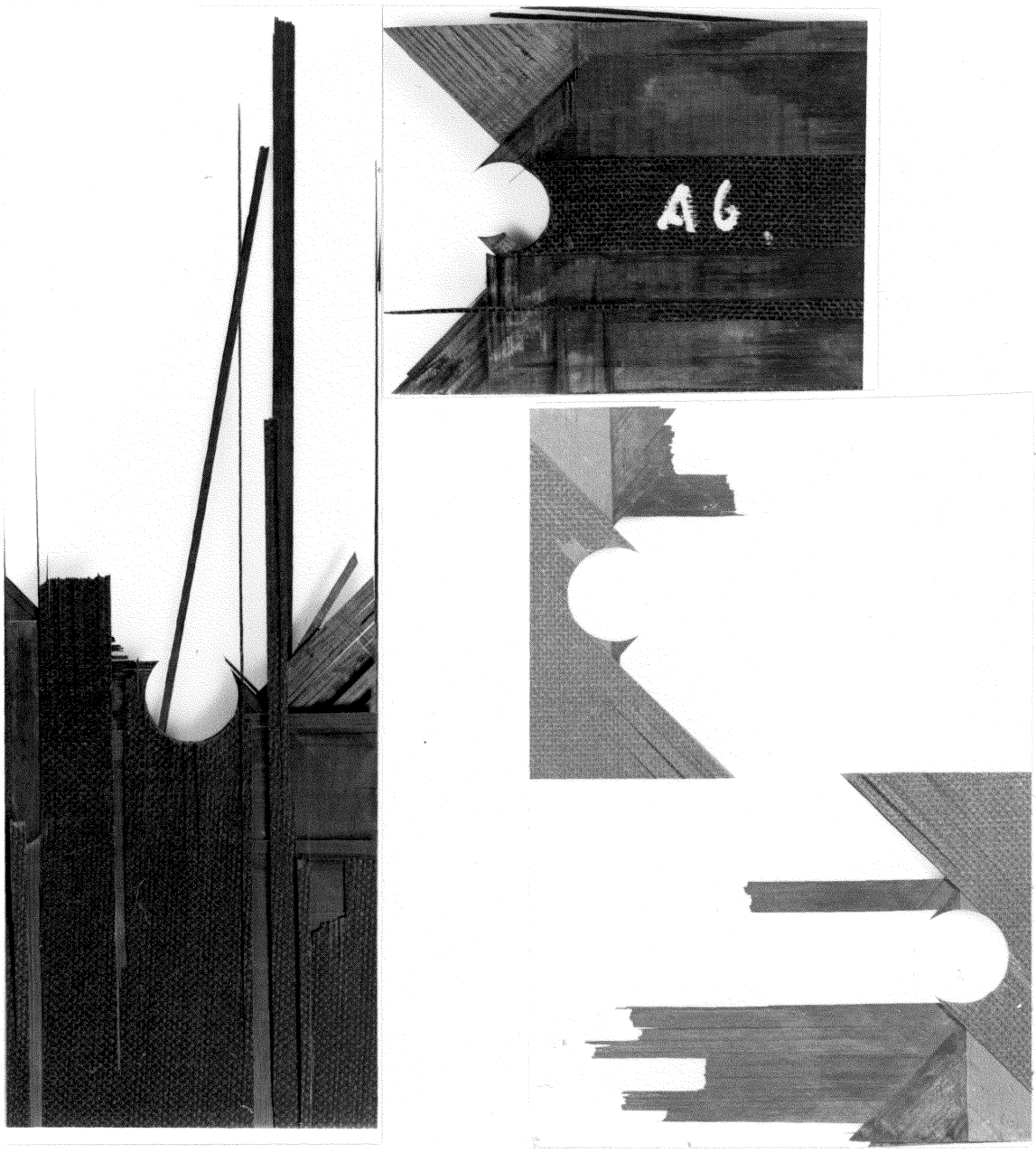

Figure 39: Fracture Surfaces of High Stress Level Fatigue Specimen

5.6 DAMAGE PATTERNS

Static damage starts with matrix cracks usually in the surface plies at 1570 lbs load for the A-laminate and 1220 lbs load for the B-laminate. At higher load levels, cracks appear in all directions. The A-laminate develops more well defined zero-deg cracks tangent to the hole while the B-laminate develops more well defined 45-deg cracks. Note that these are the directions of the surface layers, respectively. In both laminates, 45-deg and zero-deg cracks are more well defined than -45-deg and 90-deg cracks. The latter cracks are often secondary cracks in the sense that they are initiated at locations where 45-deg and zero-deg cracks already exist. Zero-deg cracks in the A-laminate grow to a length of more then five hole diameters. When the tangent zero-deg cracks approach their maximum length, cracks in 45-deg and 90-deg direction are also initiated on the straight edge. In the final stages of lifetime, a regular pattern of matrix cracks is formed between the tangent zero-deg cracks and the straight edges. The uniformity of these cracks is similar to damage patterns of unnotched laminates, so-called characteristic damage states (CDS).

The delamination zone visible on an X-ray photo consists of the superimposed images of the delaminations on the various laminate interfaces. It seems as if the tangent zero

deg cracks in both the A- and the B-laminates cause delaminations on adjacent interfaces. Those delaminations have the largest continuously connected area of all delaminations in the laminates. In general, while the A-laminate develops a much larger delamination along its tangent zero-deg cracks, the more confined delaminations of the B-laminate spread along the 45-deg direction and reach the straight edge. It is emphasized that Figure 21 and Figure 22 give the spatial distributions and the characteristic shapes as well as the proper magnitude of the delamination zones. Noting that the area of delaminations on all interfaces is higher for the A-laminate than for the B-laminate, we recall that the A-specimens experienced much higher stiffness losses during their fatigue life than the B-specimens.

5.7 DAMAGE AND MECHANICAL RESPONSE

Figure 24 shows that the tangent zero-deg cracks have a strong redistributing effect on the strain field near the hole, reducing the maximum strain concentration in x-direction. Except at the crack tips, the strain distribution along the cracks is almost uniform. Figure 40 presents the average strain concentrations as a function of the length of the tangent cracks at various fatigue stages for the A-specimen. After 600K cycles, which is estimated as being 50

percent of the expected lifetime the strain concentration is reduced to K_ε=1.46.

Figure 41 shows the decrease of strain concentration versus the logarithmically scaled number of cycles. The rate of decrease is very high during the first cycles of fatigue loading.

Recalling that the rate of increase of residual strength of both laminates is also very high at the beginning of fatigue life it seems very likely that the tangent zero-deg cracks are a main factor influencing residual strength.

Figure 42 shows the results of two strength tests performed on an A-specimen and a B-specimen versus the length of the tangential cracks obtained from X-ray photos taken after applying the fatigue load.

We note that cracks of equal length in A- and B-specimen seem to influence the strength increases of A- and B-specimens differently. As a result of a linear curve fit for the data points we find an increase-in-strength rate of 44 percent per inch for the B- and 23 percent for the A-laminate.

A residual-strength versus strain-concentration curve (Figure 43) was constructed from the data used in Figure 40 and Figure 42 by eliminating the crack length.

Figure 44 and Figure 45 show the increase of cracks in the zero-deg plies with the number of cycles under fatigue load.

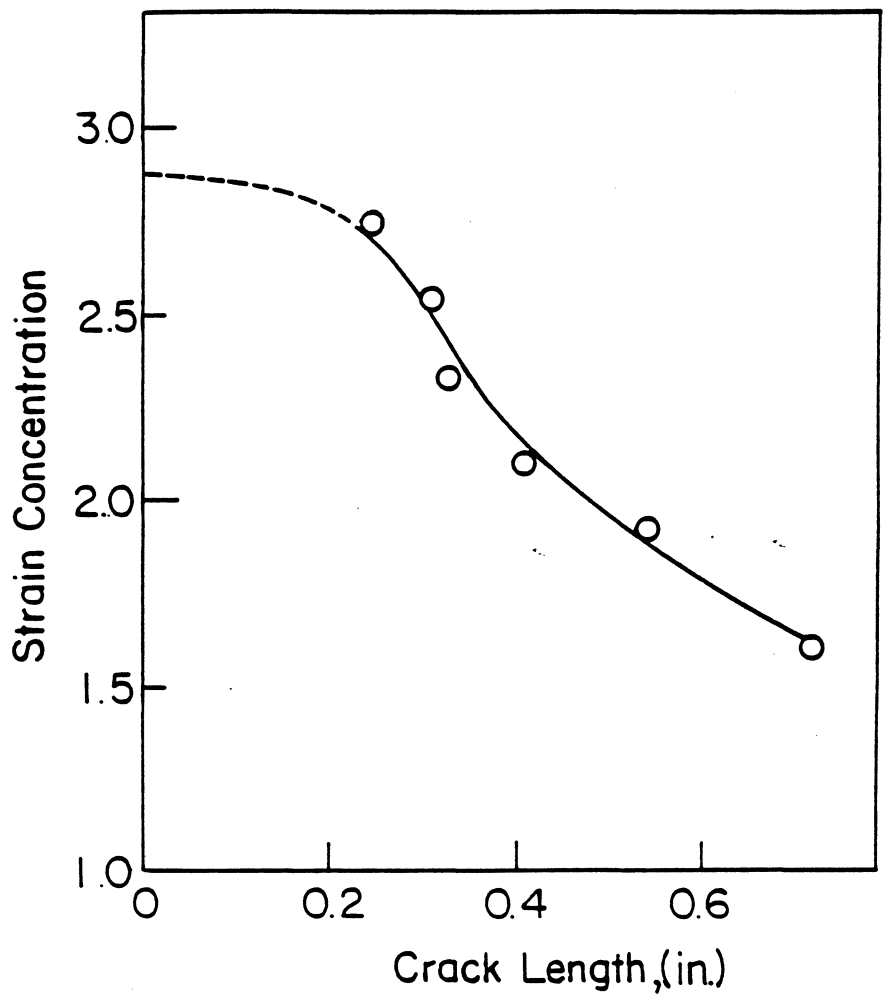

Figure 40: Strain Concentration Versus Crack Length for an A-Specimen

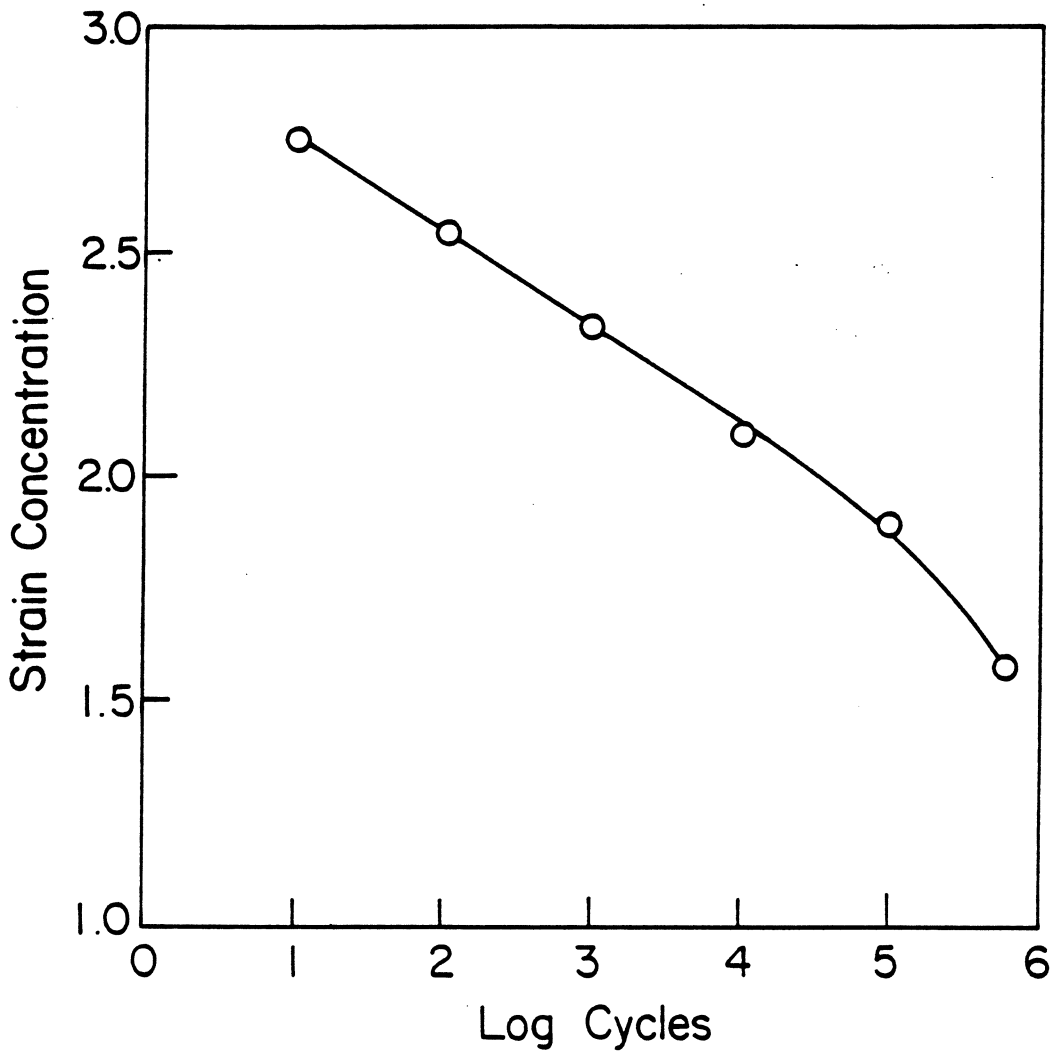

Figure 41: Strain Concentration Versus Cycles for the A-Laminate

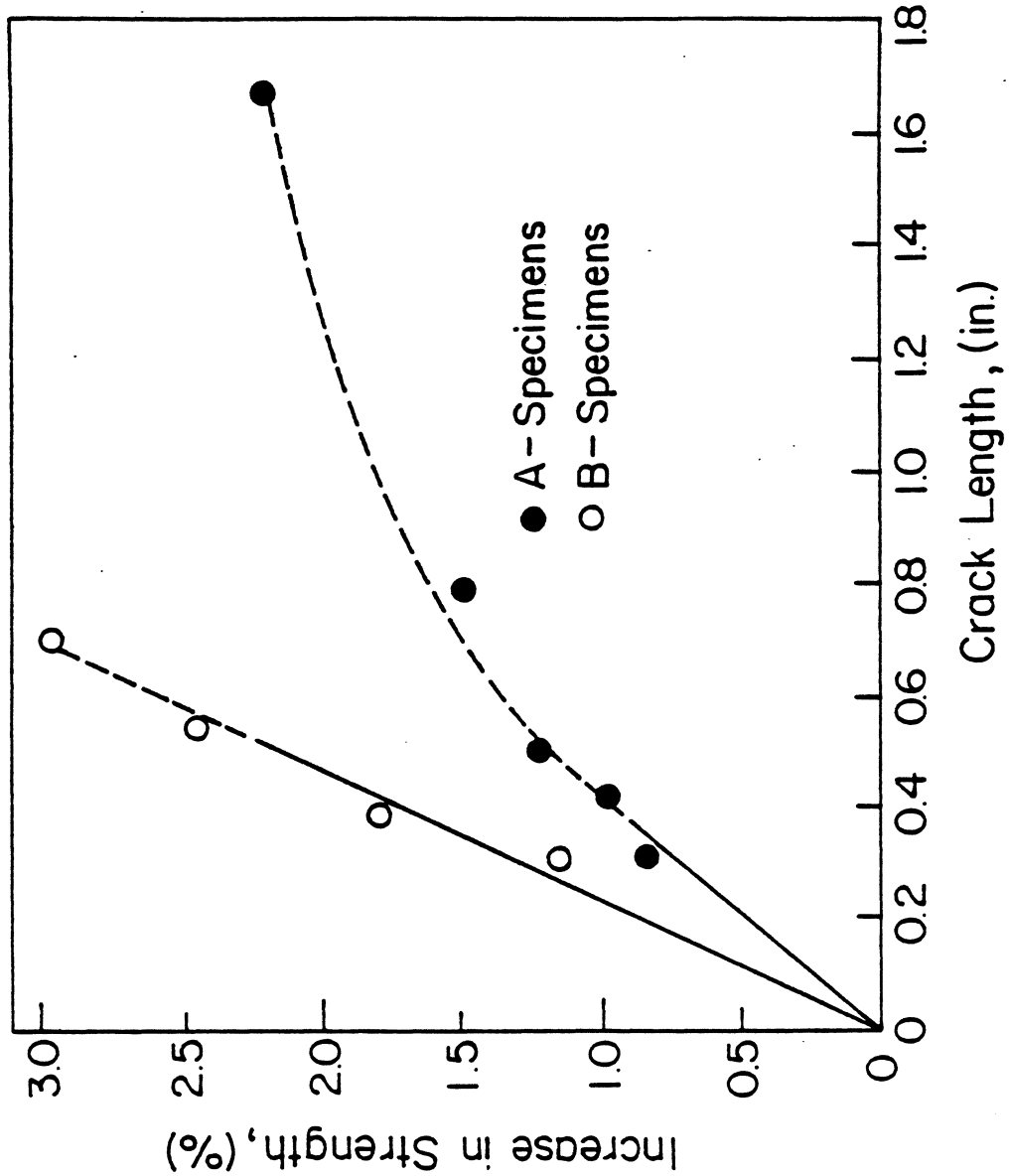

Figure 42: Residual Strength Versus Crack Length

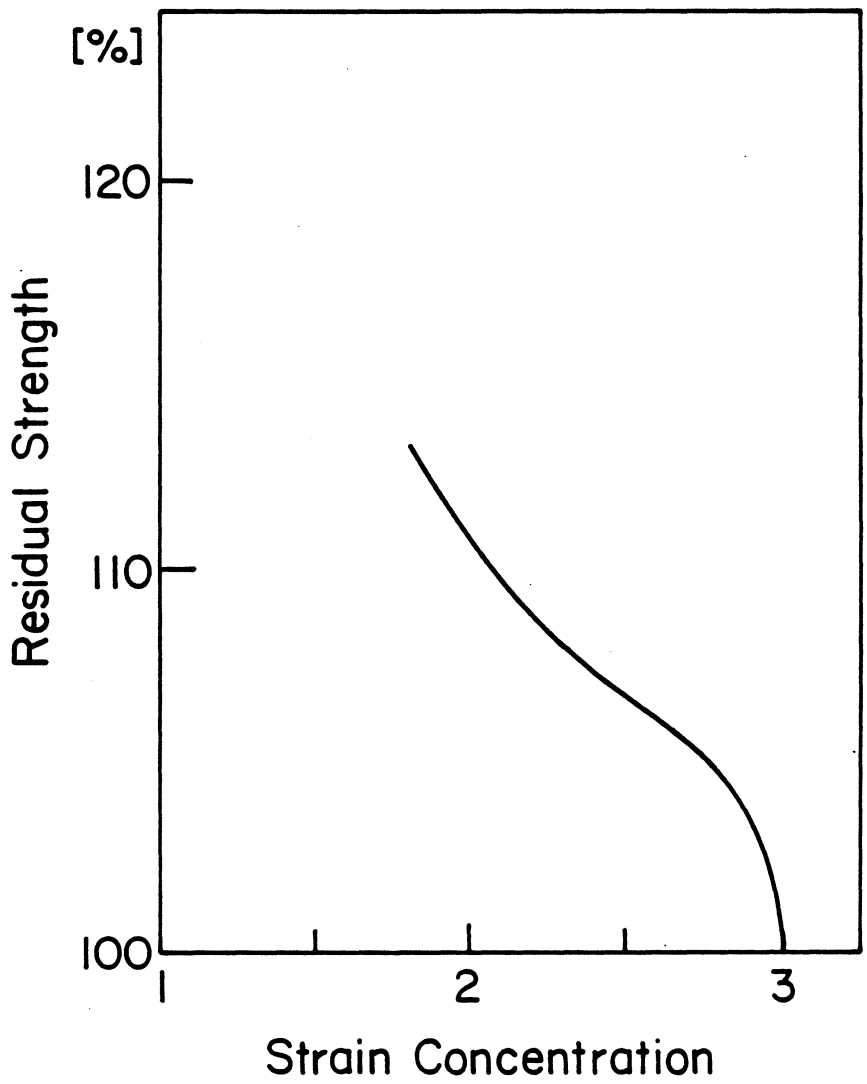

Figure 43: Strain Concentration Versus Residual Strength

The crack lengths are the average values of the length of the two cracks visible on X-ray photos. For two reasons it is difficult, however, to measure average crack lengths exactly. First, the length of the dark line on a X-ray matches the actual crack length only in the case of complete penetration with zinc iodide. Second, it is difficult to decide what the length of a crack is since a dark line on a X-ray is the superimposed image of actually two cracks on each side of the laminate midplane. If these two actual cracks are shifted in different directions, one might observe a longer crack than actually exists. Since the data for the B-laminate is more complete, Figure 45 provides also information on the influence of the load parameter on the growth rate of those cracks. Figure 44 takes the initial crack length due to static load into account, so the crack length starts with the value indicated.

The phenomenon of widely scattered fracture surfaces for specimens with high loading histories can be related to the shift of high strain concentrations away from the hole. Since those strain concentrations are presumably highest at the tips of the cracks, we conclude that catastrophic failure can be initiated right there. Specimen A-6 underwent a fatigue life test on 80 percent load and its fracture surface is shown in Figure 39. Many zero-deg fibers broke at a

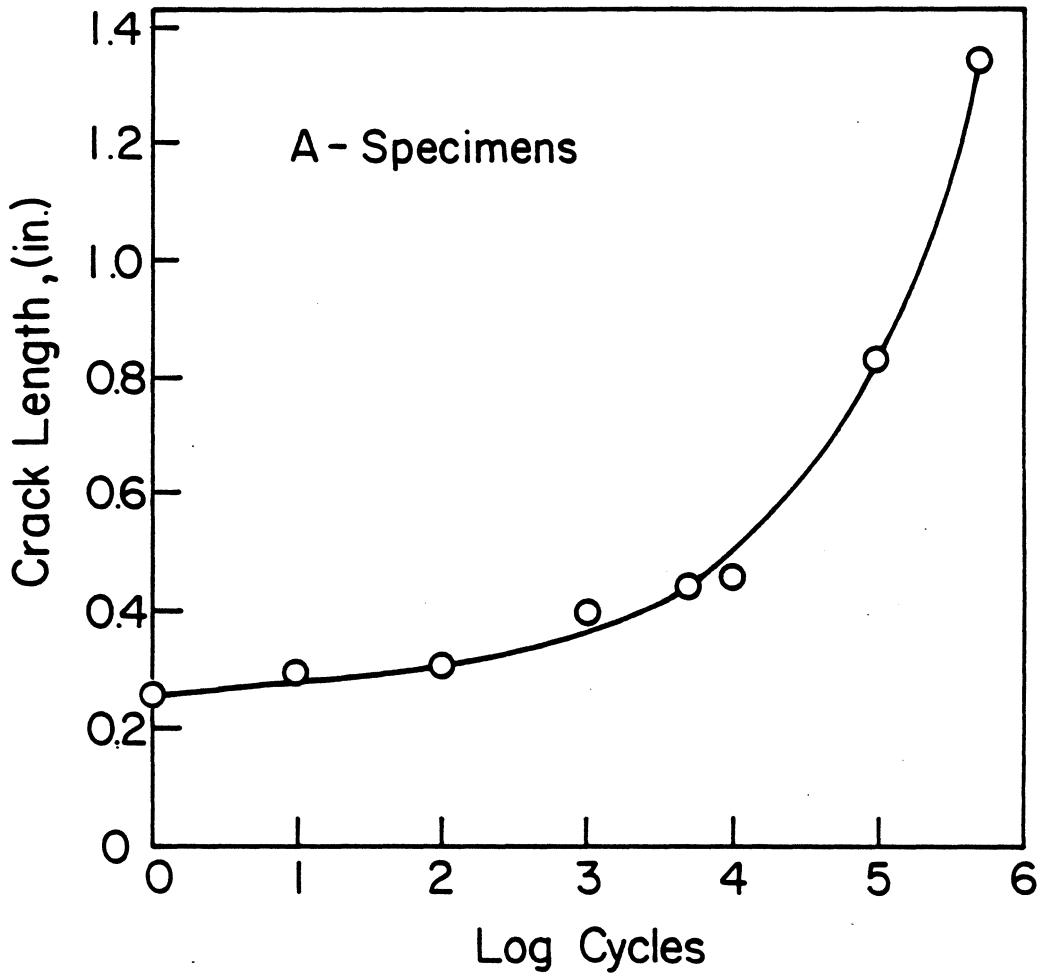

Figure 44: Zero-Deg-Crack Length Versus Number of Cycles for an A-Specimen

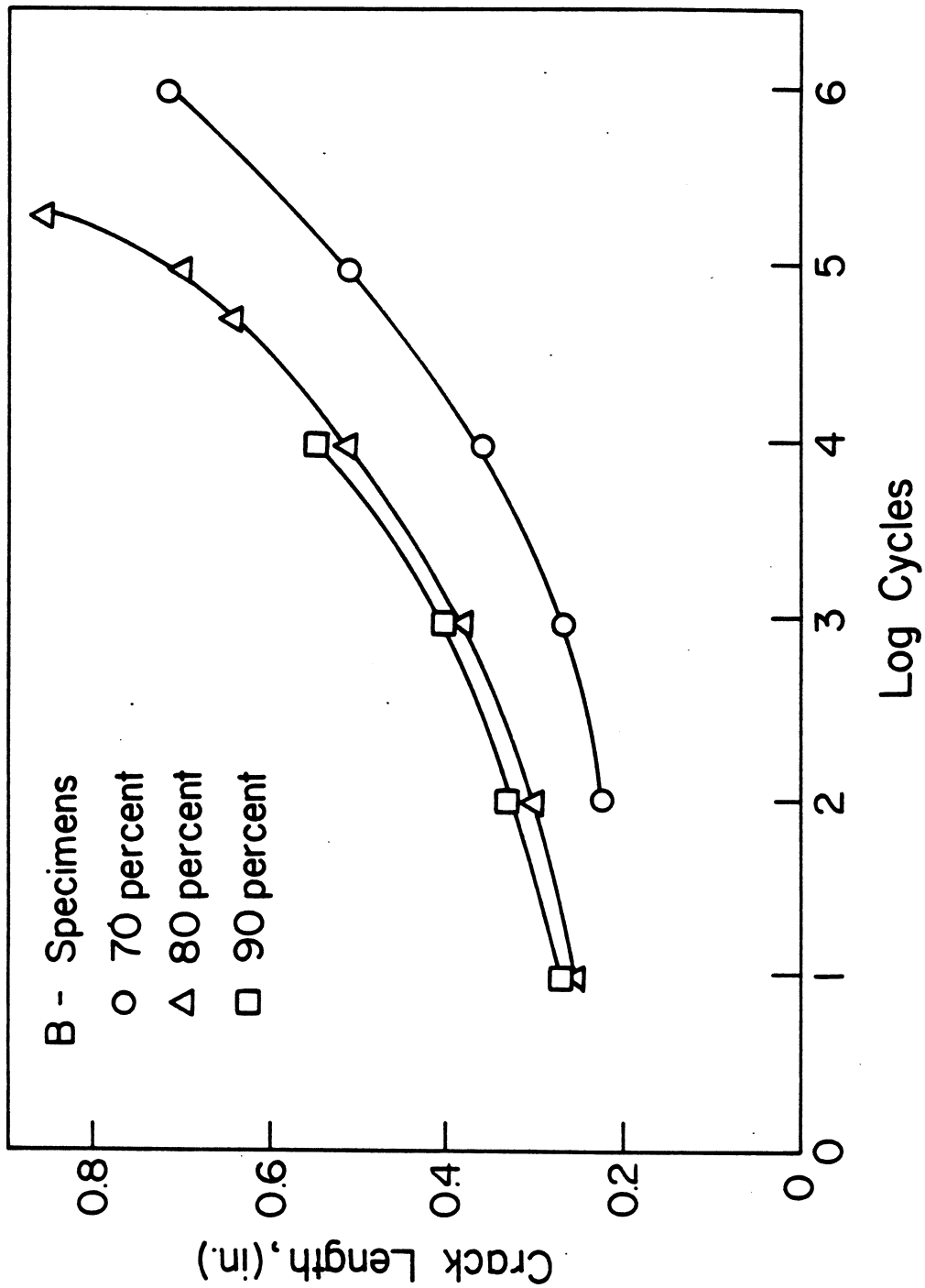

Figure 45: Zero-Deg-Crack Length Versus Number of Cycles for B-Specimens

distance from the hole of 6 to 7 hole diameters or from 2.25 inches to 2.625 inches. As for the phenomenon of stiffness degradation, we note that the A-laminate exhibits much larger delaminations than the B-laminate. These delaminations and also the buckling described in the section on continuous stiffness recording contribute to higher stiffness losses in the A-laminate than in the B-laminate.

Chapter VI

CONCLUSIONS

1. X-Radiography gives detailed information on matrix cracks that can be used to establish relations between those cracks and the fatigue response of laminates.

2. In conjunction with x-radiography, the deply technique gives the shape, size, and spatial distribution of delaminations.

3. The first strong acoustic emission signals during static loading correlated with discontinuities in the load-strain curves.

4. The Moire technique can be used to detect damage in the surface layer and related effects in the displacement field. Local stiffness can be measured for various damage situations. These results are in good agreement with extensometer measurements. The fringe patterns suggest that the sensitivity of results to eccentric attachment of extensometers is low. The Moire patterns of the laminate with the zero-deg-surface layer gave more evidence about relations between damage and response than those of the other laminate. All possibilities of the moire technique were not completely used in this work. More sophisticated data-processing methods

could help to take full advantage of this technique.

5. Stiffness losses during the lifetime reached, dependent on load levels, 20 percent for the B-laminate and 40 percent for the A-laminate. Stiffness-change versus number-of-cycles curves are typical for laminates.

6. Residual strength exceeds initial strength until final stages of lifetime are reached. Increases may reach levels of at least 26 percent for the A- and 42 percent for the B-laminate. Laminates with the higher initial strength are not necessarily those with higher residual values.

7. The observed damage patterns prior to failure consisting of matrix cracks and delaminations are characteristic for each laminate. In general, matrix cracking associated with the hole in surface layers develops quicker and extends further than the matrix cracks in in the other layers. Delaminations can be caused by certain stress situations in the undamaged or low damaged specimen as well as by stresses which are due to the presence of matrix cracks. It was found that delaminations between the surface layer and the adjacent layer where following major cracks in this layer. Moreover, tangent zero-deg cracks are well defined in both laminates and seem to cause delaminations on adjacent

interfaces. In the A-specimen, these delaminations cover a larger area than the other delaminations. In the B-specimen, the wing like delaminations between the 45-deg surface layer and the adjacent 90-deg layer extend further but do not necessarily cover a larger area than the delaminations between the zero-deg and the adjacent -45-deg layer. Since in the A-laminate the zero--deg ply is a surface layer, it has longer zero-deg cracks than the B-laminate and consequently, the area covered by the delaminations initiated by these cracks is much larger than that for the B-specimen.
After the hole-effected damage reaches a maximum, the remaining intersection area develops a uniform damage state that reminds at so called characteristic damage states (CDS) found in unnotched laminates.

8. Zero-deg-matrix cracks tangent to the hole have a major influence on residual strength via relaxation of strain concentrations near the hole. The relationship between crack length and residual strength involves a parameter dependent on the stacking sequence.
Since the zero-deg matrix cracks appear together with delaminations between the zero-deg layer and adjacent layers, and these delaminations cover a large area in both, the A- and the B-laminate compared to the area of delaminations between other layers, it seems likely

that the zero-deg matrix cracks have also a major influence on the stiffness via delamination size. Further work could better quantify these relations.

9. The behavior of the notched laminates during the final stage of lifetime is similar to the behavior of unnotched laminates.

10. The approximate stress analysis indicates where local static failure may occur first. However, it is believed that static failure of a laminate as a sequence of interacting failures at different locations in the laminate can not be predicted by an initial stress distribution alone. The stress analysis is of little use for predicting fatigue damage growth.

References

1. W.W. Stinchcomb and K.L. Reifsnider, " Fatigue Damage Mechanisms in Composite Materials: A Review," Fatigue Mechanisms, J.T. Fong, Ed., ASTM STP 675, American Society for Testing and Materials, 1979, pp. 762-787

2. W.W. Stinchcomb, K.L. Reifsnider, P. Yeung, and J. Masters, " Effect of Ply Constraint on Fatigue Damage Development in Composite Material Laminates," Fatigue of Fibrous Composite Materials, ASTM STP 723, American Society for Testing and Materials, 1981, pp. 64-84

3. G.P. Sendeckyj, G.E. Maddux, and E. Porter, " Damage Documentation in Composites by Stereo Radiography," Damage in Composite Materials, ASTM STP 775, K.L. Reifsnider, Ed., American Society for Testing and Materials, 1982, pp. 16-26

4. Daniel Post, " Optical Interference for Deformation Measurements -- Classical Holographic and Moire Interferometry," Mechanics of Nondestructive Testing, Editor W.W. Stinchcomb, Plenum Press, New York, 1980

5. T.K. O'Brien, " Stiffness Change as a Nondestructive Damage Measurement," Mechanics of Nondestructive Testing, Editor W.W. Stinchcomb, Plenum Press, New York 1980

6. E.T. Camponeschi and W.W. Stinchcomb, " Stiffness Reduction as an Indicator of Damage in Graphite/ Epoxy Laminates," Composite Materials: Testing and Design (Sixth Conference), ASTM STP 787, I.M. Daniel, Ed., American Society for Testing and Materials, 1982, pp. 225-246

7. D. Engrand, " A Boundary Layer Approach to the Calculation of Transverse Stresses along the Free Edges of a Symmetric Laminated Plate of Arbitrary With Under In-plane Loading," Composite Structures, Applied Science Publishers, London and New Jersey

8. C.T. Herakovitch, A. Nagarkar, and D.A. O'Brien, " Failure Analysis of Composite Laminates with Free Edges," Modern Development in Composite Materials and Structures, Edited by J.R. Vinson Published by The American Society of Mechanical

Engineers, New York, 1979

9. I.S. Raju and J.H. Crews,Jr., " Three-Dimensional Analysis of (0/90)s and (90/0)s Laminates With a Central Circular Hole," NASA Technical Memorandum 83300

10. I.S. Raju and J.H. Crews,Jr., " Interlaminar Stress Singularities at a Straight Edge in Composite Laminates," J. of Computers and Structures 14(1-2), 21 (1981). (Also NASA TM-81876, 1980.)

11. E.F. Rybicki and D.W. Schmueser, " Effect of Stacking Sequence and Lay-Up Angle on Free Edge Stresses Around a Hole in a Laminated Plate Under Tension," Journal for Composite Materials, Vol. 12 (July 1978), p. 300

12. S. Tang, " Interlaminar Stresses around Circular Cutouts in Composite Plates under Tension, AIAA Journal, pp.1631-1637, 1977

13. A.S.D. Wang and F.W. Crossman, " Some New Results on Edge Effect in Symmetric Composite Laminates," J. Composite Materials, Vol. 11 (Jan. 1977), p. 92

14. J.D. Whitcomb, " Experimental and Analytical Study of Fatigue Damage in Notched Graphite/Epoxy Laminates," Fatigue of Fibrous Composite Materials, ASTM STO 723, American Society for Testing and Materials, 1981, pp. 48-63

15. S.G. Lekhnitskii, " Theory of Elasticity of an Anisotropic Body," Copyright 1963 by Holden-Day, Inc., 728 Montgomery Street, San Francisco, California

16. J.M. Whitney and R.J. Nuismer, " Stress Fracture Criteria for Laminated Composites Containing Stress Concentrations," J. Composite Materials, Vol. 8/July 1974

17. J.M. Whitney and R.Y. Kim, " Effect of Stacking Sequence on the Notched Strength of Laminated Composites, Composite Materials: Testing and Design (Fourth Conference), ASTM STP 617, American Society for Testing and Materials, 1977, pp. 229-242

18. E.L. Reiss, " Extension of A Thick Infinite Plate With A Circular Hole," IMM-NYU 281, New York, 1961

19. S.P. Timoshenko and J.N. Goodier, " Theory of Elasticity," McGraw-Hill Book Company, New York, 1970

APPENDIX A

The total differential of the complementary energy per volume due to the boundary layer stresses is given by :

$$dU = \varepsilon_R d\sigma_R + \varepsilon_Z d\sigma_Z + \gamma_{Z\theta} d\sigma_{Z\theta} + \gamma_{ZR} d\sigma_{ZR} + \gamma_{R\theta} d\sigma_{R\theta} \qquad (A1)$$

Using the constitutive relation, substituting stresses for strains, and integrating from zero to the final state of stress, we obtain the complementary energy per volume in the form :

$$\begin{aligned} U = \int & (A_{11}\sigma_r + A_{13}\sigma_z + A_{16}\sigma_{R\theta})d\sigma_R \\ + & (A_{13}\sigma_r + A_{33}\sigma_z + A_{36}\sigma_{R\theta})d\sigma_Z \\ + & (A_{44}\sigma_{Z\theta} + A_{45}\sigma_{ZR})d\sigma_{Z\theta} \\ + & (A_{45}\sigma_{Z\theta} + A_{55}\sigma_{ZR})d\sigma_{ZR} \\ + & (A_{16}\sigma_R + A_{36}\sigma_Z + A_{66}\sigma_{R\theta})d\sigma_{R\theta} \end{aligned} \qquad (A2)$$

where the A_{ij} are the elements of the layer-compatibility matrix.

The integrations can be carried out easily after reordering the terms into the following sequence :

$$
\begin{aligned}
U = \int \{ & A_{11}\sigma_R d\sigma_R + A_{13}(\sigma_Z d\sigma_R + \sigma_R d\sigma_Z) + A_{16}(\sigma_{\theta R} d\sigma_R + \sigma_R d\sigma_{R\theta}) \\
+ \quad & A_{33}\sigma_Z d\sigma_Z + A_{36}(\sigma_{R\theta} d\sigma_R + \sigma_Z d\sigma_{R\theta}) \\
+ \quad & A_{44}\sigma_{Z\theta} d\sigma_{Z\theta} + A_{45}(\sigma_{ZR} d\sigma_{Z\theta} + \sigma_{Z\theta} d\sigma_{ZR}) \\
+ \quad & A_{55}\sigma_{Z\theta} d\sigma_{Z\theta} \\
+ \quad & A_{66}\sigma_{R\theta} d\sigma_{R\theta}\}
\end{aligned}
\tag{A3}
$$

The result is :

$$
\begin{aligned}
U = & \tfrac{1}{2}A_{11}\sigma_R^2 + A_{13}\sigma_Z\sigma_R + A_{16}\sigma_{R\theta}\sigma_R \\
& + \tfrac{1}{2}A_{33}\sigma_Z^2 + A_{36}\sigma_{r\theta}\sigma_Z \\
& + \tfrac{1}{2}A_{44}\sigma_{z\theta}^2 + A_{45}\sigma_{ZR}\sigma_{Z\theta} \\
& + \tfrac{1}{2}A_{55}\sigma_{ZR}^2 \\
& + \tfrac{1}{2}A_{66}\sigma_{R\theta}^2
\end{aligned}
\tag{A4}
$$

We recall the assumed stress functions :

$$
\phi = a_{(\eta)} b_{(\rho)} \ , \qquad \psi = c_{(\eta)} d_{(\rho)} \tag{A5}
$$

and express the boundary layer stresses by :

$$
\begin{aligned}
f_{R\theta} &= \psi_{,\rho} &&= cd' \\
f_{Z\theta} &= -\psi_{,\eta} &&= \dot{c}d \\
f_{R} &= \phi_{,\rho\rho} &&= ab'' \\
f_{ZR} &= -\phi_{,\rho\eta} &&= -\dot{a}b' \\
f_{ZZ} &= \phi_{,\eta\eta} &&= \ddot{a}b
\end{aligned}
\qquad \text{(A6)}
$$

where the dash stands for a derivation with respect to the normalized height coordinate ρ and the dot indicates the derivation with respect to the normalized radius η.
With this we are able to represent the complementary energy in terms of the boundary layer stress functions. In addition, we integrate the complementary energy per volume over the laminate thickness and get the average complementary energy per laminate area unit :

$$
\begin{aligned}
\int_{-1}^{1} U d\rho = \int_{-1}^{1} \Big(& \tfrac{1}{2}A_{11}a^2b''^2 + A_{13}\ddot{a}abb'' + A_{16}cd'ab'' \\
& + \tfrac{1}{2}A_{33}\ddot{a}^2b^2 + A_{36}cd'\ddot{a}b \\
& + \tfrac{1}{2}A_{44}\dot{c}^2d^2 + A_{45}\dot{a}b'\dot{c}d \\
& + \tfrac{1}{2}A_{55}\dot{a}^2b'^2 \\
& + \tfrac{1}{2}A_{66}c^2d'^2 \Big)\, d\rho
\end{aligned}
\qquad \text{(A7)}
$$

The energy term has a minimum, where its variation with respect to the functions of η and their derivatives is equal to zero :

$$\delta_a \int_{-1}^{1} U = \int_{-1}^{1} (A_{11} ab''^2 \delta a + A_{13}(a\delta\ddot{a}+\ddot{a}\delta a) + \frac{1}{2}A_{16} d'b''c\delta a + A_{33}\ddot{a}b^2\delta\ddot{a} + \frac{1}{2}A_{36}d'bc\delta\ddot{a} + \frac{1}{2}A_{45}b'd\dot{c}\delta\dot{a} + A_{55}\dot{a}b'^2\delta\dot{a})\, d\rho$$

$$\delta_c \int_{-1}^{1} U = \int_{-1}^{1} (A_{16} d'b''a\delta c + A_{36}d'b\ddot{a}\delta c + A_{44}d^2\dot{c}\delta\dot{c} + A_{45}b'd\dot{a}\delta\dot{c} + A_{66}d'^2c\delta c)\, d\rho \qquad \text{(A8)}$$

Using integration by parts ,

$$\begin{aligned}
\ddot{a}\delta\ddot{a} &= (\ddot{a}\delta\dot{a})^{\cdot} - \dddot{a}\delta\dot{a} = (\ddot{a}\delta\dot{a})^{\cdot} - (\dddot{a}\delta a)^{\cdot} + \ddddot{a}\delta a \\
\dot{a}\delta\ddot{a} &= (\dot{a}\delta\dot{a})^{\cdot} - \ddot{a}\delta\dot{a} = (\dot{a}\delta\dot{a})^{\cdot} - (\ddot{a}\delta a)^{\cdot} + \dddot{a}\delta a \\
a\delta\ddot{a} &= (a\delta\dot{a})^{\cdot} - \dot{a}\delta\dot{a} = (a\delta\dot{a})^{\cdot} - (\dot{a}\delta a)^{\cdot} + \ddot{a}\delta a \\
\dot{a}\delta\dot{a} &= (a\delta\dot{a})^{\cdot} - \ddot{a}\delta a \\
a\delta\dot{a} &= (a\delta a)^{\cdot} - \dot{a}\delta a
\end{aligned} \qquad \text{(A9)}$$

the weak form of these equations can be written as :

$$\delta_a = \int_{-1}^{1} (A_{11}b''^2 a + 2A_{13}bb''\ddot{a} + A_{16}d'b''c + A_{33}b^2\dddot{a} + A_{36}d'b\ddot{c} - A_{45}b'd\ddot{c} - A_{55}b'^2\ddot{a})\,\delta a\, d\rho \tag{A10}$$

$$\delta_c = \int_{-1}^{1} (A_{16}d'b''a + A_{36}d'b\ddot{a} - A_{44}d^2\ddot{c} - A_{45}b'd\ddot{a} + A_{66}d'^2)\delta c\, d\rho$$

The point of the minimum of the elastic energy can be determined by setting the variations equal to zero :

$$\delta_a \int_{-1}^{1} U = \delta_c \int_{-1}^{1} U = 0 \tag{A11}$$

Assuming that the values of δa and δc do not vanish over the domain, we find the equations :

$$\int_{-1}^{1} \{ A_{33}b^2\dddot{a} + (2A_{13}bb''-A_{55}b'^2)\ddot{a} + A_{11}b''^2 a + (A_{36}d'b-A_{45}b'd)\ddot{c} + A_{16}d'b''c \}\, d\rho = 0 \tag{A12}$$

$$\int_{-1}^{1} \{(A_{36}d'b-A_{45}b'd)\ddot{a} + A_{16}d'b''a - A_{44}d^2\ddot{c} + A_{66}d'^2 c \}\, d\ell = 0$$

These equations represent an eigenvalue problem which can be written in the short form :

$$[M]\{\dddot{X}\} + [N]\{\ddot{X}\} + [P]\{X\} = 0 \ , \quad \{X\} = \{{}^{c}_{a}\} \qquad (3.22)$$

APPENDIX B

```
C$JOB
C     ************************************************************************
C     *****                                                              *****
C     ***** THIS PROGRAM EVALUATES A CLOSED FORM SOLUTION FOR THE       *****
C     ***** ANALYSIS OF ALL INTERLAMINAR STRESSES OF AN INFINITE        *****
C     ***** STRIP OF A LAMINATE WITH A CIRCULAR HOLE                    *****
C     *****                                                              *****
C     ************************************************************************
C
C     -----LIST OF SUBROUTINES
C
C     -----REDATA             READ AND GENERATE DATA
C
C     -----FLEX               COMPLIANCES AND STIFFNESSES
C
C     -----PLANE              PLANE STRESS SOLUTION
C
C     -----LAMINA             LAYER STRESSES IN CYLINDRICAL COORDINATES
C
C     -----FUNETA             STRESS FUNCTIONS, FUNCTIONS OF THE HEIGHT
C
C     -----BOULAY             THREE DIMENSIONAL BOUNDARY LAYER STRESSES
C
C     -----ENERGY             STRAIN ENERGY OR TSAI-WU-FAILURE CRITERION
C
C     -----TRANS              TRANSFORM IN OTHER COORDINATE SYSTEMS
C
C     -----STRAIN             COMPUT THE STRAINS
C
C     -----PRIRES             PRINT THE RESULTS
C
C     -----PLORES             PLOT THE  RESULTS
C
C     -----MATMLT             MATRIX MULTIPLICATION
C
C     -----ANISOT             OVERALL SOLUTION FOR ANISOTROPIC LAMINATES
C
C     -----ZCPOLY             IMSL ROUTINE, FINDS COMPLEX ROOTS
C
C     -----NUMINT             NUMERICAL INTEGRATION THROUGH THE THICKNESS
C
C     -----KUPO               FAST & ACCURATE ROOTFINDER CUBIC POLYNOMIAL
C
C     -----LEQ2C              IMSL ROUTINE, SOLVE SYSTEM OF EQUATIONS
C
C     -----NEWTON             FIND ZEROS OF A FUNCTION
C
C     -----PLOTS, SCALE, AXIS, PLOT, NEWPEN, FACTOR, LINE, VPISYM, AND
C     -----NUMBER ARE LIBRARY ROUTINES
C
C    ----------------------------------FOLLOWING DIMENSIONS EQUAL TO M
      COMPLEX S1,S2,S3,S4,RMUE(3),ALPHA(3),E1(3),E2(3)
      REAL Q11(4),Q12(4),Q16(4),Q22(4),Q26(4),Q66(4)
      REAL        A11(4),A13(4),A16(4),A33(4)
      REAL A36(4),A44(4),A45(4),A55(4),A66(4)
      REAL S12(4),S22(4),S23(4),S26(4)
      REAL SR(4),ST(4),SRT(4)
      REAL THEPLY(4)
C     -------------------------------FOLLOWING DIMENSIONS EQUAL TO IDIV
      REAL STRESS(101,7),AX(101,7),AY(101,7)
      REAL SIG1(101),SIG2(101),SIG3(101)
```

```
      REAL SIG4(101),SIG5(101),SIG6(101)
      REAL ENERG(101)
      REAL ST1(6,6)
      REAL EPS1(101),EPS2(101),EPS3(101)
      REAL EPS4(101),EPS5(101),EPS6(101)
      REAL ETA(101),RHO(101)
      DOUBLE PRECISION THETA(101)
C     ------------------------------------THIS DIMENSION EQUAL TO SEVEN
      INTEGER IPLOT(7)
C     ------------------------------------------READ  AND  GENERATE DATA
      PI = 3.141592653589793
      READ 800,IWU
      READ 800,ITRANS
      READ 800,ISTRN
      READ 800,IMAT
      READ 800,M2
      M=M2/2
      IDIV = 1
      CALL REDATA(RHO,THETA,ETA,I10,J20,K30,
     $            H2,THEPLY,THICK,
     $            M2,DIAMTR,RADIUS,P,SECT,
     $            IDIV,IOPT,IPRINT,NPLOT,IPLOT)
C     ------------------------------------------------------DATA PRINTOUT
      IF(IPRINT.LE.1) GOTO 1000
      PRINT 900
      PRINT 901,ITRANS,ISTRN,IMAT,M2,H2,DIAMTR
      DO 100 I=1,M
      ANGLE   = THEPLY(I)*180.0/PI
  100 PRINT 902,I,ANGLE
      DO 200 I=1,IDIV
      ANGLE   = THETA(I)*180.0/PI
  200 PRINT 903,I,RHO(I),ANGLE,ETA(I)
      PRINT 904,THICK,IOPT
C     ------------------------------PROPERTIES OF AN ISOTROPIC MATERIAL
 1000 IF(IMAT.GT.0) GOTO 1
      E11     =  1000.0
      E22     = E11
      E33     = E11
      RNUE12 = 0.3
      RNUE13 = RNUE12
      RNUE23 = RNUE12
      G12     = E11/(2.*(1.+RNUE12))
      G13     = G12
      G23     = G12
      GOTO 3
C     ------------------------------------ PROPERTIES FOR GRAPHITE EPOXY
    1 IF(IMAT.EQ.2) GOTO 2
      E11     =  19.2          * 1000000.0
      E22     =   1.56         * 1000000.0

      E33     = E22
      G12     =   0.82         * 1000000.0
      G13     = G12
      G23     =   0.487        * 1000000.0
      RNUE12 =   0.21
      RNUE13 = RNUE12
      RNUE23 = RNUE12
      GOTO 3
C     ------------------------------------------PROPERTIES FOR BORON/EPOXY
    2 E11     =30.6            * 1000000.0
      E22     = 3.5            * 1000000.0
      E33     = E22
      G12     = 1.0            * 1000000.0
      G13     = G12
      G23     = G12
      RNUE12 = 0.36
      RNUE13 = RNUE12
      RNUE23 = RNUE12
C     ---------------------------------------INITIATE THE TOTAL STRESSES
```

```
    3 DO 300 I=1,IDIV
      SIG1(I) = 0.0
      SIG2(I) = 0.0
      SIG3(I) = 0.0
      SIG4(I) = 0.0
      SIG5(I) = 0.0
  300 SIG6(I) = 0.0
C     ------------------------------------------------CONSTITUTIVE VALUES
      ICYL = 0
      CALL FLEX(B11,B12,B16,B22,B26,B66,
     $          Q11,Q12,Q16,Q22,Q26,Q66,
     $          A11,A13,A16,A33,A36,A44,A45,A55,A66,
     $          S12,S22,S23,S26,ST1,
     $          M,H2,THEPLY,THETA,IDIV,1,M2,
     $          E11,E22,E33,G12,G13,G23,RNUE12,RNUE13,RNUE23,
     $          IPRINT,ICYL)
      ICYL = 1
      ILEK = 1
C     ------------------------------------------------LOOP ON VARIABLE RHO
      DO  10 I=1,I10
C
      IRHO    = IFIX((RHO(I)-0.00001)*FLOAT(M))
      IF(IRHO.LT.0) IRHO = 0
      IPLY    = M - IRHO
      RHOI    = FLOAT(IRHO)/FLOAT(M)
C     ------------------------------------------------LOOP ON VARIABLE THETA
    6 DO  20 J=1,J20
C
      IF(IOPT.EQ.2) ICYL = 1
                                        ISWITC = 2
      IF(IOPT.EQ.2.AND.ETA(1).NE.0.0) ISWITC = 1
      IF(IOPT.EQ.1.AND.ETA(1).NE.0.0) ISWITC = 1
C     ------------------------------------------------LOOP ON VARIABLE   ETA
      DO  30 K=1,K30
C
    4                 R = ETA(K)*H2    + DIAMTR/2.
      IF(ISWITC.EQ.1) R =                DIAMTR/2.
C     ------------------------------------OVERALL PLANE STRESS SOLUTION
      IF(IOPT.EQ.1.AND.I.GT.1.AND.ETA(K).EQ.0.0) GOTO 12
      CALL PLANE(PSR,PST,PSRT,
     $           THETA,IDIV,J,
     $           RADIUS,R,THICK,P,
     $           B11,B12,B16,B22,B26,B66,
     $           RNUE12,G12,
     $           S1,S2,S3,S4,
     $           ILEK,IPRINT,M,H2)
      IF(IPRINT.EQ.3) PRINT 907,PSR,PST,PSRT
      ILEK = 0
C     ------------------------------------------------LAMINA STRESSES
      CALL LAMINA(SR,ST,SRT,
     $            PSR,PST,PSRT,
     $            Q11,Q12,Q16,Q22,Q26,Q66,
     $            B11,B12,B16,B22,B26,B66,
     $            THETA,J,IDIV,M,
     $            IPRINT)
      IF(IMAT.EQ.0) GOTO 15
C     ------------------------------------COMPUTE THE STRESSFUNCTIONS
      IF(ISWITC.LT.1.OR.K.NE.1) GOTO 5
C     ---------------------------------COMPUTE A-MATRIX FOR NEW ANGLES
      IF(IOPT.NE.2.AND.ICYL.NE.1) GOTO 12
      CALL FLEX(B11,B12,B16,B22,B26,B66,
     $          Q11,Q12,Q16,Q22,Q26,Q66,
     $          A11,A13,A16,A33,A36,A44,A45,A55,A66,
     $          S12,S22,S23,S26,ST1,
     $          M,H2,THEPLY,THETA,IDIV,J,IPLY,
     $          E11,E22,E33,G12,G13,G23,RNUE12,RNUE13,RNUE23,
     $          IPRINT,ICYL)
      ICYL = 0
```

```
C     ------------------------------------------------STRESSFUNCTIONS
   12 II = I
      IF(IOPT.EQ.3.AND.K.GT.1) GOTO 14
      IFAIL = 0
      CALL FUNETA(ALPHA,
     $            B,BP,BPP,D,DP,
     $            RMUE,E1,E2,
     $                A11,A13,A16,A33,
     $            A36,A44,A45,A55,A66,
     $            SR,SRT,
     $            RHO,IDIV,RHOI,
     $            M,H2,II,
     $            IPRINT,IFAIL,IOPT)
      IF(IFAIL.NE.0) GOTO 13
   14 IF(IOPT.EQ.2.AND.K30.EQ.1) ISWITC = ISWITC - 1
      IF(IOPT.EQ.1.AND.K30.EQ.1) ISWITC = ISWITC - 1
      IF(ISWITC.EQ.0) GOTO 4
C     ------------------------------------------BOUNDARY LAYER SOLUTION
      IF(IFAIL.EQ.2) GOTO 13
    5 CALL BOULAY(FR,FT,FZ,FRT,FZT,FZR,
     $            B,BP,BPP,D,DP,
     $            RMUE,E1,E2,
     $            ALPHA,
     $            S12,S22,S23,S26,
     $            ETA,IDIV,K,M,IPLY,IPRINT)
   13 IF(IPRINT.EQ.3) PRINT 910, FR,FT,FZ,FRT,FZT,FZR
C     ------------------------------------------------TOTAL STRESSES
   15                L=K
      IF(IOPT.EQ.2) L=J
      IF(IOPT.EQ.1) L=I
      SIG1(L)=  SR(IPLY) + FR
      SIG2(L)=  ST(IPLY) + FT
      SIG3(L)=             FZ
      SIG4(L)=             FZT
      SIG5(L)=             FZR
      SIG6(L)= SRT(IPLY) + FRT
C     ------------------------------------------------STRAIN ENERGY
      CALL ENERGY(ENERG,
     $            SIG1,SIG2,SIG3,SIG4,SIG5,SIG6,
     $            ST1,IWU,
     $            THETA,THEPLY,
     $            L,J,IPLY,IDIV,M,ITRANS)
C     ----------------------------------TRANSFORM INTO ANOTHER SYSTEM
      IF(ITRANS.EQ.0.OR.IWU.EQ.1) GOTO 7
      CALL TRANS(SIG1,SIG2,SIG3,SIG4,SIG5,SIG6,
     $           THETA,THEPLY,
     $           L,J,IPLY,IDIV,M,ITRANS)
C
    7 IF(ISTRN.NE.1.OR.ITRANS.NE.0.OR.IWU.EQ.1) GOTO 30
      CALL STRAIN(EPS1,EPS2,EPS3,EPS4,EPS5,EPS6,
     $            SIG1,SIG2,SIG3,SIG4,SIG5,SIG6,
     $            ST1,THETA,
     $            IDIV,L)
C
   30 CONTINUE
   20 CONTINUE
   10 CONTINUE
C     ------------------------------------------------PRINT THE SOLUTION
      IF(IPRINT.EQ.0) GOTO 8
      CALL PRIRES(SIG1,SIG2,SIG3,SIG4,SIG5,SIG6,ENERG,
     $            THETA,ETA,RHO,
     $            IDIV,IOPT)
C     ------------------------------------------------PLOT THE STRESSES
    8 I1=NPLOT+1
      IF(NPLOT.EQ.0.OR.ISTRN.EQ.1) GOTO 9
      CALL PLORES(SIG1,SIG2,SIG3,SIG4,SIG5,SIG6,ENERG,
     $            RHO,THETA,ETA,THEPLY,
     $            DIAMTR,THICK,
     $            M,IOPT,NPLOT,IPLOT,IMAT,ITRANS,I1,IDIV,IWU)
```

```
C     ------------------------------------------------PLOT THE STRAINS
    9 IF(ISTRN.NE.1) GOTO 11
      CALL PLORES(EPS1,EPS2,EPS3,EPS4,EPS5,EPS6,ENERG,
     $            RHO,THETA,ETA,
     $            DIAMTR,THICK,
     $            M,IOPT,NPLOT,IPLOT,IMAT,ITRANS,I1,IDIV,IWU)
   11 STOP
C
C     ***************************************************************************
C     *****                                                                 *****
C     *****       F   O   R   M   A   T   S                                 *****
C     *****                                                                 *****
C     ***************************************************************************
C
  800 FORMAT(I5)
  900 FORMAT(1H1,/,' * * * * * * * * * * * * * * * * * * * * * * * * * * * * * *
     $ * * * * * * * * * * * * * * * * * * * * * * * * * * * * * * * * * * * *',/,
     $              ' * * * * * * * * * * * * *
     $                                * * * * * * * * * * * * * * * * * * * * *',/,
     $              ' * * * * * * * * * * * * *                 D         A
     $       T          A             * * * * * * * * * * * * * * * * * * * * *',/,
     $              ' * * * * * * * * * * * * *
     $                                * * * * * * * * * * * * * * * * * * * * *',/,
     $              ' * * * * * * * * * * * * * * * * * * * * * * * * * * * * * *
     $ * * * * * * * * * * * * * * * * * * * * * * * * * * * * * * * * * * * *',//
     $///)
  901 FORMAT(' ITRANS=',I2,//,
     $' ITRANS=0         RESULTS IN CYLINDRICAL COORDINATES',/,
     $' ITRANS=1         RESULTS IN SYSTEM      COORDINATES',/,
     $' ITRANS=2         RESULTS IN MATERIAL    COORDINATES',///,
     $' ISTRN= ',I2,//,
     $' ISTRN=0          STRESSES',/,
     $' ISTRN=1          STRAINS',///,
     $' IMAT=  ',I2,//,
     $' IMAT=0           ISOTROPIC MATERIAL STEEL',/,
     $' IMAT=1           GRAPHITE/EPOXY PROPERTIES',/,
     $' IMAT=2           BORON/EPOXY PROPERTIES',///,
     $' NUMBER OF LAYERS    :',I2,/,
     $' LAYERTHICKNESS      :',F7.4,/,
     $' HOLE DIAMETER       :',F7.4,//)
  902 FORMAT(1H ,' LAYER',I2,'          FIBER DIRECTION :',F7.1//)
  903 FORMAT(' POINT',I3,': RHO =',F5.2,' THETA =',F5.1,' ETA =',F9.4,/)
  904 FORMAT(' LAMINATE THICKNESS =',F7.4,///,' OPTION',I2,/
     $/,' OPTION 1 :       STRESSES ALONG THE VARIABLE RHO  (HEIGHT)',/,
     $  ' OPTION 2 :       STRESSES ALONG THE VARIABLE THETA (ANGLE)',/,
     $  ' OPTION 3 :       STRESSES ALONG THE RADIUS',///)
  907 FORMAT(' SX :',E14.4,'    SY :',E14.4,'    SXY :',E14.4,//)
  910 FORMAT('  FR :',F14.4,/,'  FT :',F14.4,/,'  FZ :',F14.4,/,' FRT :'
     $,F14.4,/,' FZT :',F14.4,/,' FZR :',F14.4,///)
      END
C
C     ***************************************************************************
C     *****                                                                 *****
C     *****       S   U   B   R   O   U   T   I   N   E   S                 *****
C     *****                                                                 *****
C     ***************************************************************************
C
      SUBROUTINE REDATA(RHO,THETA,ETA,I10,J20,K30,
     $                  H2,THEPLY,THICK,
     $                  M2,DIAMTR,RADIUS,P,SECT,
     $                  IDIV,IOPT,IPRINT,NPLOT,IPLOT)
C
C     ***************************************************************************
C     *****                                                                 *****
C     *****  R E A D I N G  A N D  G E N E R A T I N G  D A T A              *****
C     *****                                                                 *****
C     ***************************************************************************
C
```

```
      DOUBLE PRECISION THETA(101)
      REAL             ETA(101),RHO(101),THEPLY(4)
      INTEGER          IPLOT(7)
C     ------------------------------------------------------------READING
      PI        =3.141592653589793
      M         =M2/2
      THICK     =0.0
      READ 900,H2
      DO  10  I=1,M
      READ 900,THEPLY(I)
      THEPLY(I)=THEPLY(I)*PI/180.0
   10 THICK     =THICK+H2*2.
      READ 900,DIAMTR,P
      READ 900,COORD1,COORD2,COORD3,COORD4,IDIV
      READ 910,IOPT,IPRINT
      READ 910,NPLOT
      IF(NPLOT.EQ.0) GOTO 12
      DO  11  I=1,NPLOT
   11 READ 911,IPLOT(I)
   12 RADIUS    =DIAMTR/2.
      KDIV      = IDIV - 1
C     ------------------------------------------------------------GENERATE
      I10 = 1
      J20 = 1
      K30 = 1
C     ----------------------------------OPTION 1       (HEIGHT VARIABLE)
      IF(IOPT.NE.1) GOTO 2
      I10       = IDIV
      SECT      =COORD2-COORD1
      RHODIV  = (COORD2-COORD1)/FLOAT(KDIV)
      DO  20 I=1,IDIV
      RHO(I)  = RHODIV*(I-1) + COORD1
      THETA(I)= COORD3*PI/180.0
   20 ETA(I)  = COORD4
      GOTO 4
C     ----------------------------------OPTION 2       (ANGLE  VARIABLE)
    2 IF(IOPT.NE.2) GOTO 3
      J20       = IDIV
      SECT      =(COORD3-COORD2)*PI/180.0
      THEDIV  =((COORD3-COORD2)*PI/180.0)/FLOAT(KDIV)
      DO  30 I=1,IDIV
      RHO(I)  =COORD1
      THETA(I)=COORD2*PI/180.0+THEDIV*(I-1)
   30 ETA(I)  = COORD4
      GOTO 4
C     ----------------------------------OPTION 3       (RADIUS VARIABLE)
    3 K30       = IDIV
      SECT      = COORD4-COORD3
      ETDIV   = SECT/FLOAT(KDIV)
      DO  40 I=1,IDIV
      RHO(I)  = COORD1
      THETA(I)= COORD2*PI/180.0
   40 ETA(I)  = ETDIV*(I-1)+COORD3
C     ---------------------------------END
    4 RETURN
  900 FORMAT(4F10.4,I5)
  910 FORMAT(2I5)
  911 FORMAT(I5)
      END
C
C     ---------------------------------------------------------------
C
      SUBROUTINE FLEX(B11,B12,B16,B22,B26,B66,
     $                Q11,Q12,Q16,Q22,Q26,Q66,
     $                A11,A13,A16,A33,A36,A44,A45,A55,A66,
     $                S12,S22,S23,S26,ST1,
     $                M,H2,THEPLY,THETA,IDIV,JJ,IPLY,
     $                E11,E22,E33,G12,G13,G23,RNUE12,RNUE13,RNUE23,
     $                IPRINT,ICYL)
```

```
C
C     ************************************************************************
C     *****                                                              *****
C     *****          F  L  E  X  I  B  I  L  I  T  I  E  S               *****
C     *****                                                              *****
C     ************************************************************************
C
      REAL A11(M),A13(M),A16(M),A33(M),A36(M),A44(M),A45(M),A55(M)
      REAL A66(M)
      REAL S12(M),S22(M),S23(M),S26(M)
      REAL S0(6,6),T(6,6),TT(6,6),ST(6,6),ST1(6,6),ZW(6,6)
      REAL Q11(M),Q12(M),Q16(M),Q22(M),Q26(M),Q66(M)
      REAL THEPLY(M)
      DOUBLE PRECISION THETA(IDIV)
C     ------------------------------------------------COMPLIANCE MATRIX
      DO  10 I=1,6
      DO  10 J=1,6
   10 S0(I,J) = 0.0
C
      S0(1,1) =       1./E11
      S0(1,2) = - RNUE12/E11
      S0(1,3) = - RNUE13/E11
      S0(2,2) =       1./E22
      S0(2,3) = - RNUE23/E22
      S0(3,3) =       1./E33
      S0(4,4) =       1./G23
      S0(5,5) =       1./G13
      S0(6,6) =       1./G12
C
      DO  20 I=1,6
      DO  20 J=1,I
   20 S0(I,J)=S0(J,I)
C     ----------------------------------------LOOP ON NUMBER OF LAYERS
      RA11 = 0.0
      RA12 = 0.0
      RA16 = 0.0
      RA22 = 0.0
      RA26 = 0.0
      RA66 = 0.0
C
      DO  30 N=1,M
      ARG =   THEPLY(N)
      IF(ICYL.NE.0) ARG =   THEPLY(N) - THETA(JJ)
      RN = SIN(ARG)
      RM = COS(ARG)
C     ------------------------------------------TRANSFORMATION MATRIX
      DO  31 I=1,6
      DO  31 J=1,6
   31 T(I,J) = 0.0
C
      T(1,1) = RM*RM
      T(1,2) = RN*RN
      T(1,6) = 2.0*RM*RN
      T(2,1) = T(1,2)
      T(2,2) = T(1,1)
      T(2,6) =-T(1,6)
      T(3,3) = 1.0
      T(4,4) = RM
      T(4,5) =-RN
      T(5,4) =-T(4,5)
      T(5,5) = T(4,4)
      T(6,1) = T(2,6)/2.0
      T(6,2) =-T(6,1)
      T(6,6) = RM*RM-RN*RN
C     ----------------------------THE TRANSPOSED TRANSFORMATION MATRIX
      DO  40 I=1,6
      DO  40 J=1,6
   40 TT(I,J)=T(J,I)
C     ---------------------------------COMPLIANCE IN SYSTEM COORDINATES
      CALL MATMLT(TT,6,6,S0,6,ZW)
      CALL MATMLT(ZW,6,6,T,6,ST)
```

```
C     ---------------------------LAYER COMPLIANCE FOR STRAIN COMPUTATION
      IF(N.NE.IPLY) GOTO 1
      DO  50 I=1,6
      DO  50 J=1,6
   50 ST1(I,J)=ST(I,J)
C
    1 S12(N) = ST(1,2)
      S22(N) = ST(2,2)
      S23(N) = ST(2,3)
      S26(N) = ST(2,6)
C     ------------------------------------REDUCED COMPLIANCE COEFFICIENTS
      A11(N) = ST(1,1) - ST(1,2)*ST(2,1)/ST(2,2)
      A13(N) = ST(1,3) - ST(1,2)*ST(2,3)/ST(2,2)
      A16(N) = ST(1,6) - ST(1,2)*ST(2,6)/ST(2,2)
      A33(N) = ST(3,3) - ST(3,2)*ST(2,3)/ST(2,2)
      A36(N) = ST(3,6) - ST(3,2)*ST(2,6)/ST(2,2)
      A44(N) = ST(4,4)
      A45(N) = ST(4,5)
      A55(N) = ST(5,5)
      A66(N) = ST(6,6) - ST(6,2)*ST(2,6)/ST(2,2)
C     ------------------------------------------------MAKE ZEROS EXACT

      EPS                    = 1.E-5*A33(N)
      APS                    = ABS(A16(N))
      IF(APS.LT.EPS) A16(N) = 0.0
      APS                    = ABS(A36(N))
      IF(APS.LT.EPS) A36(N) = 0.0
      APS                    = ABS(A45(N))
      IF(APS.LT.EPS) A45(N) = 0.0
C     ---------------------------------------PRINT LAMINA COMPLIANCES
      IF(IPRINT.EQ.4) PRINT 900,N,THEPLY(N),A11(N),A13(N),A16(N),
     $                     A33(N),A36(N),A44(N),A45(N),A55(N),A66(N)
      IF(ICYL.NE.0) GOTO 30
C     ---------------------------------PLANE STRESS STIFFNESS MATRIX
      DET = ST(1,1)*ST(2,2)*ST(6,6)+ST(1,2)*ST(2,6)*ST(1,6)
     $                             +ST(1,2)*ST(2,6)*ST(1,6)
     $    - ST(1,6)*ST(2,2)*ST(1,6)-ST(2,6)*ST(2,6)*ST(1,1)
     $                             -ST(1,2)*ST(1,2)*ST(6,6)
      Q11(N) = (ST(2,2)*ST(6,6)-ST(2,6)*ST(2,6))/DET
      Q12(N) =-(ST(1,2)*ST(6,6)-ST(2,6)*ST(1,6))/DET
      Q16(N) = (ST(1,2)*ST(2,6)-ST(2,2)*ST(1,6))/DET
      Q22(N) = (ST(1,1)*ST(6,6)-ST(1,6)*ST(1,6))/DET
      Q26(N) =-(ST(1,1)*ST(2,6)-ST(1,2)*ST(1,6))/DET
      Q66(N) = (ST(1,1)*ST(2,2)-ST(1,2)*ST(1,2))/DET
      EPS                    = 1.E-4*Q66(N)
      APS                    = ABS(Q16(N))
      IF(APS.LT.EPS) Q16(N) = 0.0
      APS                    = ABS(Q26(N))
      IF(APS.LT.EPS) Q26(N) = 0.0
      IF(IPRINT.EQ.4)PRINT 902,Q11(N),Q12(N),Q16(N),Q22(N),Q26(N),Q66(N)
C     ---------------------------------------ASSEMBLE THE B(I,J) MATRIX
      RA11 = RA11 + 2.*Q11(N)*H2
      RA12 = RA12 + 2.*Q12(N)*H2
      RA16 = RA16 + 2.*Q16(N)*H2
      RA22 = RA22 + 2.*Q22(N)*H2
      RA26 = RA26 + 2.*Q26(N)*H2
      RA66 = RA66 + 2.*Q66(N)*H2
   30 CONTINUE
      IF(ICYL.NE.0) GOTO 999
C     ---------------------------------------INVERSION OF THE A MATRIX
      DET = RA11*RA22*RA66+RA12*RA26*RA16
     $                             +RA12*RA26*RA16
     $    - RA16*RA22*RA16-RA26*RA26*RA11
     $                             -RA12*RA12*RA66
      B11 = (RA22*RA66-RA26*RA26)/DET
      B12 =-(RA12*RA66-RA26*RA16)/DET
      B16 = (RA12*RA26-RA22*RA16)/DET
      B22 = (RA11*RA66-RA16*RA16)/DET
      B26 =-(RA11*RA26-RA12*RA16)/DET
      B66 = (RA11*RA22-RA12*RA12)/DET
```

```
      EPS                = 1.E-05*B66
      APS                = ABS(B16)
      IF(APS.LT.EPS) B16 = 0.0
      APS                = ABS(B26)
      IF(APS.LT.EPS) B26 = 0.0
      IF(IPRINT.EQ.4) PRINT 901,B11,B12,B16,B22,B26,B66
  999 RETURN
  901 FORMAT('  B11=',F20.15,'  B12=',F20.15,'  B16=',F20.15,/,
     $       '  B22=',F20.15,'  B26=',F20.15,'  B66=',F20.15,///)
  902 FORMAT(' Q11=',F20.10,'  Q12=',F20.10,'  Q16=',F20.10,/,'  Q22=',
     $F20.10,'  Q26=',F20.10,'  Q66=',F20.10,///)
  900 FORMAT('  NUMBER OF LAYER :',I2,'  FIBERORIENTATION :',F10.4,//,
     $'  A11=',E9.2,'  A13=',E9.2,
     $'  A16=',E9.2,'  A33=',E9.2,'  A36=',E9.2,'  A44=',E9.2,
     $'  A45=',E9.2,'  A55=',E9.2,/,'  A66=',E9.2,///)
      END
C
C     ------------------------------------------------------------------
C
      SUBROUTINE MATMLT(A,M,N,B,L,C)
      DIMENSION A(M,N),B(N,L),C(M,L)
      DO  10 I=1,M
      DO  10 J=1,L
      C(I,J)  =0.0
      DO  10 K=1,N
   10 C(I,J)  =C(I,J)+A(I,K)*B(K,J)
      RETURN
      END
C
C     ------------------------------------------------------------------
C
      SUBROUTINE PLANE(PSR,PST,PSRT,
     $                 THETA,IDIV,J,
     $                 RADIUS,R,THICK,P,
     $                 B11,B12,B16,B22,B26,B66,
     $                 RNUE12,G12,
     $                 S1,S2,S3,S4,
     $                 ILEK,IPRINT,M,H2)
C
C     ********************************************************************
C     *****                                                          *****
C     *****       P L A N E    S T R E S S    S O L U T I O N      *****
C     *****                                                          *****
C     ********************************************************************
C
      COMPLEX S1,S2,S3,S4
      DOUBLE PRECISION THETA(IDIV)
C     ---------------------------------------CRITERIONS FOR QUASIISOTROPY
      QUAS1 = ABS(B16)
      QUAS2 = ABS(B26)
      QUAS3 = ABS((B22-B11)/B11)
      QUAS4 = ABS(B12/B11+RNUE12)
      QUAS5 = ABS(2.*(B11-B12)-1./(2.*H2*M*G12))
      QUASI =   QUAS1  +  QUAS2  +  QUAS3  +  QUAS4  +  QUAS5
      IF(IPRINT.EQ.3.AND.ILEK.EQ.1)PRINT 800,QUAS1,QUAS2,QUAS3,QUAS4,
     $QUAS5
  800 FORMAT(' QUASIISOTROPIC CRITERIA :',5E9.2,/)
      IF(QUASI.LT.1.E-01) GOTO 1
C     ------------------------------------------------ANISOTROPIC PROPERTIES
      CALL ANISOT(PSR,PST,PSRT,
     $            THETA,IDIV,J,
     $            RADIUS,R,THICK,P,
     $            B11,B12,B16,B22,B26,B66,
     $            S1,S2,S3,S4,
     $            ILEK,IPRINT)
      GOTO 999
```

```
C     ------------------------------------------QUASIISOTROPIC PROPERTIES
    1 ARG = 2.*THETA(J)
      A   = RADIUS/R
      PSR =  0.5*P*THICK*((1.-A*A)+(1.+3.*A*A*A*A-4.*A*A)*COS(ARG))
      PST =  0.5*P*THICK*((1.+A*A)-(1.+3.*A*A*A*A)       *COS(ARG))
      PSRT= -0.5*P*THICK*( 1.-3.*A*A*A*A+2.*A*A )         *SIN(ARG)
C
  999 RETURN
      END
C
C     ---------------------------------------------------------------
C
      SUBROUTINE ANISOT(PSR,PST,PSRT,
     $                  THETA,IDIV,J,
     $                  RADIUS,R,THICK,P,
     $                  B11,B12,B16,B22,B26,B66,
     $                  S1,S2,S3,S4,
     $                  ILEK,IPRINT)
C
C     ********************************************************************
C     *****                                                          *****
C     *****    PLANE STRESS SOLUTION FOR ANISOTROPIC LAMINATES       *****
C     *****                                                          *****
C     ********************************************************************
C
      REAL        RA(10),RZ(8)
      COMPLEX     A(5),Z(4),S1,S2,S3,S4
      EQUIVALENCE (A(1),RA(1)),(Z(1),RZ(1))
      COMPLEX     UNITR,UNITI,CX,CY,CR,Z1,Z2
      COMPLEX     PI1,PI2,PHI0,PSI0,RAD1,RAD2,CVAL1,CVAL2,ROOT1,ROOT2
      COMPLEX     CP,C1,CDIV1,CDIV2
      DOUBLE PRECISION THETA(IDIV)
C
      IF(ILEK.EQ.0) GOTO 4
C
      A1 =       B11
      A2 = - 2.*B16
      A3 =   2.*B12+B66
      A4 = - 2.*B26
      A5 =       B22
      A(1) = CMPLX(A1,0.0)
      A(2) = CMPLX(A2,0.0)
      A(3) = CMPLX(A3,0.0)
      A(4) = CMPLX(A4,0.0)
      A(5) = CMPLX(A5,0.0)
C     ------------------------------------------COMPUTE THE COMPLEX ROOTS
      CALL ZCPOLY(RA,4,RZ,IER)
C     ------------------------------------------BRING THE ROOTS IN ORDER
      RMAX    = 0.0
      IMAX    = 1
      DO 100 I=1,4
      ABSRES  = ABS( REAL(Z(I))   )
      IF(ABSRES.GT.RMAX) IMAX = I
  100 RMAX    = ABS( REAL(Z(IMAX)))
      ALPHA1  =      REAL(Z(IMAX))
      PRO     = ALPHA1*ABS(ALPHA1)
      BETA1   = ABS(AIMAG(Z(IMAX)))
      RMIN    = RMAX
      IMIN    = 1
      DO 200 I=1,4
      ABSRES  = ABS( REAL(Z(I))   )
      IF(ABSRES.LT.RMIN) IMIN = I
  200 RMIN    = ABS( REAL(Z(IMIN)))
      ALPHA2  =      REAL(Z(IMIN))
      BETA2   = ABS(AIMAG(Z(IMIN)))
      IF(PRO) 1,1,2
    1 S2 = CMPLX(ALPHA1,BETA1)
      S1 = CMPLX(ALPHA2,BETA2)
      GOTO 3
    2 S2 = CMPLX(ALPHA2,BETA2)
      S1 = CMPLX(ALPHA1,BETA1)
    3 S3 = CONJG(S1)
      S4 = CONJG(S2)
```

```
C
      CRIT = ABS((REAL(S1)-REAL(S2))/REAL(S2))
      IF(CRIT.GT.1.E-03) GOTO 4
      D=(ABS( REAL(S1))+ABS( REAL(S2))+ABS( REAL(S3))+ABS( REAL(S4)))/4.
      E=(ABS(AIMAG(S1))+ABS(AIMAG(S2))+ABS(AIMAG(S3))+ABS(AIMAG(S4)))/4.
      S1 = CMPLX(D,E)
      S2 = CMPLX(-D,E)
C
    4 IF(IPRINT.GT.4) PRINT 900,S1,S2,S3,S4
  900 FORMAT(2E15.7,/,2E15.7,/,2E15.7,/,2E15.7,//)
C     ------------------------------------------------LEKHNITSKII FORMULAS
      X      = R * DCOS(THETA(J))
      Y      = R * DSIN(THETA(J))
      UNITR = CMPLX(1.0,0.0)
      UNITI = CMPLX(0.0,1.0)
      CX     = CMPLX(X,0.0)
      CY     = CMPLX(Y,0.0)
      CR     = CMPLX(RADIUS,0.0)
      CP     = CMPLX(P,0.0)
      IF(IPRINT.GT.4) PRINT 801,CX,CY,CR,CP
      Z1     = CX + S1*CY
      Z2     = CX + S2*CY
      PI1    = CMPLX(2.*RADIUS,0.0)
      PI2    = CMPLX(2.*RADIUS,0.0)
      IF(IPRINT.GT.4) PRINT 802,Z1,Z2,PI1,PI2
      CVAL1 = CR + CR*UNITI*S1
      CVAL2 = CR + CR*UNITI*S2
      IF(IPRINT.GT.4) PRINT 803,CVAL1,CVAL2
      RAD1   = Z1*Z1 - CR*CR*(UNITR + S1*S1)
      RAD2   = Z2*Z2 - CR*CR*(UNITR + S2*S2)
      ROOT1 = CSQRT(RAD1)
      ROOT2 = CSQRT(RAD2)
      IF(IPRINT.GT.4) PRINT 804.RAD1.RAD2.ROOT1.ROOT2
      C1     = UNITR
      CDIV1 = Z1/ROOT1
      CDIV2 = Z2/ROOT2
      RDIV1 = REAL(CDIV1)
      RDIV2 = REAL(CDIV2)
      ADIV1 = ABS(RDIV1)
      ADIV2 = ABS(RDIV2)
      IF(IPRINT.GT.4) PRINT 805,CDIV1,CDIV2,RDIV1,RDIV2,ADIV1,ADIV2
      PRO1   = RDIV1*ADIV1
      PRO2   = RDIV2*ADIV2
      IF(PRO1.LT.0.0) CDIV1 = - CDIV1
      IF(PRO2.LT.0.0) CDIV2 = - CDIV2
      PHI0   = - UNITI*CP*PI1/(4.*(S1-S2)*CVAL1)*(UNITR-CDIV1)
      PSI0   =   UNITI*CP*PI2/(4.*(S1-S2)*CVAL2)*(UNITR-CDIV2)
      IF(IPRINT.GT.4) PRINT 806,PHI0,PSI0
  801 FORMAT(' CX=',F10.4,' CY=',F10.4,' CR=',F10.4,' CP=',F10.4,/)
  802 FORMAT(' Z1=',2E15.7,' Z2=',2E15.7,/,' PI1=',2E15.7,' PI2=',2E15.7
     $,/)
  803 FORMAT(' CVAL1=',2E15.7,' CVAL2=',2E15.7,/)
  804 FORMAT(' RAD1=',2E15.7,' RAD2=',2E15.7,/,' ROOT1=',2E15.7,' ROOT2=
     $',2E15.7,/)
  805 FORMAT(' CDIV1=',2E15.7,' CDIV2=',2E15.7,/,' RDIV1=',2E15.7,' RDIV
     $2=',2E15.7,/,' ADIV1=',2E15.7,' ADIV2=',2E15.7,/)
  806 FORMAT(' PHI0=',2E15.7,' PSI0=',2E15.7,/)
C
      SX   = P + 2.*REAL(S1*S1 * PHI0 + S2*S2 * PSI0)
      SY   =     2.*REAL(         PHI0 +          PSI0)
      SXY =    - 2.*REAL(    S1 * PHI0 +     S2 * PSI0)
C
      IF(IPRINT.EQ.3) PRINT 901,SX,SY,SXY
  901 FORMAT(' S1 =',F20.15,' S2 =',F20.15,' S12 =',F20.15,//)
C     ----------------------------TRANSFORM INTO CYLINDRICAL COORDINATES
      ARG = THETA(J)
      RN = SIN(ARG)
      RM = COS(ARG)
C
      PSR  = (RM*RM*SX + RN*RN*SY + 2.*RN*RM*SXY)*THICK
      PST  = (RN*RN*SX + RM*RM*SY - 2.*RN*RM*SXY)*THICK
      PSRT = (RN*RM*(SY-SX)  + (1.-2.*RN*RN)*SXY)*THICK
C
```

```
      IF(IPRINT.EQ.3) PRINT 901,PSR,PST,PSRT
C
      RETURN
      END
C
C     ------------------------------------------------------------------
C
      SUBROUTINE LAMINA(SR,ST,SRT,
     $                  PSR,PST,PSRT,
     $                  Q11,Q12,Q16,Q22,Q26,Q66,
     $                  B11,B12,B16,B22,B26,B66,
     $                  THETA,J,IDIV,M,
     $                  IPRINT)
C
C     ******************************************************************
C     *****                                                        *****
C     *****       LAMINA STRESSES IN CYLINDRICAL COORDINATES       *****
C     *****                                                        *****
C     ******************************************************************
C
      DOUBLE PRECISION THETA(IDIV)
      REAL QA(3,3),BA(3,3),EPS(3),S(3)
      REAL Q11(M),Q12(M),Q16(M),Q22(M),Q26(M),Q66(M)
      REAL SR(M),ST(M),SRT(M)
C     ---------------------------------------------LAMINA STIFFNESS ARRAY
      PI = 3.141592653589793
C
      DO 100 JJ = 1,M
C
      QA(1,1) = Q11(JJ)
      QA(1,2) = Q12(JJ)
      QA(1,3) = Q16(JJ)
      QA(2,2) = Q22(JJ)
      QA(2,3) = Q26(JJ)
      QA(3,3) = Q66(JJ)
C     ----------------------------------------LAMINATE COMPLIANCE ARRAY
      BA(1,1) = B11
      BA(1,2) = B12
      BA(1,3) = B16
      BA(2,2) = B22
      BA(2,3) = B26
      BA(3,3) = B66
C     ------------------------------------------------------STRESS VECTOR
      ARG  = - THETA(J)
      RN   = SIN(ARG)
      RM   = COS(ARG)
      S(1) = RM*RM*PSR + RN*RN*PST + 2.*RN*RM*PSRT
      S(2) = RN*RN*PSR + RM*RM*PST - 2.*RN*RM*PSRT
      S(3) = RN*RM*(PST-PSR) + (1.-2.*RN*RN)*PSRT
C     ----------------------------LOWER TRIANGLE OF QA(I,K) AND BA(I,K)
      DO  10 I = 1,3
      DO  10 K = 1,I
      QA(I,K)  = QA(K,I)
   10 BA(I,K)  = BA(K,I)
C     ---------------------------------------------------OVERALL STRAINS
      DO  20 I = 1,3
      EPS(I)   = 0.0
      DO  20 K = 1,3
   20 EPS(I)   = EPS(I) + BA(I,K)*S(K)
C     ----------------------------------------CARTESIAN LAMINA STRESSES
      DO  30 I = 1,3
      S(I)     = 0.0
      DO  30 K = 1,3
   30 S(I)     = S(I) + QA(I,K)*EPS(K)
C     ----------------------------TRANSFORM INTO CYLINDRICAL COORDINATES
      ARG = THETA(J)
      RN  = SIN(ARG)
      RM  = COS(ARG)
C
      SR(JJ) = RM*RM*S(1) + 2.*RN*RM*S(3) + RN*RN*S(2)
```

```
      ST(JJ) = RN*RN*S(1) - 2.*RN*RM*S(3) + RM*RM*S(2)
      SRT(JJ)= RN*RM*(S(2)-S(1)) + (1.-2.*RN*RN)*S(3)
  100 IF(IPRINT.EQ.3) PRINT 900,JJ,SR(JJ),ST(JJ),SRT(JJ)
C
      RETURN
  900 FORMAT(' LAYER',I2,'   SR=',E15.4,'  ST=',E15.4,'  SRT=',E15.4,/)
      END
C
C     ------------------------------------------------------------------
C
      SUBROUTINE BOULAY(FR,FT,FZ,FRT,FZT,FZR,
     $                  B,BP,BPP,D,DP,
     $                  RMUE,E1,E2,
     $                  ALPHA,
     $                  S12,S22,S23,S26,
     $                  ETA,IDIV,K,M,IPLY,IPRINT)
C
C     ********************************************************************
C     *****                                                          *****
C     *****   B O U N D A R Y   L A Y E R   S T R E S S E S          *****
C     *****                                                          *****
C     ********************************************************************
C
      COMPLEX RMUE(3),RMU2(3),E1(3),E2(3),ALPHA(3),EX(3),FU(3)
      REAL    ETA(IDIV)
      REAL    S12(M),S22(M),S23(M),S26(M)
C
      DO 100 I=1,3
      EX(I)   = - RMUE(I) * CMPLX(ETA(K),0.0)
      FU(I)   =  ALPHA(I) * CEXP(EX(I))
  100 RMU2(I) =   RMUE(I) * RMUE(I)
C
      FRT = REAL
     $(E2(1)        *FU(1)+E2(2)        *FU(2)+E2(3)        *FU(3))*DP
C
      FZT = REAL
     $(E2(1)*RMUE(1)*FU(1)+E2(2)*RMUE(2)*FU(2)+E2(3)*RMUE(3)*FU(3))*D
C
      FR  = REAL
     $(E1(1)        *FU(1)+E1(2)        *FU(2)+E1(3)        *FU(3))*BPP
C
      FZR = REAL
     $(E1(1)*RMUE(1)*FU(1)+E1(2)*RMUE(2)*FU(2)+E1(3)*RMUE(3)*FU(3))*BP
C
      FZ  = REAL
     $(E1(1)*RMU2(1)*FU(1)+E1(2)*RMU2(2)*FU(2)+E1(3)*RMU2(3)*FU(3))*B
C
      FT  =  -(S12(IPLY)*FR+S23(IPLY)*FZ+S26(IPLY)*FRT)/S22(IPLY)
      RETURN
      END
C
C     ------------------------------------------------------------------
C
      SUBROUTINE ENERGY(ENERG,
     $                  ST1,ST2,ST3,ST4,ST5,ST6,
     $                  S,IWU,
     $                  THETA,THEPLY,
     $                  L,J,IPLY,IDIV,M,ITRANS)
C
C     ********************************************************************
C     *****                                                          *****
C     *****   S T R A I N   E N E R G Y   P E R   V O L U M E        *****
C     *****                                                          *****
C     *****                       O R                              *****
C     *****                                                          *****
C     *****  T S A I - W U   F A I L U R E   C R I T E R I O N      *****
C     *****                                                          *****
C     ********************************************************************
C
      REAL          S(6,6),ENERG(IDIV),THEPLY(M)
      REAL          ST1(IDIV),ST2(IDIV),ST3(IDIV)
      REAL          ST4(IDIV),ST5(IDIV),ST6(IDIV)
      DOUBLE PRECISION  THETA(IDIV)
```

```
      IF(IWU.EQ.1) GOTO 2
C
      S1 = ST1(L)
      S2 = ST2(L)
      S3 = ST3(L)
      S4 = ST4(L)
      S5 = ST5(L)
      S6 = ST6(L)
      ENERG(L)=(0.5*S(1,1)*S1 + S(1,2)*S2 + S(1,3)*S3 + S(1,6)*S6)*S1 +
     $         (0.5*            S(2,2)*S2 + S(2,3)*S3 + S(2,6)*S6)*S2 +
     $         (0.5*                        S(3,3)*S3 + S(3,6)*S6)*S3 +
     $         (0.5*            S(4,4)*S4 + S(4,5)*S5)*S4             +
     $         (0.5*                        S(5,5)*S5)*S5             +
     $         (0.5*                                  S(6,6)*S6)*S6
      GOTO 999
C     -----------------------------------------------------STRENGTH VALUES
    2 XT  =  219500.0
      XC  = -246000.0
      YT  =    6350.0
      YC  = - 23850.0
      ZT  =  YT
      ZC  =  YC
      S23 =    9800.0
      S13 =   12600.0
      S12 = S13
C     ---------------------------------------FAILURE TENSOR COMPONENTS
      F1 = 1./XT + 1./XC
      F2 = 1./YT + 1./YC
      F3 = F2
      F11= -1./(XT*XC)
      F22= -1./(YT*YC)
      F33= F22
      F44=  1./(S23*S23)
      F55=  1./(S13*S13)
      F66= F55
      F12= -1./2.*SQRT(1./(XT*XC*YT*YC))
      F13= F12
      F23= -1./2.*SQRT(1./(YT*YC*ZT*ZC))
C
C     ----------------------TRANSFORM STRESSES INTO MATERIAL COORDINETES
C
      CALL TRANS(ST1,ST2,ST3,ST4,ST5,ST6,
     $           THETA,THEPLY,
     $           L,J,IPLY,IDIV,M,2)
C     ------------------------------------------------FAILURE CRITERION
      S1 = F1*ST1(L)
      S2 = F2*ST2(L)
      S3 = F3*ST3(L)
      S11= F11*ST1(L)*ST1(L)
      S22= F22*ST2(L)*ST2(L)
      S33= F33*ST3(L)*ST3(L)
      S44= F44*ST4(L)*ST4(L)
      S55= F55*ST5(L)*ST5(L)
      S66= F66*ST6(L)*ST6(L)
      S12= F12*ST1(L)*ST2(L)
      S13= F13*ST1(L)*ST3(L)
      S23= F23*ST2(L)*ST3(L)
      ST1(L) = S1+S11+S12+S13
      ST2(L) = S2+S22+S12+S23
      ST3(L) = S3+S33+S23+S13
      ST4(L) = S44
      ST5(L) = S55
      ST6(L) = S66
      ENERG(L) = S1+S11+S12+S13 + S2+S22+S12+S23 + S3+S33+S13+S23
     $             +S44             +S55             +S66
  999 RETURN
      END
C
C     ----------------------------------------------------------------
C
```

```
      SUBROUTINE TRANS(SIG1,SIG2,SIG3,SIG4,SIG5,SIG6,
     $                 THETA,THEPLY,
     $                 L,J,IPLY,IDIV,M,ITRANS)
C
C     ***************************************************************
C     *****                                                     *****
C     *****    TRANSFORMATION  INTO  SYSTEM  OR  MATERIAL  AXES    *****
C     *****                                                     *****
C     ***************************************************************
C
      REAL SIG1(IDIV),SIG2(IDIV),SIG3(IDIV)
      REAL SIG4(IDIV),SIG5(IDIV),SIG6(IDIV)
      REAL SIG(6),T(6,6),SIGTRA(6)
      REAL THEPLY(M)
      DOUBLE PRECISION THETA(IDIV)
C
      ARG     = - THETA(J)
      IF(ITRANS.EQ.2) ARG=-THETA(J)+THEPLY(IPLY)
      DO  10 I=1,6
      DO  10 K=1,6
   10 T(I,K)  = 0.0
C
      RN=SIN(ARG)
      RM=COS(ARG)
C     ------------------------------------------------INITIATE THE T MATRIX
      DO  20 I=1,6
      DO  20 N=1,6
   20 T(I,N) = 0.0
C
      T(1,1) =      RM*RM
      T(1,2) =      RN*RN
      T(1,6) = 2. *RN*RM
      T(2,1) =      RN*RN
      T(2,2) =      RM*RM
      T(2,6) =-2. *RN*RM
      T(3,3) = 1.0
      T(4,4) =      RM*RM
      T(4,5) =      RN*RN
      T(5,4) =-     RN*RN
      T(5,5) =      RM*RM
      T(6,1) =-     RN*RM
      T(6,2) =      RN*RM
      T(6,6) = RM*RM-RN*RN
C
      SIG(1) = SIG1(L)
      SIG(2) = SIG2(L)
      SIG(3) = SIG3(L)
      SIG(4) = SIG4(L)
      SIG(5) = SIG5(L)
      SIG(6) = SIG6(L)
C
      CALL MATMLT(T,6,6,SIG,1,SIGTRA)
C
      SIG1(L) = SIGTRA(1)
      SIG2(L) = SIGTRA(2)
      SIG3(L) = SIGTRA(3)
      SIG4(L) = SIGTRA(4)
      SIG5(L) = SIGTRA(5)
      SIG6(L) = SIGTRA(6)
C
      RETURN
      END
C
C     ---------------------------------------------------------------
C
```

```
      SUBROUTINE STRAIN(EPS1,EPS2,EPS3,EPS4,EPS5,EPS6,
     $                  SIG1,SIG2,SIG3,SIG4,SIG5,SIG6,
     $                  ST1,THETA,
     $                  IDIV,L)
C
C     ************************************************************************
C     *****                                                              *****
C     *****      S      T      R      A      I      N      S           *****
C     *****                                                              *****
C     ************************************************************************
C
      REAL  EPS1(IDIV),EPS2(IDIV),EPS3(IDIV)
      REAL  EPS4(IDIV),EPS5(IDIV),EPS6(IDIV)
      DOUBLE PRECISION  THETA(IDIV)
      REAL  SIG1(IDIV),SIG2(IDIV),SIG3(IDIV)
      REAL  SIG4(IDIV),SIG5(IDIV),SIG6(IDIV)
      REAL  ST1(6,6),S(6),T(6,6),TT(6,6),BETW(6,6),SBAR(6,6),EPS(6)
C     ------------------------------------------STRESSES IN SYSTEM AXES
      RN=DSIN(THETA(L))
      RM=DCOS(THETA(L))
C     ------------------------------------------TRANSFORMATION MATRIX
      DO  10 I=1,6
      DO  10 J=1,6
   10 T(I,J) = 0.0
C
      T(1,1) = RM*RM
      T(1,2) = RN*RN
      T(1,6) =-RM*RN
      T(2,2) = T(1,1)
      T(2,6) =-T(1,6)
      T(3,3) = 1.0
      T(4,4) = RM
      T(4,5) = RN
      T(5,4) =-T(4,5)
      T(5,5) = RM
      T(6,1) = T(2,6)*2.0
      T(6,2) =-T(6,1)
      T(6,6) = RM*RM-RN*RN
C
      DO  20 I=1,6
      DO  20 J=1,6
   20 TT(I,J) = T(J,I)
C
      S(1) = SIG1(L)
      S(2) = SIG2(L)
      S(3) = SIG3(L)
      S(4) = SIG4(L)
      S(5) = SIG5(L)
      S(6) = SIG6(L)
C
      CALL MATMLT(T,6,6,ST1,6,BETW)
      CALL MATMLT(BETW,6,6,TT,6,SBAR)
      CALL MATMLT(SBAR,6,6,S,1,EPS)
C
      EPS1(L)  = EPS(1)
      EPS2(L)  = EPS(2)
      EPS3(L)  = EPS(3)
      EPS4(L)  = EPS(4)
      EPS5(L)  = EPS(5)
      EPS6(L)  = EPS(6)
C
      RETURN
      END
C
C     ------------------------------------------------------------------
C
```

```
      SUBROUTINE FUNETA(ALPHA,
     $                  B,BP,BPP,D,DP,
     $                  RMUE,E1,E2,
     $                      A11,A13,A16,A33,
     $                  A36,A44,A45,A55,A66,
     $                  SR,SRT,
     $                  RHO,IDIV,RHOI,
     $                  M,H2,II,
     $                  IPRINT,IFAIL,IOPT)
C
C     ************************************************************************
C     *****                                                            *******
C     *****   S  T  R  E  S  S       F  U  N  C  T  I  O  N  S       *******
C     *****                                                            *******
C     *****   -    COMPUTE THE FUNCTIONS OF RHO B,BP,BPP,D,DP          *******
C     *****                                                            *******
C     *****   -    COMPUTE THE ELEMENTS OF MIJ,NIJ,PIJ                 *******
C     *****                                                            *******
C     *****   -    SOLVE THE EIGENVALUE PROBLEM                        *******
C     *****                                                            *******
C     *****   -    COMPUTE THE COEFFICIENTS ALPHA                      *******
C     *****                                                            *******
C     ************************************************************************
C
      COMPLEX*16 DMUE(3)
      COMPLEX*16 DENUM(3),DENOM(3),CHE1,CHE2,CHE3
      COMPLEX    ALPHA(3),A(3,3),WA(15),WK(3),CRAD,RMUE(3),E1(3),E2(3)
      COMPLEX CANOM
      REAL SR(M),SRT(M),RHO(IDIV)
      REAL        A11(M),A13(M),A16(M),A33(M)
      REAL A36(M),A44(M),A45(M),A55(M),A66(M)
      REAL M11,N11,N12,N22,P11,P12,P22
C     ----------------------------------------------------------INITIALIZE
      B  = 0.0
      BP = 0.0
      D  = 0.0
C     -------------------------FIND THE STRESSFUNCTIONS DEPENDENT ON RHO
      K  = M + 1 - IFIX(RHOI*FLOAT(M))
      K1 = K-1
C     PRINT 903,RHO(II),RHOI,K,K1
C     ----------------------------------INTEGRATE FROM MINUS ONE TO ZERO
      DO 100 I=1,M
      B  =  B  -   (0.5*SR(I)/FLOAT(M)       -   BP)      /FLOAT(M)
      BP =  BP -         SR(I)/FLOAT(M)
  100 D  =  D  -        SRT(I)/FLOAT(M)
C 100 PRINT 904,I,SR(I),SRT(I),B,BP,D
C     ---------------------------------------INTEGRATE FROM ZERO TO RHOI
      IF(K.GT.M) GOTO 1
      DO 110 J=K,M
      I  =  M  +  K  -  J
      B  =  B  -  (0.5* SR(I)/FLOAT(M)       -   BP)      /FLOAT(M)
      BP =  BP -         SR(I)/FLOAT(M)
  110 D  =  D  -        SRT(I)/FLOAT(M)
C 110 PRINT 905,J,I,SR(I),SRT(I),B,BP,D
C     ---------------------------------------INTEGRATE FROM RHOI TO RHO
    1 B  =  B  -  (0.5*SR(K1)*(RHO(II)-RHOI)   -   BP) * (RHO(II)-RHOI)
      BP =  BP -       SR(K1)*(RHO(II)-RHOI)
      D  =  D  -      SRT(K1)*(RHO(II)-RHOI)
      DP =     -      SRT(K1)
      BPP=     -       SR(K1)
C
      IF(IPRINT.EQ.3) PRINT 900,B,BP,BPP,D,DP
C
      IF(IOPT.EQ.1.AND.II.GT.1) GOTO 999
C
C     ------------------------------------------------MATRIX COEFFICIENTS
      MM = 2*M
```

```
      CALL NUMINT(M11,N11,P11,N12,P12,N22,P22,
     $            A11,A13,A16,A33,A36,A44,A45,A55,A66,
     $            SR,SRT,
     $            H2,M,MM,
     $            IPRINT)
C
C     ----------------CALCULATE THE ROOTS OF THE CHARACTERISTIC EQUATION
      IF(IPRINT.EQ.9) PRINT 901,M11,N11,N12,N22,P11,P12,P22
      AN12=ABS(N12)
      AP12=ABS(P12)
      IF(AN12.LT.1.E-3.AND.AP12.LT.1.E-3) GOTO 3
      Q0 = M11*N22
      Q1 = M11*P22 + N11*N22 - N12*N12
      Q2 = N11*P22 + P11*N22 - N12*P12 - N12*P12
      Q3 = P11*P22 - P12*P12
      IF(IPRINT.EQ.9) PRINT 902,Q0,Q1,Q2,Q3
C     ------------------------------------------------------EIGENVALUES
      CALL KUPO(DMUE,Q0,Q1,Q2,Q3,IPRINT)
C     ------------------------------------------------------EIGENVECTORS
      DO 200 I=1,3
      E1(I)=  CMPLX(1.0,0.0)
      E2(I)= E1(I)
      DENUM(I)=  DMUE(I)*DMUE(I)*DCMPLX(DBLE(M11),DBLE(0.0))
     $          +         DMUE(I)*DCMPLX(DBLE(N11),DBLE(0.0))
     $          +                 DCMPLX(DBLE(P11),DBLE(0.0))
      DENOM(I)=           DMUE(I)*DCMPLX(DBLE(N12),DBLE(0.0))
     $          +                 DCMPLX(DBLE(P12),DBLE(0.0))
      IF(IPRINT.EQ.9) PRINT 906,DENUM(I),DENOM(I)
      CANOM = DENOM(I)
      ANOM = CABS(CANOM)
      IF(ANOM.NE.0.0) GOTO 200
      DENUM(I) = DENOM(I)
      DENOM(I) =          DMUE(I)*DCMPLX(DBLE(N22),DBLE(0.0))
     $          +                 DCMPLX(DBLE(P22),DBLE(0.0))
      IF(IPRINT.EQ.9) PRINT 906,DENUM(I),DENOM(I)
      CANOM = DENOM(I)
      ANOM = CABS(CANOM)
      IF(ANOM.NE.0.0) GOTO 200
      DENUM(I) =                  DCMPLX(DBLE(N12),DBLE(0.0))
      DENOM(I) =                  DCMPLX(DBLE(N22),DBLE(0.0))
      IF(IPRINT.EQ.9) PRINT 906,DENUM(I),DENOM(I)
  200 E2(I) = - DENUM(I)/DENOM(I)
      GOTO 4
C
    3 RADI = (N11/(M11*2.))*(N11/(M11*2.))-P11/M11
      CRAD = CSQRT(CMPLX(RADI,0.0))
      RM1 = -N11/(2.*M11)
      RMUE(1) = CMPLX(RM1,0.0) + CRAD
      RMUE(2) = CMPLX(RM1,0.0) - CRAD
      RMUE(3) = CMPLX(1.E50,0.0)
      IF(IPRINT.EQ.9) PRINT 903,RMUE
      R2 = -P22/N22
      IF(N22.NE.0.0) RMUE(3) = CMPLX(R2,0.0)
      E2(1) = CMPLX(0.0,0.0)
      E1(1) = CMPLX(1.0,0.0)
      E2(2) = E2(1)
      E1(2) = E1(1)
      E2(3) = E1(1)
      E1(3) = E2(1)
C
    4 DO 250 I=1,3
C     ------------------------------------COMPLEX EQUATION COEFFICIENTS
      RMUE(I) = DMUE(I)
      RMUE(I) = CSQRT(RMUE(I))
      A(1,I) = - RMUE(I)*E1(I)
      A(2,I) =           E1(I)
  250 A(3,I) =           E2(I)
      ALPHA(1) = CMPLX(0.0,0.0)
      ALPHA(2) = CMPLX(1.0,0.0)
      ALPHA(3) = CMPLX(1.0,0.0)
```

```
      CHE1 = CMPLX(0.0,0.0)
      CHE2 = CHE1
      CHE3 = CHE1
C     ---------------------------------------SOLVE THE COMPLEX EQUATIONS
      CALL LEQ2C(A,3,3,ALPHA,1,3,0,WA,WK,IER)
C     -------------------------------------------CHECK THE SOLUTION
      DO 300 I=1,3
      CHE1 = CHE1 + ALPHA(I)*RMUE(I)*E1(I)
      CHE2 = CHE2 + ALPHA(I)        *E1(I)
      CHE3 = CHE3 + ALPHA(I)        *E2(I)
  300 IF(IPRINT.EQ.9)PRINT 910,(A(I,J),J=1,3)
      IF(IPRINT.EQ.9)PRINT 910,ALPHA
      IF(IPRINT.EQ.9)PRINT 910,CHE1,CHE2,CHE3
  910 FORMAT(6E9.2,/)
  999 RETURN
C     ------------------------------------------------------------FORMATS
  900 FORMAT(/,' COEFFICIENTS DEPENDENT ON THE THIRD DIRECTION :',//
     $' B=',E15.7,'     BP=',E15.7,'     BPP=',E15.7,/,
     $' D=',E15.7,'     DP=',E15.7,//)
  901 FORMAT(' M11=',E9.2,/,' N11=',E9.2,' N12=',E9.2,' N22=',E9.2,/,' P
     $11=',E9.2,' P12=',E9.2,' P22=',E9.2,/)
  902 FORMAT(' Q0= ',E9.2,' Q1= ',E9.2,' Q2= ',E9.2,' Q3= ',E9.2,/)
  903 FORMAT(' RMUE(1)=',2E9.2,' RMUE(2)=',2E9.2,' RMUE(3)=',2E9.2,
     $' IER=',I4,/,'    ER(1)=',2E9.2,'    ER(2)=',2E9.2,'    ER(3)=',2E9.2
     $,/)
C 904 FORMAT(' FROM 0 TO 1 : I=',I2,' SR=',F10.4,' SRT=',F10.5,' B=',
C    $E15.7,' BP=',E15.7,' D=',E15.7,/)
C 905 FORMAT(' J=',I2,' I=',I2,' SR=',F10.5,' SRT=',F10.5,' B=',
C    $E15.7,' BP=',E15.7,' D=',E15.7,/)
  906 FORMAT(' NUMERATOR =',2E9.2,' DENOMINATOR =',2E9.2,/)
      END
C
C     ---------------------------------------------------------------
C
      SUBROUTINE KUPO(RMUE,Q0,Q1,Q2,Q3,IPRINT)
      COMPLEX*16 RMUE(3),E
      DOUBLE PRECISION X,B,C,D,R1,R2,R3,A1,A2,A3,RAD,PART,STEP,DR(2)
      B = Q1/Q0
      C = Q2/Q0
      D = Q3/Q0
      X = 0.0
      ICOUNT = 0
      EPS = ABS(Q0)
      STEP = 1.0
      REM = D
    1 IF(ICOUNT.EQ.1) X=STEP
      FUN = X*X*X + B*X*X + C*X + D
      SIGN = FUN * REM
      IF(SIGN.LT.0.0) STEP = - STEP/2.
      ABSFUN = ABS(FUN)
      IF(IPRINT.EQ.9) PRINT 700,X,FUN,REM,ICOUNT
      X = X + STEP
      REM = FUN
      ICOUNT = ICOUNT + 1
      IF(ABSFUN.GT.EPS.AND.ICOUNT.LT.100) GOTO 1
      CALL NEWTON(X,Q0,Q1,Q2,Q3)
      R1 = X
      RAD = B*B/4. - R1*B/2. - 3.*R1*R1/4. - C
      PART = DSQRT(DABS(RAD))
      A1 = DBLE(0.0)
      IF(RAD.LT.0.0) GOTO 2
      R2 = -(B+R1)/2. + PART
      CALL NEWTON(R2,Q0,Q1,Q2,Q3)
      R3 = -(B+R1)/2. - PART
      CALL NEWTON(R3,Q0,Q1,Q2,Q3)
      A2 = 0.0
      A3 = 0.0
      GOTO 3
    2 R2 = -(B+R1)/2.
      R3 = R2
      A2 =   PART
      A3 = - PART
```

```
    3 RMUE(1) = DCMPLX(R1,A1)
      RMUE(2) = DCMPLX(R2,A2)
      RMUE(3) = DCMPLX(R3,A3)
      DO 100 I=1,3
      E = Q0*RMUE(I)*RMUE(I)*RMUE(I)+Q1*RMUE(I)*RMUE(I)+Q2*RMUE(I)+Q3
  100 IF(IPRINT.EQ.9) PRINT 900,RMUE(I),E
      RETURN
  700 FORMAT(' X = ',E15.8,' FUN = ',E15.8,' REM = ',E15.8,' I = ',I2,/)
  900 FORMAT(' ROOT :',2E15.8,' ERROR : ',2E15.8,/)
      END
      SUBROUTINE NEWTON(X,Q0,Q1,Q2,Q3)
      DOUBLE PRECISION X
      EPS = 1.E-30
      ICOUNT = 0
    4 FUN = Q0*X*X*X + Q1*X*X + Q2*X + Q3
      DER = 3.*Q0*X*X + 2.*Q1*X + Q2
      IF(IPRINT.EQ.9) PRINT 700,X,FUN,ICOUNT
      X = X - FUN / DER
      ICOUNT = ICOUNT + 1
      ABSFUN= ABS(FUN)
      IF(ABSFUN.GT.EPS.AND.ICOUNT.LT.5) GOTO 4
      RETURN
  700 FORMAT(' X = ',E15.8,' FUN = ',E15.8,' I = ',I2,/)
      END
C
C     ------------------------------------------------------------------
C
      SUBROUTINE NUMINT(M11,N11,P11,N12,P12,N22,P22,
     $                  A11,A13,A16,A33,A36,A44,A45,A55,A66,
     $                  SR,SRT,
     $                  H2,M,MM,
     $                  IPRINT)
C
C     ********************************************************************
C     *****                                                          *****
C     *****     NUMERICAL INTEGRATIONS THROUGH THE THICKNESS         *****
C     *****                                                          *****
C     *****     FIVE POINT FORMULA ,     THREE POINT FORMULA         *****
C     *****                                                          *****
C     ********************************************************************
C
      REAL M11,N11,P11,N12,P12,N22,P22
      REAL SR(M),SRT(M),SSR(8),SSRT(8)
      REAL A11(M),A13(M),A16(M),A33(M),A36(M)
      REAL A44(M),A45(M),A55(M),A66(M)
      REAL AA11(8),AA13(8),AA16(8),AA33(8),AA36(8)
      REAL AA44(8),AA45(8),AA55(8),AA66(8)
      REAL X13(3),W3(3),X15(5),W5(5),BB(5),X3(3),X5(5)
C     ------------------------------------------------------WEIGHT FACTORS
      F = 1./FLOAT(M)/2.
      W3(1) = 0.555555555555556*F
      W3(2) = 0.888888888888889*F
      W3(3) = W3(1)
      W5(1) = 0.236926885056189*F
      W5(2) = 0.478628670499366*F
      W5(3) = 0.568888888888889*F
      W5(4) = W5(2)
      W5(5) = W5(1)
C     ----------------------------------------------INTEGRATION POINTS
      X13(1) = (1.-0.774596669241483)*F
      X13(2) =                       1.*F
      X13(3) = (1.+0.774596669241483)*F
      X15(1) = (1.-0.906179845938664)*F
      X15(2) = (1.-0.538469310105683)*F
      X15(3) =                       1.*F
      X15(4) = (1.+0.538469310105683)*F
```

```
      X15(5) = (1.+0.9061798459386 64)*F
      X3(1)  = X13(1)
      X3(2)  = X13(2) - X13(1)
      X3(3)  = X13(3) - X13(2)
      X5(1)  = X15(1)
      X5(2)  = X15(2) - X15(1)
      X5(3)  = X15(3) - X15(2)
      X5(4)  = X15(4) - X15(3)
      X5(5)  = X15(5) - X15(4)
C     ------------------------------------------------COMPLETE THE ARRAYS
      DO 100 I = 1,MM
                J = I
      IF(I.GT.M) J = 2*M + 1 - I
      SSR(I)  =  SR(J)
      SSRT(I) = SRT(J)
      AA11(I) = A11(J)
      AA13(I) = A13(J)
      AA16(I) = A16(J)
      AA33(I) = A33(J)
      AA36(I) = A36(J)
      AA44(I) = A44(J)
      AA45(I) = A45(J)
      AA55(I) = A55(J)
      AA66(I) = A66(J)
      IF(IPRINT.EQ.7) PRINT 799,J
      IF(IPRINT.EQ.7)PRINT 800, A11(J), A13(J), A16(J), A33(J), A36(J),
     $                          A44(J), A45(J), A55(J), A66(J)
      IF(IPRINT.EQ.7) PRINT 799,I
  100 IF(IPRINT.EQ.7)PRINT 800,AA11(I),AA13(I),AA16(I),AA33(I),AA36(I),
     $                         AA44(I),AA55(I),AA66(I)
  799 FORMAT(' INDEX =',I3)
  800 FORMAT(9E12.3)
C     ------------------------------------------------------------INITIALIZE
      BP  = 0.0
      D   = 0.0
      B5  = 0.0
      BP5 = 0.0
      B3  = 0.0
      BP3 = 0.0
      D3  = 0.0
      M11 = 0.0
      N11 = 0.0
      P11 = 0.0
      N12 = 0.0
      P12 = 0.0
      N22 = 0.0
      P22 = 0.0
C     ---------------------------------------------LOOP ON NUMBER OF LAYERS
      DO 200 I = 1,MM
      BPP = -  SSR(I)
      DP  = - SSRT(I)
      IF(IPRINT.EQ.7) PRINT 900,BPP,DP
C     ------------------------------------------------------FIVE POINT FORMULA
      IF(IPRINT.EQ.7) PRINT 901,AA33(I)
      DO 210 J = 1,5
      B5    = B5  +   BPP * X5(J)*X5(J)/2.   +   BP5 * X5(J)
      BP5   = BP5 +   BPP * X5(J)
      BB(J) = B5*B5
      M11   =    M11   +       AA33(I)*B5* B5                      * W5(J)
  210 IF(IPRINT.EQ.7) PRINT 902,BP5,B5,BB(J),M11
      B5    = B5  +   BPP * X5(1)*X5(1)/2.   +   BP5 * X5(1)
      BP5   = BP5 +   BPP * X5(1)
      BBS   = B5*B5
      IF(IPRINT.EQ.7) PRINT 902,BP5,B5,BBS
C     ----------------------------------------------------THREE POINT FORMULA
      DO 220 J = 1,3
      B3    = B3  +   BPP * X3(J)*X3(J)/2.   +   BP3 * X3(J)
      BP3   = BP3 +   BPP * X3(J)
      D3    = D3  +   DP  * X3(J)
      N11   =  N11  + (2.0*AA13(I)*B3*BPP -     AA55(I)*BP3*BP3) * W3(J)
      N12   =  N12  + (    AA36(I)*DP* B3 -     AA45(I)*BP3* D3) * W3(J)
      N22   =  N22  + (                   -     AA44(I)* D3* D3) * W3(J)
```

```
      P11    =   P11   + (     BPP*BPP*AA11(I))                        * W3(J)
      P12    =   P12   + (     BPP* DP*AA16(I))                        * W3(J)
      P22    =   P22   + (     DP * DP*AA66(I))                        * W3(J)
      IF(IPRINT.EQ.7) PRINT 903,BP3,B3,D3
  220 IF(IPRINT.EQ.7) PRINT 904,N11,N12,N22,P11,P12,P22
      B3     = B3   +    BPP * X3(1)*X3(1)/2.    +    BP3 * X3(1)
      BP3    = BP3  +    BPP * X3(1)
      D3     = D3   +    DP  * X3(1)
      IF(IPRINT.EQ.7) PRINT 903,BP3,B3,D3
  200 CONTINUE
      N11 = N11/M11
      P11 = P11/M11
      N12 = N12/M11
      P12 = P12/M11
      N22 = N22/M11
      P22 = P22/M11
      M11 = 1.0
      IF(IPRINT.EQ.7) PRINT 904,N11,N12,N22,P11,P12,P22
      RETURN
  900 FORMAT(' BPP=',E15.7,'  DP=',E15.7,/)
  901 FORMAT(' AA33 = ',E15.7)
  902 FORMAT(' BP5=',E15.7,'  B5=',E15.7,'  BB=',E15.7,' M11=',E15.7,/)
  903 FORMAT(' BP3=',E15.7,'  B3=',E15.7,'  D3=',E15.7,/)
  904 FORMAT(' N11=',E15.7,' N12=',E15.7,' N22=',E15.7,/,
     $       ' P11=',E15.7,' P12=',E15.7,' P22=',E15.7,/)
      END
C
C     ------------------------------------------------------------------
C
      SUBROUTINE PRIRES(SIG1,SIG2,SIG3,SIG4,SIG5,SIG6,ENERG,
     $                  THETA,ETA,RHO,
     $                  IDIV,IOPT)
C
C     ********************************************************************
C     *****                                                          *****
C     *****           P       R       I       N       T              *****
C     *****                                                          *****
C     ********************************************************************
C
      REAL SIG1(IDIV),SIG2(IDIV),SIG3(IDIV)
      REAL SIG4(IDIV),SIG5(IDIV),SIG6(IDIV)
      REAL ENERG(IDIV)
      REAL RHO(IDIV),ETA(IDIV)
      DOUBLE PRECISION THETA(IDIV)
C
      PI = 3.141592653589793
C
      PRINT 900
C
      KOPT=IOPT-2
      IF(KOPT)1,2,3
C
    1 PRINT 910,THETA(1),ETA(1)
      PRINT 911,(RHO(I),SIG1(I),SIG2(I),SIG3(I),SIG4(I),SIG5(I),
     $                  SIG6(I),ENERG(I),I=1,IDIV)
      GOTO 4
C
    2 PRINT 920
      PRINT 921,ETA(1),RHO(1)
      DO  20 I=1,IDIV
      ANGLE=THETA(I)*180.0/PI
      PRINT 922,ANGLE,SIG1(I),SIG2(I),SIG3(I),SIG4(I),SIG5(I),
     $                                        SIG6(I),ENERG(I)
   20 CONTINUE
      GOTO 4
C
    3 PRINT 930,THETA(1),RHO(1)
      DO  30 I=1,IDIV
      PRINT 931,ETA(I),SIG1(I),SIG2(I),SIG3(I),SIG4(I),SIG5(I),
     $                                       SIG6(I),ENERG(I)
   30 CONTINUE
C
```

```
  900 FORMAT(1H1,/,' * * * * * * * * * * * * * * * * * * * * * * * * * * * * *
     $ * * * * * * * * * * * * * * * * * * * * * * * * * * * * * * * * * * *',/,
     $              ' * * * * * * * * * * * * * *
     $                                          * * * * * * * * * * * * * * *',/,
     $              ' * * * * * * * * * * * * * *          S O L U T I O N
     $      P R I N T O U T                     * * * * * * * * * * * * * * *',/,
     $              ' * * * * * * * * * * * * * *
     $                                          * * * * * * * * * * * * * * *',/,
     $              ' * * * * * * * * * * * * * * * * * * * * * * * * * * * * *
     $ * * * * * * * * * * * * * * * * * * * * * * * * * * * * * * * * * * *',//
     $/////)
  910 FORMAT(1H ,'STRESSES ALONG THE COORDINATES :',///,
     $           ' THETA=',F8.4,/,' ETA  =',F8.4,//)
  911 FORMAT(' STRESSES AT NORMALIZED HEIGHT RHO =',F7.4,//,
     $' SIG 1 =',E9.2,'  SIG 2 =',E9.2,'  SIG 3 =',E9.2,
     $'  SIG 4 =',E9.2,'  SIG 5 =',E9.2,'  SIG 6 =',E9.2,
     $'  ENRG:',E9.2,      ///)
C
  920 FORMAT(1H ,'STRESSDISTRIBUTION ALONG THE COORDINATES :',////)
  921 FORMAT(1H ,'ETA =',F8.4,/,' RHO =',F8.4,//)
  922 FORMAT(1H ,'STRESSES AT ANGLE THETA =',F10.4,':',//,
     $' SIG 1 =',E9.2,'  SIG 2 =',E9.2,'  SIG 3 =',E9.2,
     $'  SIG 4 =',E9.2,'  SIG 5 =',E9.2,'  SIG 6 =',
     $E9.2,'  ENRG:',E9.2,      ///)
C
  930 FORMAT(1H ,'STRESSDISTRIBUTION ALONG THE COORDINATES THETA =',
     $F10.4,      '       AND RHO =',F10.4,//)
  931 FORMAT(1H ,'STRESSES AT THE NORMALIZED RADIUS ETA =',F10.4,':',//,
     $' SIG 1 =',E9.2,'  SIG 2 =',E9.2,'  SIG 3 =',E9.2,
     $'  SIG 4 =',E9.2,'  SIG 5 =',E9.2,'  SIG 6 =',
     $E9.2,'  ENRG:',E9.2,   ///)
    4 RETURN
      END
C
C     ------------------------------------------------------------------
C
      SUBROUTINE PLORES(SIG1,SIG2,SIG3,SIG4,SIG5,SIG6,ENERG,
     $                  RHO,THETA,ETA,THEPLY,
     $                  DIAMTR,THICK,
     $                  M,IOPT,NPLOT,IPLOT,IMAT,ITRANS,I1,IDIV,IWU)
C
C     ******************************************************************
C     *****                                                        *****
C     *****         P          L          O          T            *****
C     *****                                                        *****
C     ******************************************************************
C
      REAL              LABELX(1),LABELY(1)
      REAL              AX(101,7),AY(101,7),X(103),Y(103)
      REAL              STRESS(101,7)
      REAL              SIG1(IDIV),SIG2(IDIV),SIG3(IDIV)
      REAL              SIG4(IDIV),SIG5(IDIV),SIG6(IDIV)
      REAL              ENERG(IDIV)
      REAL              ASCALE(4),VSCALE(4)
      REAL              RHO(IDIV),ETA(IDIV)
      REAL              THEPLY(4)
      DOUBLE PRECISION THETA(IDIV)
      INTEGER IPLOT(NPLOT)
      DATA LABELX/'    '/
      DATA LABELY/'    '/
      PI = 3.141592653589793
      CALL PLOTS(0,0,50)
      I1=NPLOT
C     ------------------------------------------------------STRESS ARRAY
      DO  10 I    = 1,IDIV
      STRESS(I,1) = SIG1(I)
      STRESS(I,2) = SIG2(I)
      STRESS(I,3) = SIG3(I)
      STRESS(I,4) = SIG4(I)
      STRESS(I,5) = SIG5(I)
   10 STRESS(I,6) = SIG6(I)
```

```
C     ----------------------------------------FIND EXTREM STRESS VALUES
      STRMAX = 0.0
      STRMIN = 0.0
      DO  20 I=1,NPLOT
      DO  20 J=1,IDIV

      NI       = IPLOT(I)
      STR      = STRESS(J,NI)
      IF(STR.GT.STRMAX) STRMAX =      STR
   20 IF(STR.LT.STRMIN) STRMIN =      STR
C     ----------------------------------------SCALE THE ENERGY ARRAY
      IF(IWU.EQ.1) GOTO 32
      S2MIN = 0.0
      ENRMAX       = 0.0
      DO  30      I=1,IDIV
      ENR          = ABS(ENERG(I))
      IF(ENR.LE.ENRMAX) GOTO 30
      ENRMAX       = ENR
   30 CONTINUE
      SCALEF = ENRMAX/STRMAX
      DO       31 I=1,IDIV
   31 STRESS(I,7) = ENERG(I)/SCALEF
   32 KOPT = IOPT-2
      IF(KOPT)1,2,1
C     ---------------------------------------SCALING FOR OPTIONS 1 AND 3
    1 ASCALE(1) = STRMIN
      IF(STRMIN.GT.0.0) ASCALE(1) = 0.0
      IF(IOPT.EQ.3) GOTO 9
      ASCALE(1) = STRMIN
      ASCALE(2) = STRMAX
      VSCALE(1) = RHO(1)
      VSCALE(2) = RHO(IDIV)
      GOTO 11
    9 VSCALE(1) = ETA(1)
      VSCALE(2) = ETA(IDIV)
      ASCALE(1) = STRMIN
      ASCALE(2) = STRMAX
   11 CALL SCALE(ASCALE,4.,2,1)
      CALL SCALE(VSCALE,4.,2,1)
C
      IF(IOPT.EQ.3) GOTO 5
C     ------------------------------------------------ARRAYS FOR OPTION 1
                    DO  40 J=1,IDIV
                    DO  40 I=1,NPLOT
                    NI       = IPLOT(I)
                    AY(J,I) = RHO(J)
   40               AX(J,I) = STRESS(J,NI)
      GOTO 3
C     ------------------------------------------------ARRAYS FOR OPTION 3
    5 DO  41 J=1,IDIV
      DO  41 I=1,NPLOT
      NI       = IPLOT(I)
      AX(J,I) = ETA(J)
   41 AY(J,I) = STRESS(J,NI)
      GOTO 3
C     ------------------------------------------------SCALING FOR OPTION 2
    2                     QUOT       = 10.
      IF(STRMIN.NE.0.0) QUOT       = ABS(STRMAX/STRMIN)
                        ASCALE(1) = 0.0
                        ASCALE(2) = STRMAX
      IF(QUOT.LT.6.0)   ASCALE(2) = ABS(STRMIN)
                        BSCALE     = 3.0
      IF(QUOT.LT.6.0)   BSCALE     = 0.5
      CALL SCALE(ASCALE,BSCALE,2,1)
C     ---------------------------MODIFY DATA FOR CIRCULAR REPRESENTATION
      DO  50 J=1,IDIV
      DO  50 I=1,NPLOT
      NI       = IPLOT(I)
      ARG      = THETA(J)
      AX(J,I) = (STRESS(J,NI) + ASCALE(4)) * COS(ARG)
      AXNEW = AX(J,I)
      IF(AXNEW.LT.S2MIN) S2MIN = AXNEW
   50 AY(J,I) = (STRESS(J,NI) + ASCALE(4)) * SIN(ARG)
```

```
C     ------------------------------------------------------CIRCLE ARRAY
      I1       =NPLOT + 1
      DO  60 J=1,IDIV
      ARG      =THETA(J)
      AX(J,I1)=ASCALE(4) * COS(ARG)
   60 AY(J,I1)=ASCALE(4) * SIN(ARG)
C     ------------------------------------------------DEFINE THE AXES
    3 STRTXX=1.0
      STRTXY=2.5
      STRTYX=1.0
      STRTYY=2.5
      AXL    =  4.
      ILAB1 = -4
      ILAB2 =  4
      RD1    =  0.
      RD2    = 90.
      IF(IOPT.NE.1) GOTO 6
      ILAB1 =  4
      ILAB2 = -4
      RD1   = 90.
      RD2    =  0.
    6 IF(IOPT.NE.2) GOTO 4
      VSCALE(3) = ASCALE(3)
      VSCALE(4) = ASCALE(4)
      STRTXX=5.0
      STRTYX=4.0
      STRTYY=3.5
      AXL    =  2.
    4 CALL AXIS(STRTXX,STRTXY,LABELX,ILAB1,AXL,RD1,VSCALE(3),VSCALE(4))
      CALL AXIS(STRTYX,STRTYY,LABELY,ILAB2,AXL,RD2,ASCALE(3),ASCALE(4))
      STPLX = STRTXX
      STPLY = STRTYY
      IF(IOPT.EQ.2) STPLX = STRTXX - 1.
      IF(IOPT.EQ.2) STPLY = STRTYY - 1.
      CALL PLOT(STPLX,STPLY,-3)
C     -------------------------------LOOP ON THE NUMBER OF STRESSCURVES
      I1 = NPLOT
      IF(IOPT.EQ.2) I1 = I1 + 1
      CALL NEWPEN(3)
      DO  70 J=1,I1
      IF(IOPT.EQ.2.AND.J.EQ.I1) CALL NEWPEN(1)
      DO  80 I=1,IDIV
      X(I)=AX(I,J)
   80 Y(I)=AY(I,J)
      N1=IDIV+1
      N2=N1+1
      IF(IOPT.EQ.3) GOTO 7
      X(N1)=ASCALE(3)
      X(N2)=ASCALE(4)
      Y(N1)=VSCALE(3)
      Y(N2)=VSCALE(4)
      GOTO 8
    7 X(N1)=VSCALE(3)
      X(N2)=VSCALE(4)
      Y(N1)=ASCALE(3)
      Y(N2)=ASCALE(4)
    8 CALL FACTOR(1.)
      CALL LINE(X,Y,IDIV,1,0,0)
   70 CALL FACTOR(1.)
C     ------------------------------------------------TEXT INFORMATIONS
      CALL NEWPEN(2)
      XS = S2MIN/ASCALE(4)
      IF(IOPT.NE.2) XS = XS - 3./4.
      YS = 6.5
      HGT = 0.08
      ANG = 0.0
C     ------------------------------------------------------------MATERIAL
      IF(IMAT.EQ.1)CALL VPISYM(XS,YS,HGT,'MATERIAL GRAPHITE EPOXY',
     $                         ANG,23)
      IF(IMAT.EQ.2)CALL VPISYM(XS,YS,HGT,'MATERIAL BORON EPOXY',
     $                         ANG,20)
```

```
C     ------------------------------------------------STACKING SEQUENCE
      YS = YS - 3.*HGT
      CALL VPISYM(XS,YS,HGT,'STACKING SEQUENCE                  &(',ANG,3
     $6)
      X2 = XS + 39.*HGT
      M1 = M-1
      IF(M1.EQ.0) GOTO 27
      DO 800 I=1,M1
      TPLY = THEPLY(I) * 180.0/PI
      IF(TPLY.LT.9.5.AND.TPLY.GE.0.0) X2 = X2 + HGT
      IF(TPLY.LT.-9.)                 X2 = X2 - HGT
      CALL NUMBER(X2,YS,HGT,TPLY,ANG,-1)
      IF(TPLY.LT.-9.)                 X2 = X2 + HGT
      IF(TPLY.LT.9.5.AND.TPLY.GT.0.0) X2 = X2 - HGT
      CALL VPISYM(X2,YS,HGT,'   , ',ANG,4)
  800 X2 = X2 + 4.*HGT
   27 TPLY = THEPLY(M)*180.0/PI
      IF(TPLY.LT.0.0) X2 = X2 - HGT
      CALL NUMBER(X2,YS,HGT,TPLY,ANG,-1)
      CALL VPISYM(X2,YS,HGT,'    &)SS',ANG,8)
C     ------------------------------------------------------GEOMETRY
      X2 = XS + 36.*HGT
      YS = YS - 3.*HGT
      XSI= XS + 46.*HGT
      CALL VPISYM(XS,YS,HGT,'HOLE DIAMETER',ANG,13)
      CALL VPISYM(XSI,YS,HGT,'INCHES',ANG,6)
      CALL NUMBER(X2,YS,HGT,DIAMTR,ANG,3)
      YS = YS - 3.*HGT
      CALL VPISYM(XS,YS,HGT,'LAMINATE THICKNESS',ANG,18)
      CALL VPISYM(XSI,YS,HGT,'INCHES',ANG,6)
      CALL NUMBER(X2,YS,HGT,THICK,ANG,3)
C     ------------------------------------------------FIXED COORDINATES
      IF(IOPT.EQ.1) GOTO 21
      YS = YS - 3.*HGT
      CALL VPISYM(XS,YS,HGT,'Z/(M*H)        = ?&Q',ANG,20)
      RH = RHO(1)
      CALL NUMBER(X2,YS,HGT,RH,ANG,3)
   21 IF(IOPT.EQ.2) GOTO 22
      YS = YS - 3.*HGT
      CALL VPISYM(XS,YS,HGT,'ANGLE THETA',ANG,11)
      THET = THETA(1)*180.0/PI
      CALL NUMBER(X2,YS,HGT,THET,ANG,3)
   22 IF(IOPT.EQ.3) GOTO 23
      YS = YS - 3.*HGT
      CALL VPISYM(XS,YS,HGT,'(R - RADIUS)/H = ?&G',ANG,20)
      ET = ETA(1)
      CALL NUMBER(X2,YS,HGT,ET,ANG,3)
C     ------------------------------------------------------------LABELS
   23 HL  = HGT
      XLX = STRTXX - STPLX +0.5
      YLX = -0.5
      XLY =                -0.5
      YLY = STRTYY - STPLY +0.5
      IF(IOPT.NE.1) GOTO 24
      CALL VPISYM(XLX,YLX,HL,'STRESS CONCENTRATION',0.0,20)
      CALL VPISYM(XLY,YLY,HL,'?&Q = Z/THICK*2',90.,15)
   24 IF(IOPT.NE.2) GOTO 25
      CALL VPISYM(XLX,YLX,HL,'STRESS CONCENTRATION',0.0,20)
      CALL VPISYM(XLY,YLY,HL,'STRESS CONCENTRATION',90.,20)
   25 IF(IOPT.NE.3) GOTO 26
      CALL VPISYM(XLX,YLX,HL,'?&G = (R - RADIUS)/H',0.0,20)
      CALL VPISYM(XLY,YLY,HL,'STRESS CONCENTRATION',90.,20)
```

```
C     ----------------------------------------STRESS / STRAIN COMPONENTS
   26 YS= YLX - 5.*HGT
      XC = XS
      XI = XC + HGT
      HG = 2.*HGT
      DO 801 I=1,NPLOT
      IPL = IPLOT(I)
      IF(ISTRN.EQ.0.AND.IPL.NE.7)CALL VPISYM(XC,YS,HG,'?&R',0.0,3)
      IF(ISTRN.EQ.1.AND.IPL.NE.7)CALL VPISYM(XC,YS,HG,'?&E',0.0,3)
      IF(IPL.EQ.1)CALL VPISYM(XI,YS,HGT,'$#11',0.0,4)
      IF(IPL.EQ.2)CALL VPISYM(XI,YS,HGT,'$#22',0.0,4)
      IF(IPL.EQ.3)CALL VPISYM(XI,YS,HGT,'$#33',0.0,4)
      IF(IPL.EQ.4)CALL VPISYM(XI,YS,HGT,'$#23',0.0,4)
      IF(IPL.EQ.5)CALL VPISYM(XI,YS,HGT,'$#13',0.0,4)
      IF(IPL.EQ.6)CALL VPISYM(XI,YS,HGT,'$#12',0.0,4)
      XC = XC + 5.*HGT
  801 XI = XI + 5.*HGT
C     ------------------------------------------------COORDINATE SYSTEM
      YS = YS - 3.*HGT
      IF(ITRANS.EQ.0)CALL VPISYM(XS,YS,HGT,'IN CYLINDRICAL COORDINATES
     $                          ',0.0,26)
      IF(ITRANS.EQ.1)CALL VPISYM(XS,YS,HGT,'IN SYSTEM COORDINATES',
     $                           0.0,21)
      IF(ITRANS.EQ.2)CALL VPISYM(XS,YS,HGT,'IN NATURAL COORDINATES',
     $                           0.0,22)
C
C     IF(IOPT.EQ.2)CALL VPISYM(0.,0.,HGT,'1',0.,-1)
      CALL PLOT(0.0,0.0,999)
      RETURN
  900 FORMAT(' SCALE FACTOR FOR THE STRAIN ENERGY PLOT :  SCALE=',E15.7)
      END
C
C     ---------------------------------------------------------------
C
      SUBROUTINE PRI(F,I,J)
      REAL F(I,J)
      DO 10 K=1,I
   10 PRINT 900,(F(K,L),L=1,J)
      PRINT 901
  900 FORMAT(6E14.6)
  901 FORMAT(1H ,/)
      RETURN
      END
C$ENTRY
```

The vita has been removed from the scanned document